An *In Vitro* Model of Mouse Corneal Endothelial Development

Mohammed Mubeen Goolam

Supervisor: Prof. S. Kidson

Presented in fulfilment of the requirements for the degree of
Master of Science in Medicine

Division of Cell Biology
Department of Human Biology
Faculty of Health Sciences
University of Cape Town

July 2012

This thesis is dedicated to the memory of my sister, Feroza Goolam. Everything I do, I do in the hope that it would make you proud. I miss you.

Declaration

I, Mohammed Mubeen Goolam, hereby declare that the work on which this dissertation/thesis is based is my original work (except where acknowledgements indicate otherwise) and that neither the whole work nor any part of it has been, is being, or is to be submitted for another degree in this or any other university.

I empower the university to reproduce for the purpose of research either the whole or any portion of the contents in any manner whatsoever.

Signature: _____ Date:_____

Acknowledgements:

I think I can sum up this thesis in one word. Phew. It has been a long and tiring journey. The burdens I had to face to get to this point were made considerably easier because of the people I was surrounded with. Their input, advice, help, and support along the way has been outstanding and the only reason I got this far. It is all these people that I would like to thank for helping me get here. I know it would not be possible without all of you.

To my parents. You have provided me with a secure and stable home environment allowing me to focus on my studies and not have to worry about the day to day or how I was going to support myself. Thank you for your love and support.

To Prof. Sue Kidson. Thank you for your guidance. Your enthusiasm and dedication to science has been an inspiration. Thank you for sharing your knowledge with me, and introducing me to the wonderful world of developmental biology.

To all members of the Kidson lab past and present, Dennis, Landi and Anita. It has been a pleasure to have such wonderful lab mates. A very special thanks is owed to Robea, who is the glue that keeps the Kidson lab together. Thank you for always providing all the support in the lab that I ever needed. A double thanks is owed to Robea and Landi for reading parts of this thesis and giving me valuable feedback.

To Lester and the rest of the Redox lab for always including us, especially in lab meetings, and for always making me feel very welcome and a part of your lab.

There is a whole army of people who keep things running smoothly in the anatomy building. To all the technical and administrative staff thank you for taking care of all the details.

To Dr Paula Sommer from UKZN for all the help to get things started and sharing so much of what you had, including the data from Prof. Beebe, to whom I am also very grateful. Special thanks also go to Dr Leana Maree for the gift of the MDCK cells.

To the team at the animal unit, and especially Jaap, thank you for setting up the all the mice matings and providing me with the primary tissue needed to realise this study.

To Prof. Kellaway, Iekraam and Charles for the technical assistance with the establishing the electrophysiology component of this project, thank you for your time.

To Dirk and Susan for the help on the microscope and Morea for the help with the histology, thank you.

A special thanks to Wendy for taking time to read parts of this thesis and for providing such wonderful insight as well as to Prof. Mulder for the assistance with mining the microarray data.

To my funders, the NRF and Ernst and Ethel Erikson Foundation. Thank you for the financial support.

Lastly, I owe an enormous debt to the many mice used in this project. Your sacrifice deserves thanks most of all. Scientific research and progress, particularly in the medical field, would be impossible without the massive contribution of animals. I hope in setting up this model system that the forfeit of your lives was not in vain.

To everyone mentioned here, and to all those who I have forgotten to credit, I owe parts of this project, and thus, a part of my development over the course of the past two years, to you. This thesis is a collaborative effort in every sense. You all are the players who set the pieces in motion. To all of you my gratitude is endless and eternal.

Table of Contents:

List of Figures:

List of Tables:

Abstract:

The corneal endothelium serves to maintain the transparency of the cornea and is critical to the function of the eye. Any damage or disease which affects this layer will result in a dysfunction of this task and will lead to a loss of vision. While transplantation is a successful form of treatment there are limitations to the procedure; principally a short supply of donor corneas, especially in South Africa, and a rapid loss of cells post-surgery. There is thus a need to investigate other regenerative techniques to overcome corneal endothelial dysfunction as well as further our knowledge of the development of this critical tissue.

The principle aim of this study was to derive an *in vitro* model that could be used to study corneal endothelial development. This was done by investigating methods to induce a mesenchymal-to-epithelial transition (MET) in mouse periocular mesenchyme cells to drive them to form fully differentiated adult corneal endothelial cells in culture. Periocular mesenchyme surrounding the optic cup was dissected from E12.5 and E13.5 mouse embryos and immortalised with the SV40 large T-antigen. Two cell lines were thus derived and named E12.5POM and E13.5POM respectively. Growth analyses determined that these cell lines were able to grow rapidly at both the permissive (33°C) and non-permissive (39°C) temperatures for the large T-antigen while quantitative real-time polymerase chain reaction (qPCR) indicated a maintenance of the expected *Foxc1* and *Tgf*β*1i4* expression patterns. No expression of *Pitx2* was noted in the cell lines.

To induce a MET in the cell lines, two methods were attempted. Firstly, the E12.5POM cell line was cultured in serum free conditions. This resulted in the formation of non-adherent spheres in culture that were morphologically similar to those noted in cultures of corneal endothelial precursors. Secondly, both cell lines were grown at 39°C in reduced serum conditions. This resulted in a change in the growth and morphology of the cell lines. A statistically significant drop in *Foxc1* and increase in *Tgf*β*1i4* expression was noted when analysed by qPCR. These changes indicated that the cells were more similar to adult corneal endothelial cells than periocular mesenchyme cells. ICC revealed the expression of both adherens junctions (as

witnessed by N-cadherin expression in the cell membrane) and tight junctions (as witnessed by ZO-1 expression in the cell membrane). These results indicate that a reduction in serum in the medium together with the inactivation of the SV40 large T-antigen is sufficient to drive differentiation of periocular mesenchyme cell lines into corneal endothelial-like cells.

To identify a candidate signalling molecule secreted by the embryonic lens which could affect the differentiation of the corneal endothelium, microarray data comparing gene expression in the E12.5 lens epithelium vs. the fibre mass (kindly shared by Prof. Beebe) was examined. Follistatin was found to be highly expressed in the E12.5 lens epithelium and reverse transcription PCR (RT-PCR) analyses indicated that follistatin was specifically expressed in the embryonic and not the adult lens. The addition of follistatin to the culture medium did not have any significant effect on the cell lines.

Immortalised E12.5 and E13.5 periocular mesenchyme cell lines were successfully used to model corneal endothelial development *in vitro*. They serve as an excellent tool to elucidate the mechanisms controlling the development of the corneal endothelium.

Chapter 1: Introduction and Aims

Corneal disease and malfunction is a major cause of blindness worldwide and is, according to the World Health Organization, second only to cataract formation in its importance. The principle function of the corneal endothelium is to preserve corneal transparency by maintaining optimal stromal hydration. A decrease in density in the corneal endothelium through aging (Laing et al. 1976) or diseases such as glaucoma (Gagnon et al. 1997) and Fuchs' dystrophy (Bourne 2003) results in stromal oedema, corneal opacity and loss of visual function. The most common and successful form of treatment for patients with endothelial dysfunction is penetrating or endothelial keratoplasty (Price et al. 2010). However, there is a severe shortage of donor corneas worldwide (Lai et al. 2006). In addition, a major complication of these intraocular surgeries is a rapid post-surgery loss of endothelial cells which leads to a subsequent loss in barrier integrity, loss of corneal endothelial function and therefore, a loss in vision. There is thus a need to further develop our understanding of the corneal endothelium, its development, and physiological maintenance. An effective way to accomplish this is through developing an *in vitro* model of corneal endothelial development. Mammalian animal models would be required for preclinical research and the well-understood genetics of the mouse present it as an ideal candidate. This study will therefore focus on developing an *in vitro* mouse model of the corneal endothelium.

1.1 The Vertebrate Eye

The eye is a round, fluid-filled organ with much the same structure and function in all sighted vertebrates (Figure 1.1). The eye is responsible for translating visual information from the environment into electrical impulses which can be interpreted by the brain in order to form an image. This complex process requires a variety of different structures with specific properties that allow for a successful conversion of energy into information.

The eye is covered in the sclera, a tough fibrous layer consisting of parallel collagen fibres that is responsible for protecting and maintaining the shape of the eye. The sclera is continuous with the cornea (situated in the front of the eye) which transmits and focuses incoming light. Situated directly proximal to the cornea is the anterior chamber which is filled with the aqueous humour, tasked with providing nutrients to the avascular cornea and lens. (Snell et al. 1998)

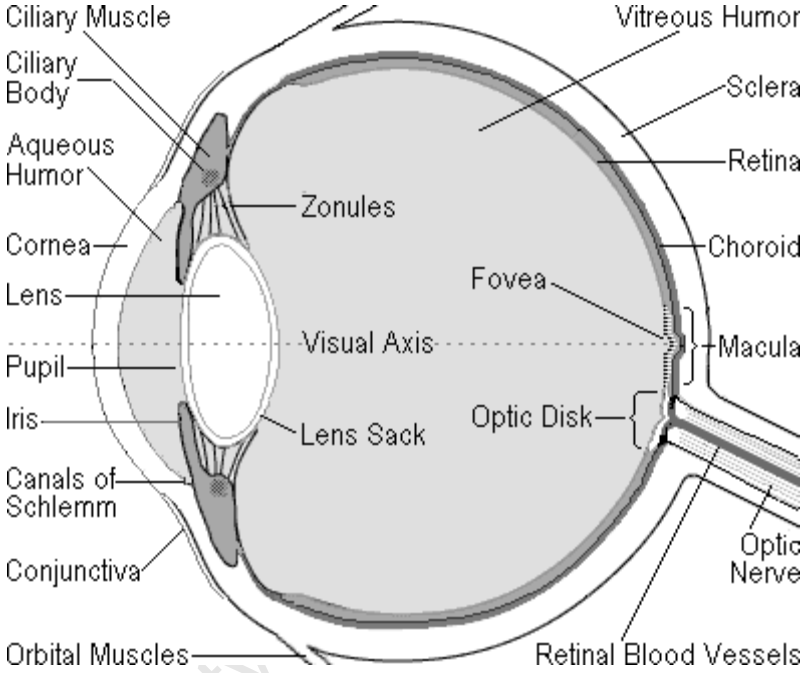

Figure 1.1: Anatomy of the vertebrate eye. Image from: http://www.99main.com/~charlief/Blindness.htm

Defining the boundary between the anterior chamber and the posterior chamber is a pigmented diaphragm known as the iris which contracts and expands to regulate the amount of light that enters the eye. The iris lies on top of the lens which, similar to the cornea, is responsible for focusing incoming light. The posterior chamber is filled with a second, transparent, gel like fluid called the vitreous humour which makes up the bulk of the eye and is primarily involved in maintaining its structure. (Snell et al. 1998)

The innermost portion of the eye consists of the retina and retinal pigmented epithelium. The rods and cones of the retina are responsible for converting light information into electrical impulses to be interpreted by the brain while the retinal pigmented epithelium absorbs excess light and prevents glare from affecting the image formed by the retina. (Snell et al. 1998)

1.2 The Cornea

The cornea is the most distal structure of the eye and provides both physical protection from the environment and allows the convergence of light on the lens to be focused on the retina. The structure and the interaction between the cornea's three distinct layers, the epithelium, stroma and endothelium (Figure 1.2) ensure that it has both transparent and refractive properties.

1.2.1 The corneal epithelium

The corneal epithelium is a stratified squamous epithelium consisting of about four to six layers in mice (Figure 1.2). The basal, cuboidal layer undergoes constant turnover throughout adulthood and in humans is responsible for renewing cells in the epithelium. These basal cells in turn are replenished by a population of stem cells in the palisades of Vogt in the corneal limbus, located at the corneoscleral border (Davanger et al. 1971; Schermer et al. 1986). Despite the state of constant change, the basal cells of the epithelium are kept in close contact through the presence of tight junctions, thus enabling the epithelium to be an effective barrier against the environment. The corneal epithelium is supported by a basement membrane known as Bowman's layer.

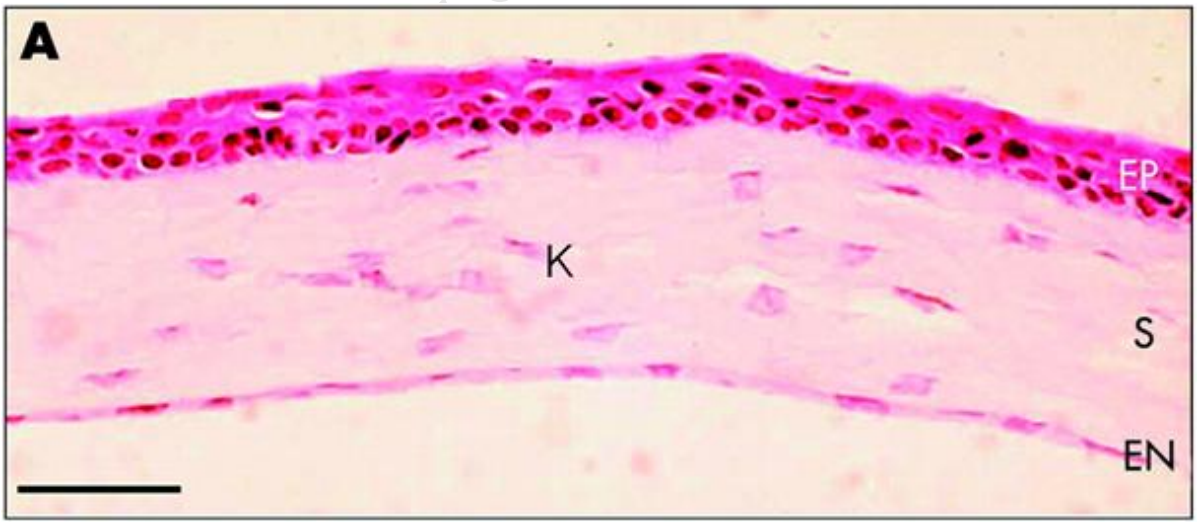

Figure 1.2: Layers of the cornea. EP - epithelium. S - stroma. EN - endothelium**.** K- keratocyte (Image from Ramalho et al. 2004)

1.2.2 The corneal stroma and endothelium

In the mouse, the normal stroma makes up 90% of the cornea (Kaufman et al. 2003 - Figure 1.2) and determines the visual and structural characteristics of the eye. The

stroma is an unusual connective tissue in that it is avascular, a characteristic necessary in order for the cornea to remain completely transparent. In humans the stroma consists of around 200 – 250 lamellae containing type I collagen fibrils running approximately parallel to the corneal surface with a matrix of proteoglycans interwoven between the individual fibres. Flattened stromal keratocytes are arranged between the lamellae (Figure 1.2) and are responsible for synthesising all of the components that make up the stroma. The stroma is maintained in the correct hydration state by the corneal endothelium.

The mouse corneal endothelium is a single layer of polygonal, mostly hexagonal, cells which rests on a basement membrane called Descemet's membrane and forms the most posterior part of the cornea (Figure 1.2). Its main function is to regulate the flow of ions and nutrients from the aqueous humour into the corneal stroma. It is critical that, concurrent to supplying the stroma with nutrients and removing waste, the osmotic potential of the stroma remains constant. Tight junctions, present on the apical surface of the corneal endothelium, help to create a barrier that allows for the hydration of the stroma to be tightly regulated (Hirsch et al. 1977; Kidson et al. 1999; McLaughlin et al. 1985; Stiemke et al. 1991). Adherens junctions strengthen cell-to-cell attachment in the corneal endothelium and so assist in maintaining the corneal endothelium's integrity (Beebe et al. 2000; Reneker et al. 2000; Joyce 2003). Both types of cell junctions are discussed in more detail in section 1.4.

The corneal endothelium uses the 'pump–leak' mechanism to regulate the passage of fluid into and out of the stroma (for a recent review see Srinivas 2011). Aqueous humour passively 'leaks' into the stroma through paracellular gaps and binds to the hydrophilic stromal proteoglycans. If there were no counter movement the stroma would become overly hydrated which would lead to corneal swelling and opacity. Therefore, this flow of water must be counteracted. The excess fluid is thus removed by Na^+/K^+- and Mg^{2+}-ATPases that are present in the corneal endothelium (Iwamoto et al. 1965; Hirsch et al. 1977) and 'pump' Na^+, K^+, and Mg^{2+} ions from the stroma into the aqueous humour in an ATP-driven process. This creates an osmotic gradient and the excess water that is in the stroma will then flow back into the aqueous humour to

balance this gradient. By controlling the number of ions pumped out of the stroma, the corneal endothelium can control the osmotic gradient between the stroma and aqueous humour. Thereby, the hydration state is maintained for optimal visual clarity.

The adult corneal endothelium does not have the capacity to regenerate like its epithelial counterpart (for further details see section 1.5). When there is a decrease in the number of cells in the corneal endothelium due to injury or ageing the remaining cells increase in size, filling gaps that may have formed and thus ensuring that a single, continuous layer connected by tight junctions is maintained (Murphy et al. 1984; Capella 1972; Van Horn et al. 1977; Fitch et al. 1986; Jun et al. 2006). When excessive damage occurs, the cells cannot expand enough to fill the void. This results in a discontinuous corneal endothelium without tight junction contact between every cell and this leads to a loss in barrier integrity. The hydration state of the stroma can no longer be regulated and fluid will flow through the gap in the corneal endothelium uncontrollably and without being removed by the 'pump-leak' mechanism. This results in the swelling of the stroma that interferes with the uniform arrangement of the lamellae, causing light to be scattered within the stroma which leads to corneal opacity.

1.3 Vertebrate Eye Development

The vertebrate eye is derived from three distinct embryonic tissues, the neuroectoderm of the diencephalon (a part of the forebrain), the overlying surface ectoderm, and the neural crest-derived mesenchyme (Noden 1983). The first sign of eye development in mammals is the appearance of the optic pits, which in mice appear at embryonic day 8.5 (E8.5) and are initiated by the bilateral outgrowth of the forebrain on either side of the presumptive head (Pei et al. 1970). By E9.0 the optic pits begin to deepen and enlarge to form the optic vesicles which continue to grow and extend by pushing through the surrounding mesenchyme until they make contact with the surface ectoderm at E9.5 (Pei et al. 1970 and Figure 1.3.a). Contact leads to a reciprocal induction between the surface ectoderm and the optic vesicle (reviewed by Martinez-Morales et al. 2009). This causes the thickening and eventual invagination of the optic vesicle to form a double-layered optic cup which connects to the forebrain by the

narrow optic stalk (Figure 1.3.b). The inner layer of the optic cup will form the neural retina, while the outer layer will form the retinal pigment epithelium (Figure 1.3.c).

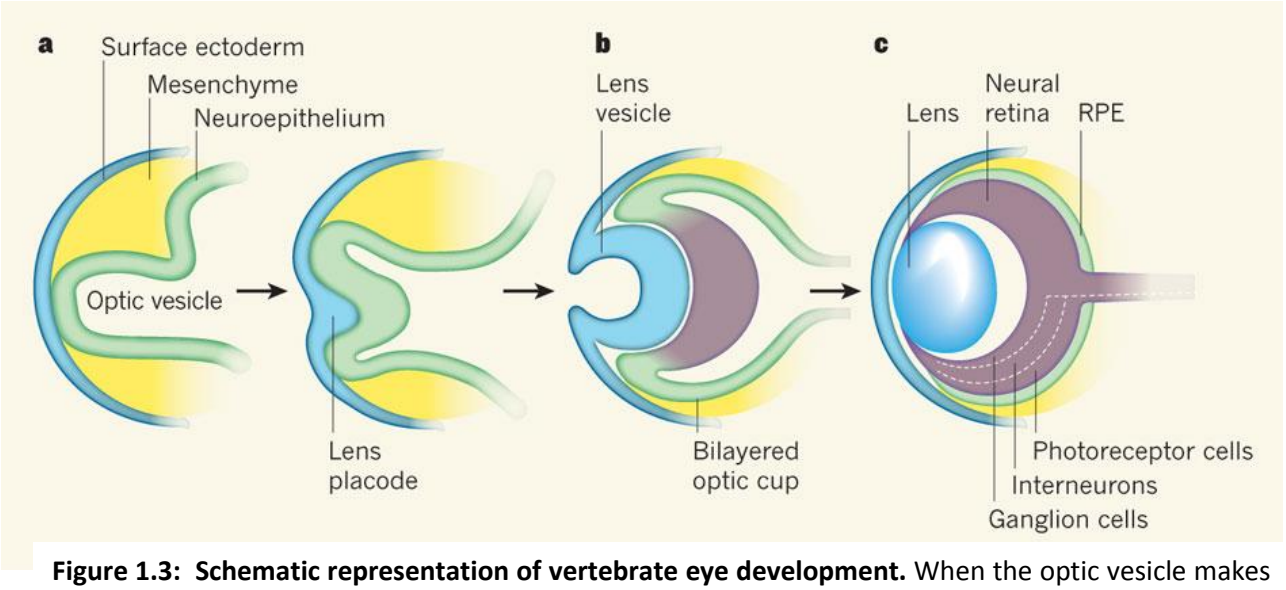

Figure 1.3: Schematic representation of vertebrate eye development. When the optic vesicle makes contact with the surface ectoderm reciprocal induction occurs. This leads to the thickening and invagination of both layers. The optic vesicle goes on to form the optic cup consisting of the neural retina and RPE (retinal pigment epithelium). The surface ectoderm forms the lens.
Image from :http://www.nature.com/nature/journal/v472/n7341/fig_tab/472042a_F1.html

At the same time as the optic cup is being formed, the surface ectoderm, which was in contact with the optic vesicle, thickens and invaginates itself to form the lens placode (Figure 1.3.a). As the optic cup begins to deepen so too is the lens drawn inwards to form a lens vesicle which separates from the surface ectoderm at E11.0 (Pei et al. 1970 and Figure 1.4.A). The cells of the posterior half of the lens vesicle are subject to signalling from the neural retina that causes them to stop dividing, elongate and differentiate into the primary lens fiber cells (reviewed by Piatigorsky 1981 and Figure 1.4.B). These fiber cells continue to elongate until they fill up the entire lumen of the lens vesicle (Figure 1.4.C). They produce the lens-specific group of proteins, the crystallins, and keep producing them until they fill up the cytoplasm of every cell. Simultaneously, the cells lose all of their organelles including the nucleus. The loss of all the organelles and expression of crystallin proteins is critical for the lens to be transparent and have the appropriate refractive index necessary to focus incoming light (reviewed by Lovicu et al. 2004). The anterior cells of the lens vesicle constitute the lens epithelium, a simple cuboidal epithelium that keeps dividing throughout development and adulthood. The cuboidal cells in the equatorial region of the lens vesicle lengthen

to surround the primary fiber cells and so form the secondary fibers (Figure 1.4.D). As the cells of the lens epithelium continue to divide more cells are pushed inwards from the equator of the lens vesicle to form additional secondary fiber cells (Figure 1.4.E). This increases the size of the lens (reviewed by Gilbert 2000; Chow et al. 2001).

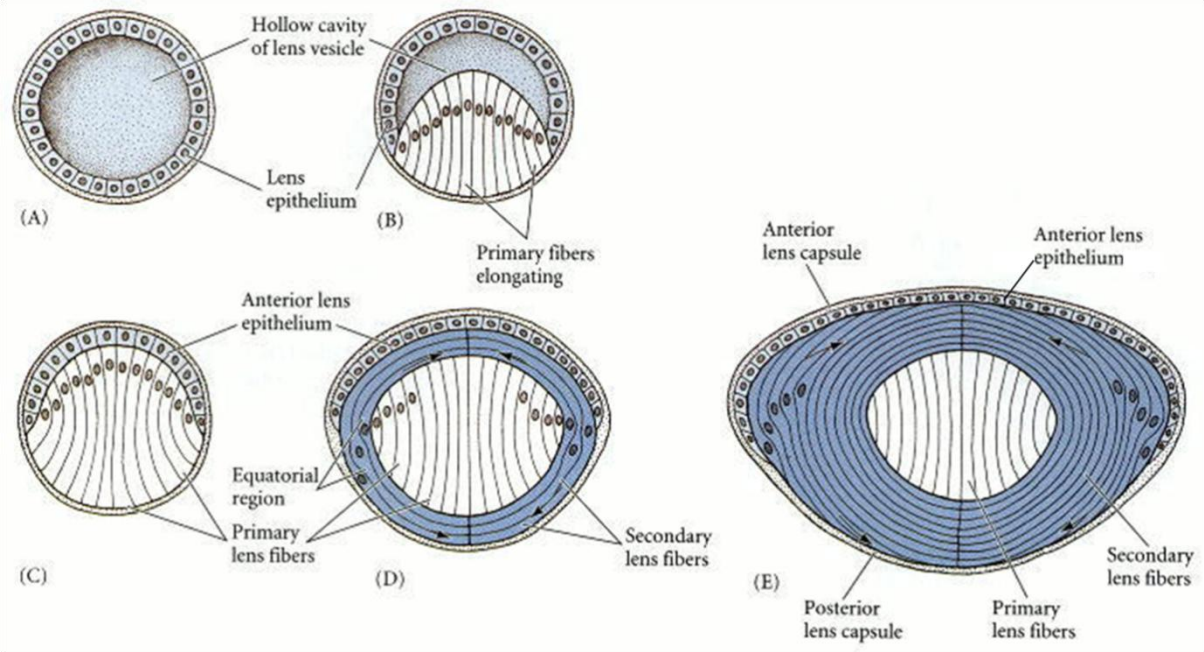

Figure 1.4: Schematic representation of vertebrate lens development. The posterior cells of the lens vesicle elongate to fill up the lens cavity with the primary fibre cells. The anterior cells form the anterior lens epithelium. The equatorial cells divide and elongate to form the secondary fibre cells. (Image adapted from Gilbert 2000)

1.3.1 Corneal development

The cornea develops from both the surface ectoderm overlying the lens and from migrating, neural crest–derived mesenchyme in a complex process with many stages (Hay 1986). The surface ectoderm gives rise to the corneal epithelium that secretes the collagen and proteoglycans that will form the stromal matrix (Hay et al. 1979). This allows a space to form between the lens and the developing epithelium which facilitates an invasion of periocular mesenchyme that forms the corneal endothelium and cells of the corneal stroma (Sevel et al. 1988).

Without any evidence to prove otherwise, it was believed that the periocular mesenchyme was derived solely from the ocular mesoderm (Noden, 1988). However, a definitive study using quail-chick chimeras revealed that the periocular mesenchyme consists of both cells from the cranial mesoderm as well as a subpopulation of neural

crest cells that migrate along the optic vesicle into the presumptive anterior segment region (Le Lièvre et al. 1975). In a later study [^{3}H]-thymidine labelled chick neural crest or mesoderm cells were transplanted into unlabelled chick hosts (Johnston et al. 1979) allowing the fate of either cell population to be visualised. The results from these experiments confirmed that the periocular mesenchyme consisted of cells derived from both the mesoderm and the neural crest (Johnston et al. 1979). It was also shown that the corneal endothelium in chicks is comprised of cells derived solely from the neural crest (Johnston et al. 1979).

The work of these early pioneers has recently been revisited in a study which repeated the exact same transplantations done by Le Lièvre et al. (1975) but identified the quail neural crest cells by immunodection for quail specific markers (Creuzet et al. 2005). Both quail neural crest and chick mesoderm cells contributed to the periocular mesenchyme and the corneal endothelium was derived solely from quail neural crest cells (Creuzet et al. 2005). The results of this study were thus consistent with the earlier reports.

The study of the mammalian cornea and its precursors has been more difficult. However, Gage et al. (2005) recently made use of double transgenic system that allowed for the permanent labelling of early neural crest cells as well as all of their progeny (a system intially developed by Danielian et al. 1998). There are two components to this system. The first is a Cre recombinase transgene under the control of a neural crest specific promoter (*Wnt*). The second is the R26R reporter allele construct which controls the expression of β-galactosidase. The expression of Cre, driven by the *Wnt* promoter, results in activation of β-galactosidase from the reporter allele which permanently labels the neural crest cells and all cells derived from them (Danielian et al. 1998). This system was repeated using an ocular mesoderm specific promoter (*αGSU*) to activate the Cre recombinase (Gage et al. 2005). The first fate maps of both the neural crest and mesoderm derivatives in the mammalian eye were thus derived. The main findings from the study were that at E11.5, the vast majority of cells in the periocular region were of a neural crest origin and by E14.5, both the

stroma and the corneal endothelium consisted almost entirely of the periocular mesenchyme cells originally derived from the neural crest (Gage et al. 2005).

In chicks every single cell in the corneal endothelium is derived from the neural crest (Le Lièvre et al. 1975; Johnston et al. 1979; Creuzet et al. 2005) whereas in mice corneal endothelial cells are derived from both the ocular mesoderm and neural crest (Gage et al. 2005). Thus, despite the highly conserved nature of the fate of neural crest and mesoderm cells in the eyes of chicks and mice, their development is not identical. The reason for this key difference in the developing eye is, as-of-yet, unknown. Variations in the neural crest development of chicks and mice have been hypothesised to be due to evolutionary differences in craniofacial development (Kulesa et al. 2004). The function of neural crest cells in human craniofacial development has yet to be uncovered.

Another difference in the development of the corneal endothelium in birds compared to mammals is in the migration of their precursor cells. In mice the invasion of the periocular mesenchyme into the space between the lens and epithelium occurs in a single wave at E11.5, with the cells most proximal to the lens giving rise to the corneal endothelium (Kidson et al. 1999). In chicks however, two waves occur, the first of which develops into the corneal endothelium and a second, later wave, which gives rise to the keratocytes of the stroma (Hay 1986). In both cases the cells most proximal to the lens undergo a mesenchymal-to-epithelial transition (MET) to form the corneal endothelium. While the cells involved and the overall process has been well investigated as discussed above (Le Lièvre et al. 1975; Johnston et al. 1979; Creuzet et al. 2005; Gage et al. 2005) the precise molecular mechanisms involved in the migration and differentiation of the periocular mesenchyme have yet to be elucidated. Research has been undertaken to identify presumptive signalling molecules responsible for the differentiation and formation of the corneal endothelium.

1.3.1.1 Signalling molecules and genes implicated in corneal endothelial development

For a cell to form part of the corneal endothelium it must first migrate into the periocular mesenchyme region and from there into the space between the lens and the surface ectoderm. As the mesenchymal cells migrate they are under the influence of

signalling from the surrounding tissue and microenvironment. These signals are responsible for inducing changes in gene expression that ultimately direct cellular differentiation into mature corneal endothelial cells.

Transforming growth factors (*TGFs*) are a group of polypeptides which have a variety of important roles in cell proliferation, differentiation, development, and adhesion (reviewed in Dünker et al. 2001). Three *β*-type *TGF*s *(*1,2 and 3) and their receptors (*TGFβRI and TGFβRII*) are found in mammals, all of which are expressed in the developing and adult eye (Joyce et al. 1997; Pelton et al. 1991). Some evidence suggests that *TGFβ*2 has a role to play in the migration of presumptive corneal endothelial cells and perhaps acts as a chemoattractant. In normal mice it is expressed in the embryonic lens from E12.5 (Saika et al. 2001). In *TGFβ*2 knockout mice the periocular mesenchymal cells do not migrate over the lens (Sanford et al. 1997; Saika et al. 2001). These mice have no corneal endothelium (Saika et al. 2001) and a stroma that is one third the size of the wildtype (Sanford et al. 1997).

Another signalling molecule of interest is *TGFα,* a member of the epidermal growth factor (EGF) superfamily. EGF and *TGFα* share the same amino acid sequence and structure of their extracellular domains and both bind the EGF receptor (EGFR) (Luetteke et al. 1990). The role of *TGFα* in ocular development has been investigated. *TGFα* null mutant mice displayed corneal scarring and inflammation due to impaired anterior segment development (Luetteke et al. 1993). It has been shown, by *in situ* hybridization, that the periocular mesenchyme cells express EGFR and have the ability to bind *TGFα* (Reneker et al. 1995). These results led researchers to believe that EGF or *TGFα* could be an important signalling molecule that controls the migration of the periocular mesenchyme. Transgenic mice that expressed either *TGFα* or *EGF* specifically in the lens under control of a crystallin promoter were thus created. The anterior segment dysgenesis in these mice was visualised using histology while the presence of the corneal endothelium was investigated by immunofluorescence using an anti-N-cadherin antibody (Reneker et al. 1995, 2000). It was found that the mutant mice had similar anterior segment dysgenesis to *TGFα* null mutant mice and had no corneal endothelium (Reneker et al. 1995, 2000). The reason for aberrant anterior segment

development in mice with *TGFα* either knocked out or over-expressed was determined to be due to the uncontrolled migration of the periocular mesenchyme cells. It has thus been hypothesised that *TGFα* is a chemoattractant of presumptive corneal endothelial cells and controls their migration over the lens. However, TGF*α* has never been found to be produced by the lens during embryonic development. The transgenic mice that ectopically over express *TGFα* in the lens epithelium are therefore not representative of normal development. While the aberrant development of *TGFα* null mutant mice and expression of EGFR in the periocular mesenchyme provide some evidence for the involvement of *TGFα* in anterior segment development, further work is still required to understand its precise role.

A considerable body of work has sought to uncover what gene expression changes are induced by the transition from periocular mesenchyme cells to corneal endothelial cells during development. Paired-like homeodomain transcription factor 2 (*Pitx2*) has been identified as a homeobox gene critical to development as homozygous mutants result in prenatal lethality (Lin et al. 1999). Various studies have provided strong evidence that *Pitx2* has a role in anterior segment development. Firstly, mutations in *PITX2* in humans are responsible for Axenfeld-Rieger syndrome that results in various anterior segment malformations including a small cornea (Tümer et al. 2009). Secondly, *Pitx2* is expressed in the mouse periocular mesenchyme at E10.5 (Semina et al. 1996) as well as in the developing corneal stroma and corneal endothelium at E14.5 (Kitamura et al. 1999). Thirdly, *Pitx2* knockout mice exhibit a host of developmental failures including a lack of extraocular muscle, a 5 to 10 fold corneal thickening and a disorganised corneal endothelium (Kitamura et al. 1999; Gage et al. 1999). The reason for the dysgenesis in *Pitx2*$^{-/-}$ mice has been determined to be due to an uncontrolled migration of periocular mesenchymal cells which invade the entire anterior segment (Gage et al. 1999; Kitamura et al. 1999). From this body of work it can be concluded that the expression of *Pitx2* is required for the controlled migration of the presumptive corneal endothelium.

Similar anterior segment dysgenesis has also been noted in LIM homeobox transcription factor 1-beta (*Lmx1b*) knockout mice. *Lmx1b* is highly expressed in the

periocular mesenchyme from as early as E10.5 and is maintained in the postnatal corneal endothelium (Pressman et al. 2000). *Lmx1b*$^{-/-}$ mutant mice lack ciliary bodies, have a reduced anterior chamber depth and have dysfunctional corneal stromal keratocytes and corneal endothelium (Pressman et al. 2000). In the mutant, the keratocytes do not secrete the proteoglycans and collagen necessary to maintain stromal transparency. It is hypothesised that undefined structural defects in the corneal endothelium result in the reduced anterior chamber depth (Pressman et al. 2000). It has been noted that while *Lmx1b* and *Pitx2* have highly similar expression patterns they function independently of one another since *Lmx1b* mutants have normal *Pitx2* expression patterns and *vice versa* (Lu et al. 1999; Pressman et al. 2000).

The transcription factor Forkhead box C1 (*Foxc1* - formally *Mf1*) belongs to the forkhead/winged helix-like family of transcription factors characterised by a specific DNA binding forkhead domain (Clark et al. 1993) and is expressed in the neural crest-derived periocular mesenchyme (Kume et al. 1998). Several lines of compelling evidence exist to suggest an important role for *Foxc1* in anterior segment development. Firstly, in humans, mutations in *FOXC1*, similarly to those in *PITX2*, are associated with Axenfeld-Rieger syndrome and are also linked to congenital glaucoma (Lehmann et al. 2000; Nishimura et al. 2001; Panicker et al. 2002). Secondly, *Foxc1*$^{-/-}$ mice die at birth and present with a variety of ocular abnormalities. They have open eyelids, no anterior chamber and the lens is attached to the cornea (Kidson et al. 1999). The cornea itself is severely affected with a thickened epithelium, disorganised stroma and no corneal endothelium. Furthermore, ultrastructural studies have shown that differentiation of the mesenchymal cells is disrupted in *Foxc1* knockout mice (Kidson et al. 1999). Thirdly, *Foxc1* is first expressed at E11.5 in the periocular mesenchyme and in the migrating mesenchymal cells at E12.5 (Kidson et al. 1999). At 13.5 no *Foxc1* is present in the differentiating corneal endothelium (Kidson et al. 1999). In normal development the periocular mesenchyme cells that migrate over the lens at E12.5 differentiate into corneal endothelial cells at E13.5. Thus, the timing of the expression of *Foxc1* is a clear indication of its critical importance in the development of the corneal endothelium.

Foxc1, Pitx2 and *Lmx1b* have overlapping expression patterns during ocular development and null mutants of all three have similar anterior segment dysgenesis. Research has thus been undertaken to elucidate the relationship between these three transcription factors. It was shown that in *Lmx1b* null mutants, normal *Foxc1* expression is disrupted in the corneal mesenchyme which fails to differentiate into endothelium (Pressman et al. 2000). Conversely, *Lmx1b* expression was unaffected in *Foxc1* mutants (Kidson et al. 1999) suggesting that *Lmx1b* regulates *Foxc1* expression. As mentioned above, mutations in *FOXC1* or *PITX2*, are both associated with Axenfeld-Rieger syndrome and congenital glaucoma (Lehmann et al. 2000; Nishimura et al. 2001; Panicker et al. 2002). The link between *Foxc1* and *Pitx2* has recently been further elucidated with a study that used immunoprecipitation experiments to show that *Pitx2* can bind and inactivate *Foxc1* and its putative targets (Berry et al. 2006). These independent researchers have therefore shown that both *Lmx1b* and *Pitx2*, while having no effect on each others' expression (Lu et al. 1999; Pressman et al. 2000), are negative regulators of *Foxc1*.

While *Foxc1* has a crucial role to play in the differentiation of the anterior segment very few of its downstream targets in the ocular region have been identified. There is thus very little information linking the *Foxc1*$^{-/-}$ genotype to its anterior segment phenotype. Transforming growth factor beta 1 induced transcript 4 (*Tgfβ1i4)* has been described as a downstream target of *Foxc1* (Sommer et al. 2006). In *Foxc1*$^{-/-}$ mice *Tgfβ1i4* is up-regulated in the E13.5 periocular mesenchyme when compared to the wildtype (Sommer et al. 2006). *In situ* hybridization has shown that *Tgfβ1i4* is expressed at low levels in the periocular mesenchyme and developing corneal endothelium at E12.5 with expression steadily increasing in intensity all the way through embryonic development (Thut et al. 2001).

Taken together, the above body of work strongly suggests that *Foxc1* is an important gene regulator involved in the differentiation of periocular mesenchyme into corneal endothelium.

1.3.1.2 The role of lenticular signalling in corneal endothelial development

Much research has focused on finding the key organisers in the development of the eye. In particular, the role of the lens in the both the migration and differentiation of the presumptive corneal endothelium from its mesenchymal precursor population has been the subject of numerous studies.

Early induction experiments in the chick attempted to identify the effect of the lens on the morphogenesis of the eye. To do this, the lens was either rotated within the eye or removed entirely, incubated for 1-7 days and then examined histologically (Genis-Galvez 1966; Genis-Galvez et al. 1967). Under these conditions the entire cornea degenerated and become disorganised (Genis-Galvez 1966; Genis-Galvez et al. 1967). More recently, a similar but more comprehensive study further investigated the role of lenticular signalling in the formation of the chick corneal endothelium (Beebe et al. 2000). In this study, histological analyses were used to investigate the morphology of the anterior segment after a variety of different surgical procedures were performed on the embryonic chick eye. Immunocytochemistry for the presence of N-cadherin was used as a marker for corneal endothelium. It was found that the complete ablation or replacement of the lens with a cellulose bead led to uncontrolled migration of periocular mesenchyme cells that filled the space below the corneal epithelium without a discernible anterior chamber (Beebe et al. 2000). In cases where the lens was replaced immediately after it was removed, a normal corneal endothelium and anterior chamber formed 2 -3 days after surgery. When the removed lens was rotated before it was replaced, only the periocular mesenchyme cells directly adjacent to the lens epithelium differentiated into corneal endothelium. Furthermore, if just the lens epithelial cells were replaced after the lens was ablated the adjacent mesenchymal cells differentiated into corneal endothelium. Conversely, when just the lens fibres were transplanted no differentiation was observed.

Additional evidence for the role of the lens in corneal endothelial differentiation comes from a study using mice. In wildtype mice, the corneal endothelium is easily identifiable by E15.5 as a prominent single layer of cells that has moved away from the lens to form the anterior chamber. Zhang et al. (2007) generated transgenic mice that specifically

expressed diphtheria toxin subunit A under control of a crystallin promoter. The diphtheria toxin is thus expressed solely in the lens epithelium resulting in its ablation. The effect this had on the anterior segment and, in particular, the corneal endothelium, was then analysed by histology and immunohistochemistry. Severe alterations in the architecture of the cornea were noted by E13.5 and were more prominent by E15.5. At E15.5 the transgenic mice with an ablated lens epithelium had a highly disorganised corneal stroma with an accumulation of periocular mesenchymal cells filling up the space beneath the corneal epithelium but with no definitive anterior chamber. In addition, it was found that the mesenchymal cells closest to the mutant lens had adherens junctions but not tight junctions. This suggests that the migrated mesenchymal cells had initiated corneal endothelial differentiation (i.e. expressed N-cadherin) but the transition to a fully differentiated corneal endothelium could not be completed without the presence of the lens epithelium. This study therefore provides strong evidence for the role of the lens epithelium in the differentiation of the corneal endothelium and the formation of the anterior chamber.

It is important to note that different researchers have used the presence of adherens junctions as a marker of both the fully differentiated corneal endothelium (Reneker et al. 2000; Beebe et al. 2000) and corneal endothelial precursors (Zhang et al. 2007). However, since adherens junctions are expressed in both adult corneal endothelial cells as well as their precursors they are insufficient as evidence or as a marker for the fully differentiated adult corneal endothelium. This underlines how the lack of a definitive marker for corneal endothelial cells can result in misleading conclusions. It would be far more stringent to look for the expression of both adherens and tight junctions as markers for the adult corneal endothelium as tight junctions have only ever been found in the adult corneal endothelium.

The effect that the lens has on the ingression of the periocular mesenchyme cells has also been investigated. *TGFβ*2, which, as mentioned earlier, has been implicated as a signalling molecule that plays a role in mesenchymal migration and is expressed specifically by the embryonic lens epithelium (Saika et al. 2001). This study gave the first indication that lens derived signals control the ingression of the presumptive

corneal endothelium. With this in mind, additional factors produced by the lens that could control periocular mesenchyme migration are of much interest. Sema3A is a chemorepellent that binds to the Npn-1 receptor and is a well characterised signalling molecule involved in axon guidance (reviewed by Goshima et al. 2000). Sema3A/Npn-1 signalling has been shown to mediate chick neural crest migration in the hindbrain (Osborne et al. 2005; McLennan et al. 2007). Its effect on chick neural crest cells during eye development has recently been investigated (Lwigale et al. 2009). By using the quail-chick chimera system pioneered in the 1970s (Le Lièvre et al. 1975; Johnston et al. 1979) Lwigale et al. transplanted quail neural crest cells into a chick host and tracked their differentiation in the anterior segment using immunofluorescence and *in situ* hybridization (Lwigale et al. 2009). It was discovered that Npn-1 expressing periocular mesenchyme cells are inhibited from migrating by Sema3A secreted by the lens vesicle (Lwigale et al. 2009). A subset of neural crest derived periocular mesenchyme cells later down-regulated their expression of Npn-1, were thus unresponsive to the inhibitory Sema3A signal, and were able to migrate over the lens and form the corneal endothelium starting at E5 (equivalent to between mouse stages E13-E13.5) (Lwigale et al. 2009). These results provide strong evidence that Sema3A/Npn-1 signalling coordinates neural crest migration in the anterior segment.

Taken together, the above body of work provides several lines of evidence supporting the role of the lens as the key organiser in the development of the anterior segment and, in particular, the corneal endothelium.

1.4 Cell Junctions in the Corneal Endothelium

A defining structural characteristic of the fully mature and functional corneal endothelium is the expression of junctions in the cell membranes. The adult corneal endothelium expresses both adherens junctions to aid cell adhesion and tight junctions to aid in the formation of a barrier.

1.4.1 Adherens junctions

Adherens junctions are required for the adhesion of adjacent cells and are present in many epithelial and non-epithelial tissues. They connect individual cells through the trans-membrane cadherin family of proteins. Cadherins appear as dimers in the cell membrane and are anchored to the actin cytoskeleton of the cell through the catenin group of proteins (Figure 1.5). The three most common cadherins are E-, N- and P-cadherin, so named due to their initial identification in epithelia, neural crest cells and placenta respectively.

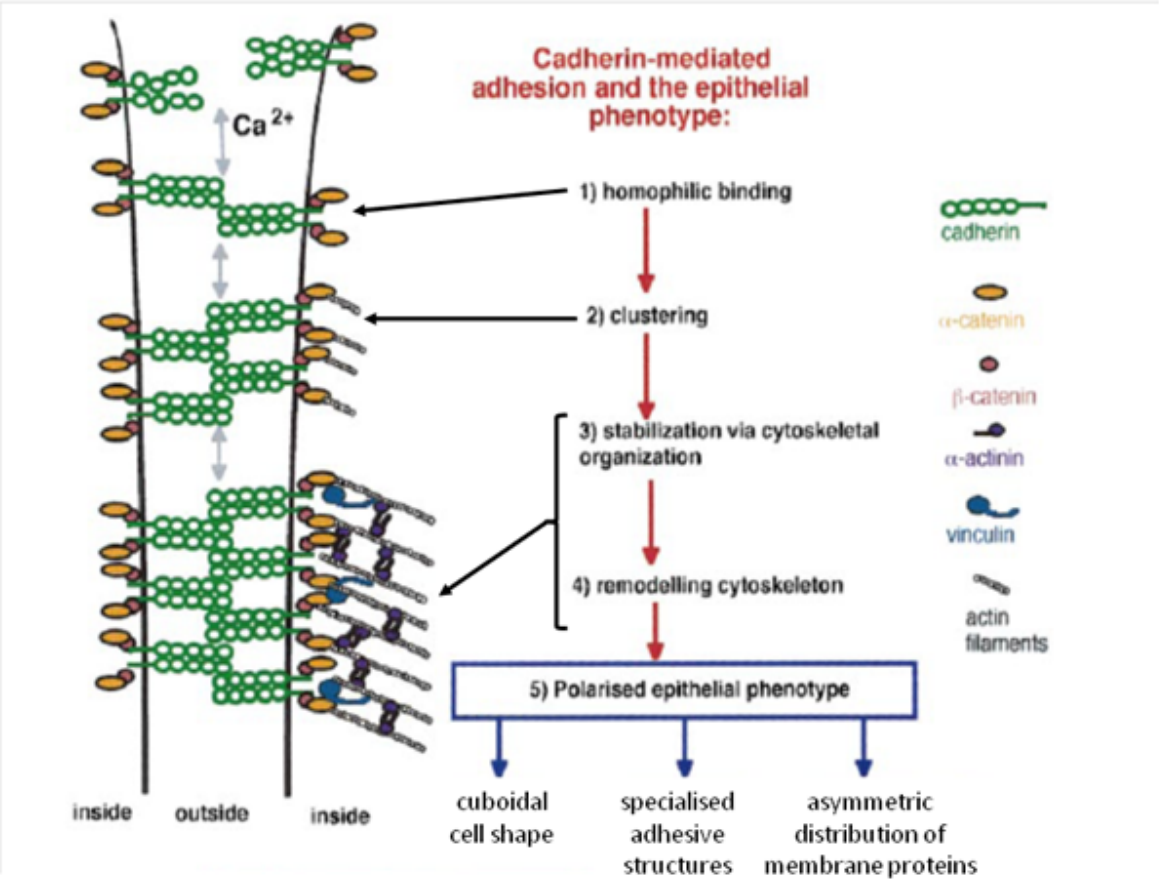

Figure 1.5: Schematic representation of adherens junction mediated formation of a polarised epithelial cell sheet. In the presence of calcium cadherin molecules bind to form dimers and then cluster. This forces a reorganization of the cytoskeleton which drives various phenotypic changes that result in the formation of a polarised epithelial cell sheet. (Image adapted from Braga 2000)

The formation of adherens junctions is a complex multistep process (reviewed in detail by Braga 2000 - see figure 1.5). Briefly, the extracellular domains of the cadherin proteins in adjacent cells form homophilic bonds in a calcium dependent process (Figure 1.5 - step 1). Upon binding, cadherin molecules cluster at the points of cellular

contact (Figure 1.5 – step 2). This results in the remodelling of the internal cytoskeleton through the catenin proteins (Figure 1.5 - steps 3 and 4). The cytoskeletal rearrangements drive a change in cell morphology, the development of specialised adhesive structures, and an asymmetric redistribution of proteins in the cell membrane (Figure 1.5 – step 5). These changes lead to the formation of a polarised epithelial cell sheet. The cytoskeletal arrangements are regulated by the Rho protein superfamily of small GTPases (for a review see Braga 2002). Three members of the Rho GTPase family, Rho, Rac, and Cdc42 have been described as mediating different processes during the formation of the polarised epithelial cell sheet. Rho regulates stress fibre formation and contraction, while Rac and Cdc42 are involved in recruiting actin to the cell membrane.

Adherens junctions have been shown to be critical to development as E-, N- and P-cadherin null mutants (all incapable of forming adherens junctions) are all embryonically lethal (Larue et al. 1994; Radice, Rayburn, et al. 1997; Radice, Ferreira-Cornwell, et al. 1997). Furthermore, the dynamics of the formation of adherens junctions in the developing neural crest population of cells has been elucidated. Chick embryos at various developmental stages were sectioned and stained with anti-N-cadherin antibodies to identify the presence of adherens junctions (Akitaya et al. 1992). It was discovered that adherens junctions only formed in neural crest cells at the completion of migration (Akitaya et al. 1992). The formation of adherens junction in the migrating neural crest has also been investigated *in vitro* using quail neural tube explants placed in an artificial extracellular matrix (Monier-Gavelle et al. 1995). In this study N-cadherin was principally localised in cytoplasmic vesicles for the duration of neural crest migration and only ever occurred in the cell membrane upon cell-to-cell-contact (Monier-Gavelle et al. 1995). Similarly to what was witnessed *in vivo*, stable expression of N-cadherin along the cell membranes was only present once the cells had completed their migration (Monier-Gavelle et al. 1995). The results achieved in the above two studies necessitated a closer investigation of the formation of adherens junctions in the neural crest derived periocular mesenchyme. Adherens junctions start to form during periocular mesenchyme migration and are present in early corneal endothelial progenitors (Beebe et al. 2000; Joyce 2003). Stable adherens junctions are

only present in the fully differentiated adult endothelium (Beebe et al. 2000; Joyce 2003; Zhang et al. 2007).

1.4.2 Tight Junctions

Tight junctions are the most apical junction in the junctional complex and are present in numerous epithelia. Their primary function is to create a barrier which allows for the regulation of solutes, ions and fluids between cells (Hirsch et al. 1977). Tight junctions also define the polarity of the cell as they prevent diffusion between the integral proteins on the apical and basal surfaces of the cell (Hirsch et al. 1977). Tight junctions can either form a very tight or a leaky barrier depending on the function of the epithelial layer (reviewed by Braga 2002). Very tight barriers, with tight junctions expressed all the way around each cell, are present in the distal convoluted tubule and collecting duct of the kidney where a high ionic gradient must be maintained across the membrane. Leaky epithelia, with fewer tight junctions and incomplete circumferential expression in the cells, are present where only a low ionic gradient must be maintained, such as the gall bladder, kidney proximal tubule and corneal endothelium.

Tight junctions consist of two main types of transmembrane proteins; the occludins and claudins. Both claudins and occludins have two extracellular domains that form a branching network of strands that bind directly to the strands of the adjacent cell and create a seal between them (Figure 1.6). The number and distribution of the extracellular strands define how permeable a barrier the tight junctions will form (reviewed by Balda et al. 2008). The occludins and claudins are connected to the actin cytoskeleton of the cell through a cytoplasmic plaque consisting of a dense meshwork of proteins, principle of which are the zona occludens ZO-1, -2 and -3 (Figure 1.6). Another transmembrane protein, the junctional adhesion molecule (JAM) is associated with tight junctions but is not involved in forming the claudin and occludin strands (Figure 1.6). The exact function of JAMs is currently unknown but they are hypothesised to be involved in strengthening cellular adhesion (reviewd by Niessen 2007).

The molecular mechanisms that control the formation of tight junctions have been the subject of much investigation. Many investigators make use of the Madin-Darby canine kidney (MDCK) cell line, which expresses tight junctions in an unbroken band around each cell, to study tight junction formation *in vitro*. When MDCK cells are treated with thapsigargin, a chelating agent that depletes endoplasmic reticulum (ER) calcium, tight junctions do not form (Stuart et al. 1996). In these calcium depleted cells ZO-1 is unable to translocate from the cytoplasm to the cell membrane and the MDCK cells do not form a tight barrier as evidenced by low transepithelial electrical resistance (TEER) measurements (Stuart et al. 1996). Thus, the formation of tight junctions is dependent on the presence of calcium. Much research has also sought to uncover the role of Rho GTPases in the *in vitro* formation of tight junctions. Numerous studies have shown that when Rho, Rac, or Cdc42 expression is repressed in MDCK cells, tight junction assembly is inhibited (Nusrat et al. 1995; Takaishi et al. 1997; Jou et al. 1998; Wójciak-Stothard et al. 2001; Bruewer et al. 2004). When taken together these reports have all indicated that the various members of the Rho GTPase family need to be expressed in a fine temporal balance for tight junctions to successfully form.

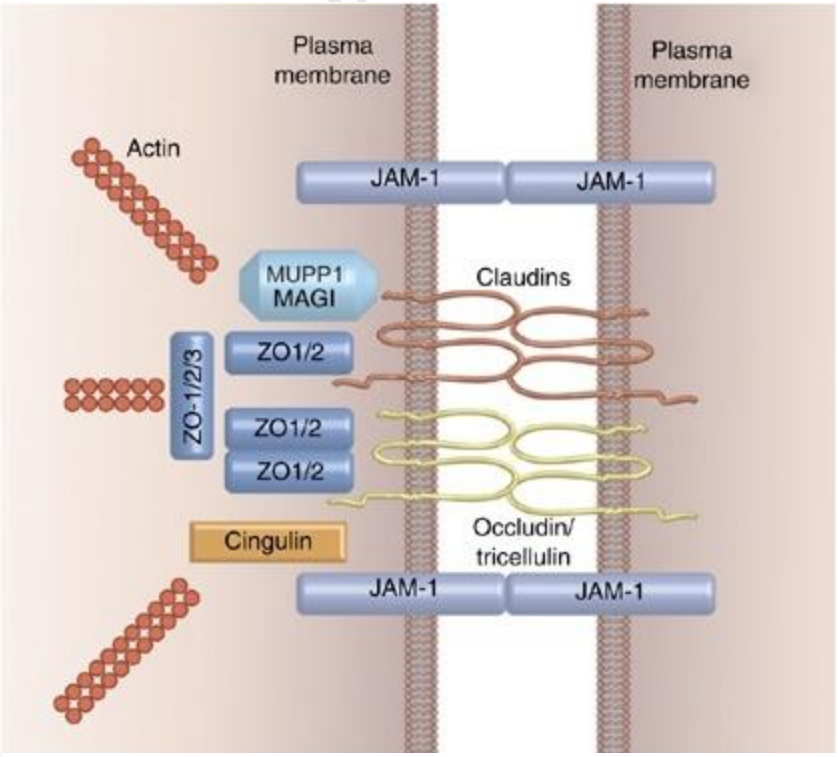

Figure 1.6: Schematic representation of the structure of a tight junction. (Image from Niessen 2007)

The link between tight and adherens junctions (besides the fact that both require calcium and the Rho GTPase family of proteins for their formation) has been the subject of numerous reports. Temporally, adherens junctions form intercellular contacts before tight junctions are expressed. This has led many researchers to hypothesise that adherens junctions trigger the formation of tight junctions (reviewed by Steed et al. 2010). In E-cadherin$^{-/-}$ mice (which cannot form adherens junction) tight junctions formation was inhibited as evidenced by the lack ZO-1 expression (Ohsugi et al. 1997). Similarly, when MDCK cells are treated with anti-E-cadherin antibodies which stop the formation of adherens junctions the assembly of tight junctions is blocked (Behrens et al. 1985; Balda et al. 1994). Conversely, when the expression of both ZO-1 and ZO-2 is suppressed by RNA interference the formation of tight junctions is blocked while adherens junctions form normally (Umeda et al. 2006). This indicates that while adherens junctions are critical for the formation of tight junctions, the opposite is not true.

The link between adherens junctions and tight junctions in the vascular endothelium has recently been studied (Taddei et al. 2008). It was found that the clustering of vascular E-cadherin (an early step in the formation of adherens junctions) activates the expression of phosphoinositide 3-kinase which then inhibits *Foxo1* by phosphorylating it (Taddei et al. 2008). *Foxo1* is normally bound to the promoter of claudin-5. When phosphorylated it is no longer able to bind and claudin-5 can be transcribed (Taddei et al. 2008). The up-regulation of claudin-5 transcription is the first step in the formation of tight junctions in the vascular endothelium. Thus, there is a direct, cell specific, mechanism by which adherens junction formation controls tight junction formation (Taddei et al. 2008).

In the corneal endothelium tight junctions are expressed in a discontinuous band around the apical surface (Petroll et al. 1999). This allows the aqueous humour to leak into the stroma through the gaps between the cells which sets the 'pump-leak' mechanism in motion. While the importance of tight junctions to the function of numerous epithelia is well documented, many of the molecular details about their formation remain unknown. In particular, the precise signalling mechanisms

responsible for tight junction assembly as well as the molecular signals involved in the cross-talk between the tight and adherens junctions have yet to be uncovered.

1.5 *In Vitro* Models of Corneal Endothelial Development

As mentioned earlier, penetrating or endothelial keratoplasty is the most common treatment for those suffering from corneal endothelial dysfunction (Price et al. 2010). However, worldwide there are insufficient donors to treat all patients and, furthermore, the success of these grafts is dependent on the age of the donor cornea as the cell density of the corneal endothelium falls rapidly as donor age increases (Laing et al. 1976; Bourne 2003, 2010; Price et al. 2010; Schwartzkopff et al. 2010).

The fact that donor grafts are so dependent on the age of the donor has meant that the proliferative potential of adult corneal endothelial cells has been the focus of much study. Numerous reports have investigated methods to culture corneal endothelium. Using electron microscopy and histological analyses it was revealed that the number of cells in the adult human corneal endothelium decreases gradually over time (Svedbergh et al. 1972; Murphy et al. 1984). The same studies also found that the individual cells of the adult corneal endothelium increase in size to fill any gaps created by cell loss in order to remain as an unbroken monolayer. Furthermore, experiments in which the rate of DNA synthesis in *in vitro* cultures of human corneal endothelial cells was measured using autoradiography showed that the cells of younger donors have a greater mitotic capacity than those of older donors (Hyldahl 1984). Primary cultures from younger as opposed to older donors were also far easier to grow (Yue et al. 1989). No matter the age, primary human corneal endothelial cultures only survive in culture for a short period, from 1-10 passages (Fabricant et al. 1981; Hyldahl 1984; Yue et al. 1989).

The lack of *in vitro* proliferation is not unique to the human corneal endothelium. When autoradiography was used to measure the DNA synthesis of monkey (Capella 1972) and cat (Van Horn et al. 1977) corneal endothelial cells *in vitro,* it was found that they had a limited capacity to proliferate and did not survive past a month in culture. Similarly,

when viewed by electron microscopy, mice showed a decrease in corneal endothelial cell density the older the donor (Fitch et al. 1986; Jun et al. 2006), consistent with the results in humans.

In contrast to the above reports, it has been repeatedly shown that the adult rabbit corneal endothelium is able to proliferate rapidly *in vitro* (Raymond et al. 1986). Further, it was found, through immunostaining of cornea sections for cell cycle associated proteins, that both human and rabbit corneal endothelium are arrested in the G1-/S-phase (Joyce et al. 1996). However, cyclin E (a cytoplasmic protein that is active during G1-/S-phase) is localised in the cytoplasm in rabbits and in the nucleus in humans (Joyce et al. 1996). Thus, because the rabbit corneal endothelium expresses active cyclin E it is able to overcome the cell cycle arrest that inhibits the proliferation of human corneal endothelium (Joyce et al. 1996). This accounts for the proliferative ability of the rabbit cornea both *in vitro* and *in vivo*. This reason for the differential expression of cyclin E in rabbits and humans has yet to be uncovered.

The inability to culture corneal endothelial cells of humans and mice continues to hamper studies on corneal endothelial development and ones that require *in vitro* cell expansion (Joo et al. 1994). This has forced researchers to investigate alternative methods to increase cell numbers in culture. One strategy has been to immortalise human adult endothelial cells with the SV40 large T-antigen to drive proliferation (Wilson et al. 1993; Aboalchamat et al. 1999; Bednarz et al. 2000). In all three studies cell lines were successfully derived and were intended to be used to investigate the function and the degeneration of the adult corneal endothelium. However, no follow up work has ever been published. In addition, studying adult cell lines does not help to develop a deeper and more accurate understanding of the formation of the corneal endothelium from its precursor population of periocular mesenchyme.

In vivo studies into the development of the corneal endothelium are exceptionally difficult in mammals as the endothelium is derived from such a small, transient population of periocular mesenchyme that is also inaccessible in the developing embryo. This is one of the reasons why so little research has been undertaken using the

periocular mesenchyme. Thus, the best way to improve our understanding of the development of the corneal endothelium would be to develop an *in vitro* model of corneal endothelial differentiation using the embryonic periocular mesenchyme.

Since the precursor population of corneal endothelial cells is so small, it was reasoned in this study that a good starting point would be to immortalise cells of the periocular mesenchyme to form stable cell lines that could be used to model corneal endothelial development. It is critical that the immortalisation procedure does not alter the gene expression or the molecular characteristics of the tissue of interest. If this were to occur one would not be able to extrapolate the *in vitro* results to the *in vivo* development. For this purpose using the established SV40 large T-antigen to immortalise the cell lines would be an effective method. The SV40 large T-antigen binds and inactivates the p53 and retinoblastoma tumour suppressors and so disrupts the G1/S and G2/M cell cycle check points (Ali et al. 2001). The disruption of these checkpoints promotes proliferation and prevents senescing thus transforming infected cells. Two previous researchers were able to immortalise cells of the E12.5 periocular mesenchyme using the large T-antigen and attempted to model corneal endothelial differentiation from them (Mgwebi 2004; Napier 2005). In both studies the immortal cell lines were successfully establish but could never be cultured in such a way as to express tight junctions. Thus, fully mature, functional corneal endothelial cells were not formed in these studies (Mgwebi 2004; Napier 2005).

1.6 Objective and Specific Aims

The broad objective of this study is to establish an *in vitro* model of mouse corneal endothelial development. This will be done by investigating methods to induce a MET in mouse periocular mesenchyme cells to drive them to form fully differentiated adult corneal endothelial cells. This will increase our understanding of anterior segment development and, in particular, the molecular cues which control the differentiation and proper formation of the corneal endothelium.

The specific aims of this study are thus:

1. To establish the immortalised cell lines needed to study the development of the corneal endothelium including;

    - E12.5 and E13.5 periocular mesenchyme cell lines to model the differentiation of the corneal endothelium *in vitro*
    - E12.5 and E13.5 lens epithelial cell lines to investigate the effect of the lens epithelium on the periocular mesenchyme
    - An adult corneal endothelial cell line to investigate the normal formation and function of the corneal endothelium.

2. To determine if immortal E12.5 and E13.5 periocular mesenchyme cell lines retain the key molecular characteristics of normal periocular mesenchyme by investigating their *Foxc1*, *Tgfβ1i4* and *Pitx2* gene expression.

3. To investigate the suitability of using immortalised E12.5 and E13.5 periocular mesenchyme cell lines to model a mesenchymal-to-epithelial transition (MET) in vitro by assessing their;

    - Morphology
    - Changes in *Foxc1*, *Tgfβ1i4* and *Pitx2* gene expression
    - Ability to form adherens and tight junctions.

4. To identify a candidate signalling molecule expressed by the embryonic lens which could affect mesenchymal differentiation and to determine its effect on the E12.5 and E13.5 periocular mesenchyme cell lines.

Chapter 2: Materials and Methods

2.1 Mice and Housing

All mice were housed in the University of Cape Town's (UCT's) Animal Unit in accordance with the ethical rules and regulations set out by the UCT Animal Ethics Committee who also approved all experimental procedures. Mice used in this study were from an inbred BALB/c genetic background and were maintained by brother-sister mating. The day that plugs were noted was considered 0.5 days post coitus (dpc) or embryonic day 0.5 (E0.5). Embryos were dissected at the appropriate developmental stages (E12.5, E13.5 and E15.5) by caesarean section.

2.1.1 Dissections and derivation of primary cultures

All dissections were done using a Wild Heerbrugg M5A microscope (Wild Heerbrugg, Switzerland) as well as tungsten needles electrolytically sharpened in a 10% sodium hydroxide (NaOH) solution at 6V, Dumont No.5 jeweler's forceps (Dumont, Switzerland) and micro-dissection scissors (Lawton, Germany). All surfaces and equipment were sterilised using 70% ethanol. Pregnant females were euthanized by cervical dissection. Embryos were excised and placed in Petri dishes on ice with 1x phosphate buffered saline (1xPBS – Appendix A.1) containing 100U/ml penicillin (Sigma-Aldrich, USA) and 100µg/ml streptomycin (Sigma-Aldrich, USA). For both embryos and the pregnant females the eyes were dissected away from the head and transferred to Petri dishes containing 1xPBS with antibiotics for extraction of specific tissues as outlined below.

2.1.1.2 Isolation of periocular mesenchyme

Primary cultures of periocular mesenchyme cells were derived from mouse embryos at both the E12.5 and E13.5 developmental stages. Small wedges of cells were then excised from the periocular mesenchyme and transferred to a 35mm tissue culture dish containing Dulbecco's Modified Eagles Medium (DMEM) (Highveld Biological, South Africa) supplemented with 10% foetal bovine serum (FBS) (Gibco, USA) and antibiotics. Four to five wedges were cultured in the same dish and allowed to expand and migrate

away from the initial explants for 48-72 hours after which they were subsequently immortalised (Section 2.2.1).

2.1.1.2 Isolation of embryonic and adult lens

Lenses from mouse embryos at E12.5, E13.5 and E15.5 developmental stages as well as those of the pregnant mothers were isolated for both culture and RNA extraction. Lenses were extracted from the eyes by tearing the anterior segment of the eye and extracting the whole lens using forceps. Any adhering tissue was removed by teasing away with either tungsten needles or forceps. The lenses to be used were then homogenised in TriPure Isolation Reagent (Roche, Germany) using siliconised corex tubes (Appendix B.4) for RNA extraction (Section 2.3). Lenses for culturing were transferred to 35mm dishes containing DMEM supplemented with 10% FBS and antibiotics for further use in a variety of different culture methods (Results - Section 3.6).

2.1.1.3 Isolation of adult corneas for culture

The corneas of the pregnant females were also isolated for culturing. Using micro-dissection scissors the entire cornea was cut off from the anterior region of the eye. Any adhering non-corneal tissue was removed using forceps. The entire cornea was then placed, endothelial side down, in 35mm dishes containing DMEM supplemented with 10% FBS and antibiotics (two corneas per dish). The corneas were divided into four quadrants by cutting them with the micro-dissection scissors. Lastly, the corneas were covered with a cover-slip to facilitate cell adhesion and migration away from the explants. After 48 – 72 hours the explants were removed.

2.1.1.4 RNA extraction from adult eyes

Additionally RNA was extracted from the entire eyes of the pregnant females. The eyes that were removed from the head of the mouse were homogenised using siliconised corex tubes. RNA was extracted in TriPure Isolation Reagent (Roche, Germany - Section 2.3).

2.2 Tissue Culture

All tissue culture was carried out in a Bio-Flow Biological Safety Cabinet Class II. Cells were incubated at 37°C, in 5% CO_2 in a Forma Scientific water-jacketed incubator (Thermo Scientific, USA) unless otherwise stated. All surfaces, microscopes, instruments, bottles, tubes, vials as well as gloves were sterilized by wiping with 70% ethanol. Cells were passaged by the addition of 1ml of 0.05% trypsin/EDTA solution (Appendix A.2) unless otherwise specified.

2.2.1 Immortalising primary cultures of periocular mesenchyme

Primary cultures of periocular mesenchyme were immortalised by infection with a retrovirus containing a temperature sensitive SV40 large T-antigen as well as a gene conferring resistance to neomycin (Jat et al. 1989). The retrovirus was obtained from the supernatant of the Ψ2 producer cell line that packages the mutant SV40. DMEM medium containing 10% FBS was added to a confluent dish of Ψ2 producer cells and grown at 33°C in 5% CO_2 for 5 hours. The supernatant was harvested and briefly centrifuged at 2000rpm. The medium was filtered through a 0.25µm filter and 8µg/ml polybrene was added before the immediate infection of primary cultures. Infected cells were incubated at 37°C in 5% CO_2 for 2 hours. Infection was repeated using fresh supernatant and following this the medium was replaced with DMEM supplemented with 10% FBS and antibiotics. Cells were kept at 37°C in 5% CO_2 overnight before being moved the next morning to 33°C in 5% CO_2. After a further 24 hours immortalised cells were selected for by the addition of 400µg/ml Geneticin (Sigma-Aldrich, USA) to the culture medium for 21 days after which time the Geneticin was removed from the culture medium. Untransformed mouse embryonic fibroblasts were used as an un-immortalised control cell line during Geneticin selection. All control cell lines died after 7-10 days of Geneticin treatment.

2.2.2 Culture of immortalised periocular mesenchyme

Once immortalised, periocular mesenchyme cell lines were grown at 33°C in 5% CO_2 in DMEM supplemented with 10% FBS and antibiotics. To inhibit their growth, serum was reduced to 2% and cell lines were incubated at 39°C in 5% CO_2.

2.2.3 Culture of Ψ2 producer cell line

Stocks of Ψ2 cells were cultured in DMEM supplemented with 5% FBS and antibiotics at 33°C in 5% CO_2 until they were required for the immortalisation procedure. At this point antibiotic free medium containing 10% FBS was used.

2.2.4 Culture of MDCK cells

MDCK cells, kindly donated by Dr Leana Maree of the Department of Medical Virology at the University of Stellenbosch, were cultured in DMEM supplemented with 10% FBS and antibiotics. When a confluent monolayer formed, cells were passaged by first treating for 10 minutes with 0.05% EDTA followed by 10 minutes in 0.05% trypsin/EDTA.

2.2.5 Culture of mouse embryonic fibroblasts and HeLa cells

Stocks of both mouse embryonic fibroblasts (MEFs) and HeLa cells were cultured in DMEM supplemented with 10% FBS and antibiotics.

2.2.6 Culture of DMEL-2 cells

Stocks of DMEL-2 cells were cultured at 33°C in 5% CO_2 in DMEM supplemented with 10% FBS and antibiotics.

2.2.7 Growth studies

Growth rates of cells were determined by calculating doubling times. A defined number of cells (5 x 10^4) were plated onto three 35 mm dishes per time point to be counted. After 1-8 days of incubation the cells were harvested using trypsin/EDTA and triturated to make a single cell suspension. For non-adherent cells all the medium on the dishes was collected and triturated to make a single cell suspension. Seven microlitres of the cell suspension was placed into a haemocytometer counting chamber and counted. Standard error of the mean was used as a statistical test of significance and is represented as the error bars seen on the bar graphs.

2.2.8 Microscopy and photography

Cultured cells were periodically visualised using either an Olympus CKX41 Microscope (Olympus, Japan) and photographed using a Canon Powershot S50 (Canon, Japan) or a Zeiss Axiovert 200M microscope and captured with a Zeiss Axiocam HR monochrome camera.

2.3 RNA Extraction

RNA extraction was undertaken by the single step phenol-chloroform method (Chomczynski et al. 1987) using TriPure Isolation Reagent (Roche, Germany) according to manufacturer's instructions (Appendix B.3). Total RNA was extracted in 1ml of TriPure from both cells being grown in culture as well as primary tissues.

2.3.1 Nanodrop quantification

RNA was quantified using a NanoDrop ND-1000 Spectrophotometer (NanoDrop Technologies, USA). Readings at OD_{260} indicated RNA concentration while the $OD_{260/280}$ ratio indicated RNA purity.

2.3.2 Gel visualisation of mRNA

mRNA integrity was tested by electrophoresis through a 1% (w/v) agarose gel using SeaKem LE Agarose (Lonza, USA) made in 1x Tris/Borate/EDTA (TBE- Appendix A.4) and containing 1mg/ml ethidium bromide at 100V for 30 minutes. Three microlitres (3µl) of loading dye was added to 1µg of RNA and loaded onto the gel. Samples were visualised using a Spectroline Transilluminator (Spectroline, USA) and KODAK EDAS 290 camera system (KODAK, USA).

2.4 Removal of Genomic DNA

To remove any contaminating genomic DNA that might remain after RNA extraction, samples were treated with RQ1 RNase free DNase (Promega, USA). A mix of 2.4 units of RQ1 DNase, 2 µg of RNA sample and 1x RQ1 RNase free DNase buffer (Promega, USA) was made up to 10 µl in nuclease free water. This mixture was incubated at 37°C for 30

minutes, after which time 1ul of RQ1 RNase free Stop Solution (Promega, USA) was added with a further incubation at 65°C for 10 minutes to inactivate the DNase.

2.5 Complementary DNA Synthesis

Complementary DNA (cDNA) was synthesised from DNase treated RNA samples using reverse transcriptase.

A reaction submix containing 1 µg of DNase treated RNA and 63pmol of Oligo dT (UCT, South Africa) was made up to 8.5µl with Sabax water (Adcock Ingram, South Africa) and incubated at 70°C for 5 minutes in a Labnet MultiGene Gradient Thermal Cycler (Labnet International Inc., USA). Samples were placed at 4°C for 10 minutes to ensure that tertiary RNA structures did not reform. Samples were made up to 20µl containing 1mM deoxynucleotide triphosphate (Fermentas, Canada), 1x Maloney-Murine Leukaemia Virus (M-MLV) reverse transcriptase buffer (Promega, USA), 1U/µl M-MLV reverse transcriptase (Promega, USA) and 20U/µl RNase Inhibitor (Promega, USA). A final concentration of 2.5 mM $MgCl_2$ was provided by the RQ1 RNase free DNase buffer. Samples were incubated at 42°C for one hour in the Thermal Cycler, after which synthesised cDNA was stored at -20°C. Each run contained a negative control, with Sabax water instead of RNA, as well as a control for genomic DNA contamination with Sabax water replacing the reverse transcriptase.

2.6 Primer Design

Primers were designed using the Primer-BLAST program (http://blast.ncbi.nlm.nih.gov/Blast.cgi) to have melting temperatures between 50-60°C and be between 18-25 base pairs (bp) in length (Table 2.1). Where possible primer sets were designed to cross an exon-exon junction to eliminate the possibility of amplifying any contaminating genomic DNA. The theoretical product size was calculated by aligning the primers on the gene of interest and counting the distance between them. The presence of secondary structures was tested for by using Integrated DNA Technologies (IDT) OligoAnalyzer

(http://www.idtdna.com/analyzer/applications/oligoanalyzer/). Primers were synthesised by IDT (IDT, USA) and reconstituted according to the instructions of Whitehead Scientific (Whitehead Scientific, South Africa). Details of primer design and reconstituting primers appear in appendix B.5.

Table 2.1: Properties of Primers used in Polymerase Chain Reactions

Gene	Sequence (5'-3')	Length (bps)	GC content (%)	Melting Temperature (°C)	Annealing Temperature (°C)	Product size (bp)
Glucuronidase B (Gus)	Forward primer – ACTGACACCTCCATGTATCCCAAG	21	50	58.3	60	172
	Reverse primer – CAGTAGGTCACCAGCCCGATG	24	61.9	59.7		
Forkhead Box C1 (*Foxc1*)	Forward primer – TCGCTTTCCTGCTCATTCGTC	21	52.4	57.6	60	559
	Reverse primer – TGCAGAAAACGCTGTAGGGG	20	55	57.8		
Transforming growth factor beta 1 induced transcript 4 (*Tgfβ1i4*)	Forward primer – TCCGTGAGACTTGACAATAGCTCTG	25	48	56.4	55	197
	Reverse primer – GCCAGCGTCTTCAGCAGATT	20	55	55.3		
Paired-like homeodomain transcription factor 2 (*Pitx2*)	Forward primer - CCTCACCCTTCTGTCACCAT	20	55	56.6	60	179
	Reverse primer – GCCCACATCCTCATTCTTTC	20	50	53.6		
Follistatin (*Fst*)	Forward primer - TATCCAGTGTGGCGGCGGGA	20	65	59.97	60	230
	Reverse primer – CCGTTTCTTCCGAGATGGAGTTGC	24	54	58.10		

2.7 Reverse Transcription Polymerase Chain Reaction (RT-PCR) (Erlich 1989)

A mastermix was made containing, at final concentrations, 1x Buffer (JMR Holdings, UK), 0.2 mM deoxynucleotide triphosphate, 1.5mM $MgCl_2$, 0.5uM of forward and reverse primer, and 1U Super-Therm Taq polymerase (JMR Holdings, UK). 1ul of cDNA

or water (no template control) was added to 19ul of mastermix in a PCR tube and incubated in a Labnet MultiGene Gradient Thermal Cycler (Labnet International Inc., USA) under the conditions seen in Table 2.2 below.

Table 2.2: Standard Conditions for RT-PCR

	Number of Cycles	Temperature (°C)	Time (min:secs)
Initial denaturation	1	94	5:00
Cycling – Denaturation Annealing Extension	30	94 Primer dependent 72	0:30 0:30 0:30
Final Extension	1	72°C	7:00

The appropriate annealing temperature during cycling was determined by running a gradient PCR for each primer set with a positive control sample and choosing the temperature at which a single product of the correct size was seen after gel electrophoresis (Section 2.8.1) with no products present in the no template samples.

2.8 Quantitative Real Time Polymerase Chain Reaction (qPCR)

Expression of genes of interest was quantified by qPCR reactions using cDNA from samples. Reactions were performed in a Roche LightCycler (Roche, Germany) using the LightCycler FastStart DNA Master^{plus} SYBR Green I system (Roche, Germany) according to manufacturer's instructions. Each reaction contained 13µl PCR grade water, 1µl 10µM forward primer, 1µl 10µM reverse primer, 4µl of the FastStart master mix and 1µl of cDNA. This cocktail was transferred to a LightCycler capillary, which was centrifuged at 2000rpm for 10 seconds in a microfuge to isolate the cocktail at the bottom of the capillary and then placed into the LightCycler Carousel.

The reaction conditions (Table 2.3) began with an activation step of 95°C for 10 minutes, followed by 30-45 cycles, each beginning with a denaturation step at 95°C for

5 seconds followed by a primer dependent annealing temperature (Table 2.1) for 5 seconds and an elongation step at 72°C of 5 seconds. Due to the large size of the product generated by the *Foxc1* primer set it had different reaction conditions (Table 2.4). Cycling was followed by a melting curve analysis, to determine the specificity of the qPCR reaction which involved setting the temperature at 65°C for 1 minute and then gradually increasing it to 95°C. Finally, the samples were cooled to 40°C for 30 seconds. A no template control was included in each run and each sample was run in triplicate.

Table 2.3: Summary of General qPCR Reaction Conditions

	Number of Cycles	**Temperature (°C)**	**Time (min:secs)**	**Ramp rate (°C/sec)**	**Acquisition Mode**	**Analysis Type**
Activation	1	95	10:00	20	None	None
Cycling –	30-45					Quantification
Denaturation		95	0:05	20	None	
Annealing		Primer dependent	0:05	20	None	
Extension		72	Primer dependent (1 sec per 25 bases of amplicon)	20	Single	
Melting Curve –	1					Melting Curve
Denaturation		95	0:00	20	None	
Annealing		65	1:00	20	None	
Extension		95	0:00	0.1	Continuous	
Cooling	1	40°C	0:30	20		None

2.8.1 Gel Visualisation of qPCR and RT-PCR products

Ten microlitres (10µl) of each qPCR or RT-PCR product was visualised after electrophoresis as above (Section 2.3.2) on a 2% (w/v) agarose gel. This confirmed the correct product size and specificity of the reactions by comparing the bands to those of the O'Generuler 100bp DNA ladder molecular weight marker (Appendix A.6).

2.8.2 Analysis of RT-PCR products

Semi-quantification of RT-PCR products was done by digitising the PCR gels using UN-SCAN-IT software (Silk Scientific, USA) and analysing the pixel density of the PCR product against the no template control. Error bars on bar graphs represent the standard deviation of the all the values of pixel densities from three separate PCR gels.

Table 2.4: qPCR Cycling Conditions for *Foxc1* primer set

	Number of Cycles	**Temperature (°C)**	**Time (min:secs)**	**Ramp rate (°C /sec)**	**Acquisition Mode**	**Analysis Type**
Cycling –	35					Quantification
Denaturation		95	0:30	20	None	
Annealing		60	0:30	20	None	
Extension		72	0:30	20	Single	

2.8.3 Analysis of qPCR

To interpret data from the qPCR reactions and gauge the relative expression of each gene, the quantification cycle values (C_q) were analyzed. This was done using the $2^{-\Delta\Delta Cq}$ method (Livak et al. 2001) to identify fold expression of the target gene relative to a calibrator sample. A reference gene (*Gus*) accounted for basal gene expression levels. See calculations below:

$\Delta C_q = C_q$ of target gene - C_q of housekeeping gene

$\Delta\Delta C_q = \Delta C_q$ (Sample) - ΔC_q (Calibrator)

Normalised expression of target gene in sample = $2^{-\Delta\Delta Cq}$

Error bars on bar graphs represent the standard deviation on all the possible values of normalised expression calculated using the triplicate values of the target and housekeeping genes.

Statistical analyses on data were completed using STATISTICA (developed by Statsoft, USA). Differences in expression were analysed by one way ANOVA with p-values <0.05 considered as significant.

Additional data used to validate qPCR reactions in accordance with the minimum information for publication of quantitative real-time PCR experiments (MIQE) guidelines (Bustin et al. 2009) can be found in appendix C.

2.9 Immunocytochemistry (Larsson 1988)

2.9.1 SV40 Large T-Antigen

Cells were grown on coverslips in 35mm dishes. After aspiration of culture medium, cells were fixed with 500µl 4% paraformaldehyde in 1xPBS (Appendix A.3) for 30 minutes at room temperature. The fixative was removed and the cells were rinsed three times in 1xPBS followed by a 10 minute 1xPBS wash. Cells were rinsed and washed after every subsequent incubation period. Following the wash, 500µl of block (5% FBS, 0.05% Triton-X 100 in 1xPBS) was added to the sample and incubated for 1 hour at room temperature. Block was aspirated and coverslips were inverted and placed on a 100ul drop of a 1:1 dilution of mouse monoclonal anti-SV40 large T-antigen clone Pab101 (ATCC TIB-117) supernatant in 1xPBS on a glass slide. Slides were incubated for 4 hours at room temperature in a humidified chamber followed by overnight at 4°C. Cells were then placed on a 100ul drop of secondary antibody, donkey anti-mouse Cy3 (Jackson ImmunoResearch, USA) at a 1:1000 dilution (made in 1xPBS) on a glass slide in a humidified chamber and incubated at room temperature for 2 hours. Cells were incubated with DAPI at a concentration of 1ug/ml for 15 minutes at room temperature. The cells were rinsed 3 times with 1xPBS including a final 10 minute 1xPBS incubation and mounted onto slides using Mowiol 4-88 (Polysciences Inc., USA). Cell were visualised using a Zeiss Axiovert 200M microscope (Carl Zeiss, Germany) and

images were captured with a Zeiss Axiocam HR monochrome camera (Carl Zeiss, Germany).

2.9.2 ZO-1 and N-cadherin

Cells were grown on coverslips in 35mm dishes. After aspiration of culture medium, cells were fixed with 500µl 4% paraformaldehyde in 1xPBS for 30 minutes at room temperature. The fixative was removed and the cells were rinsed three times in 1xPBS followed by a 10 minute 1xPBS wash. Cells were rinsed and washed after every subsequent incubation period. Following the wash, 500µl of 1% Bovine serum albumin (BSA) made in 1xPBS was added and sample was incubated for 30 minutes at room temperature. Block was aspirated and coverslips were inverted and placed on a 100ul drop of a 1:50 dilution of rabbit poly-clonal ZO-1 in PBS or mouse mono-clonal N-cadherin in 1xPBS on a glass slide. The slides were then incubated for 5 hours at room temperature in a humidified chamber followed by overnight at 4°C. Cells were then placed on a 100ul drop of secondary antibody, donkey anti-rabbit Cy3 (for ZO-1 staining - Jackson ImmunoResearch, USA) or donkey anti-mouse Cy3 (for N-cadherin staining - Jackson ImmunoResearch, USA) at a 1:1000 dilution (made in 1xPBS) on a glass slide in a humidified chamber, and incubated at room temperature for 2 hours. Cells were incubated with DAPI at a concentration of 1ug/ml for 15 minutes at room temperature. The cells were rinsed 3 times with 1xPBS including a final 10 minute 1xPBS wash and mounted using Mowiol 4-88 (Polysciences Inc., USA). Cells were visualised using a Zeiss Axiovert 200M microscope (Carl Zeiss, Germany) and images were captured with a Zeiss Axiocam HR monochrome camera (Carl Zeiss, Germany). Some samples were further visualised with a Zeiss LSM 510 META Confocal microscope (Carl Zeiss, Germany) using both a 2-photon Mai Tai DeepSee laser (Spectra-Physics, USA) and a Zeiss solid-state laser (Carl Zeiss, Germany) at a wavelength of 561nm.

2.10 Microarray Data Pathway Analysis

Pre-processed, normalized microarray data was kindly shared by Prof. David Beebe from experiments carried out in his laboratory at Washington University in St. Louis using Illumina MouseWG-6 v2.0 microarrays. The Illumina probe accessions were first

converted to unique protein IDs using UniProt (http://www.uniprot.org/) to facilitate effective annotation and pathway analysis. This also ensures that the analysis represents annotated proteins involved in biological processes. To identify pathways that were represented in the gene list the proteins IDs were analysed using the pathways mapping tool Kyoto Encyclopedia of Genes and Genomes (KEGG) Mapper (http://www.genome.jp/kegg/tool/map_pathway2.html). All the inputted IDs were mapped to their relevant pathways to analyse the reactions they may be implicated in.

2.11 Transepithelial Electrical Resistance (TEER) Measurements

TEER measurements were carried out on E12.5 and E13.5 periocular mesenchyme cells under different conditions. MDCK cells were used a positive control. Cells were seeded on 12mm Transwell 0.4µm pore polycarbonate membranes (Corning Life Sciences) at a concentration of 10^5 cells/cm. Resistance across the membrane was measured 1 day after seeding and every day subsequent to that with a Fluke 115 Multimeter (Fluke, USA) using silver electrodes. Triplicate, stable, constant readings were obtained from three sets of filters for each condition. Resistance readings of blank filters were subtracted from experimental readings of filters with cells and resistance was then calculated per cm^2.

$$\text{TEER } (\Omega.cm^2) = (\text{TEER sample } (\Omega) - \text{TEER blank } (\Omega)) \times \text{surface area of filter } (cm^2)$$

Standard error of the mean was used as a statistical test of significance and this is represented as the error bars seen on the bar graphs.

Chapter 3: Results

3.1 Establishment of Immortalised Cell Lines

The first aim of this project was to establish immortal cell lines of the various tissues needed to study corneal endothelial development. Cell lines from the periocular mesenchyme of E12.5 and E13.5 embryos were successfully derived (Section 3.1.1) and attempts were made to establish an adult corneal endothelial cell line (Section 3.5) and an embryonic lenticular cell line (Section 3.6).

3.1.1 E12.5 and E13.5 periocular mesenchyme cell lines

The corneal endothelium develops from a population of neural crest-derived periocular mesenchyme cells that migrate into the region between the surface ectoderm and the newly formed lens vesicle at E12.5 (Kidson et al. 1999). Thereafter, at E13.5, they begin to differentiate into the corneal endothelium. It was reasoned that obtaining immortalised cell lines of the periocular mesenchyme from these two developmental stages would provide the precursor cells that could potentially enable one to form a model of corneal endothelial development. To obtain periocular mesenchymal cells, wedges of periocular mesenchyme were dissected away from the eye tissue of E12.5 and E13.5 mouse embryos with tungsten needles. Between 8 and 12 embryos were isolated from each developmental stage. For each embryo, 4-5 wedges of mesenchymal cells were dissected from the periocular mesenchyme and incubated in the same 35mm dish. Explants readily attached to the culture dishes after 24 hours and, over the course of the next 72 hours, numerous cells were seen to migrate away from the initial explant and form a monolayer of cells around its border (Figure 3.1). These cells had a distinctive dendritic morphology with numerous processes extending away from the cell body.

In order to derive cell lines from these explants, they were immortalised as described in the methods - section 2.2.1. Briefly, three days after the wedges of periocular mesenchyme were seeded onto the 35mm dishes they were infected with a retrovirus containing the temperature sensitive SV40 large T-antigen. After infection, selection

was carried out in the presence of 400µg/ml Geneticin for 21 days at 33°C, the permissive temperature for the SV40 large T-antigen. Once the selection pressure was removed cells were sub-cultured by the standard procedure. The immortalised cell lines thus derived will be referred to from here on as E12.5POM and E13.5POM. The cell lines were morphologically similar to each other in appearance and presented as stellate cells in areas of low confluency and were much rounder when tightly packed (Figure 3.2). The cell lines were also morphologically similar to a primary culture of periocular mesenchyme (Figure 3.3).

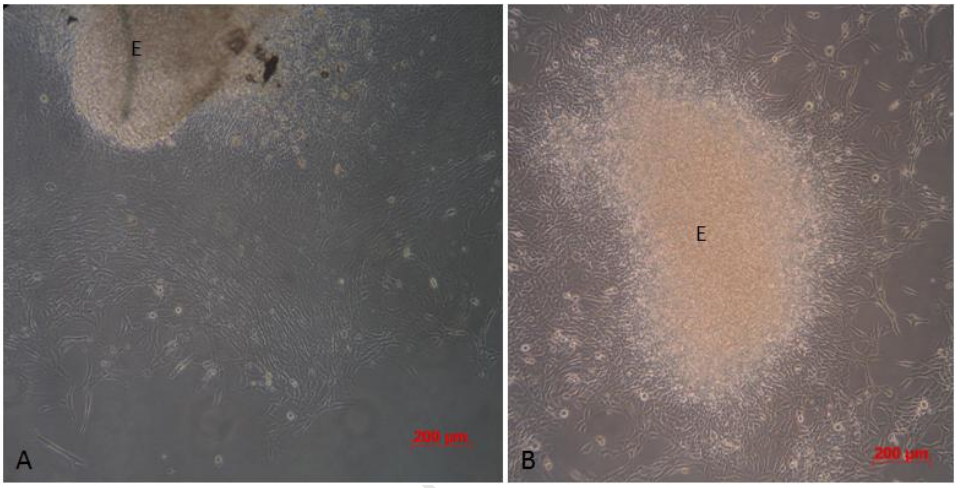

Figure 3.1: Primary cultures of mouse (A) E12.5 and (B) E13.5 periocular mesenchyme cells 3 days after dissection. 'E' denotes the explanted wedges isolated from the eyes of the mouse embryos. Numerous cells have migrated out to form a monolayer surrounding the explants.

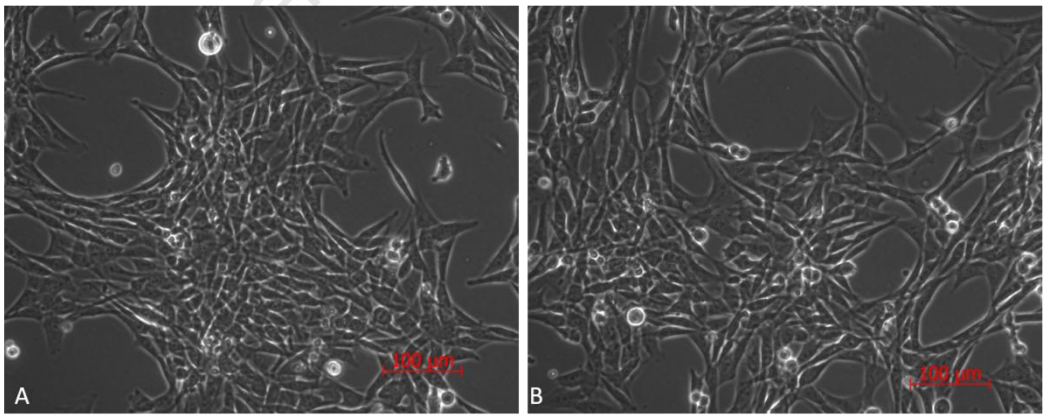

Figure 3.2: Immortalised cell lines of (A) E12.5 and (B) E13.5 periocular mesenchyme. Immortalised periocular mesenchyme cells from both cell lines at passage 2. Individual cells are elongated in areas of low confluency. At high confluency cells appear rounder and more tightly packed.

Both cell lines could be grown and expanded for many passages with no evident changes in morphology. After 13-16 passages all cells in the primary cultures senesced or otherwise died in culture. At the time of writing the derived cell lines have been passaged more than 40 times with no changes in cell growth or morphology. For all experiments cells between passages 15-30 were used.

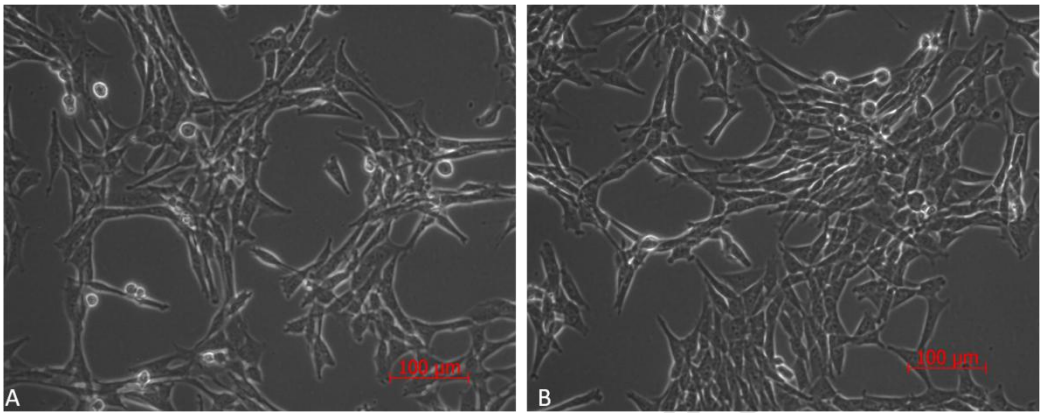

Figure 3.3: Morphology of (A) a primary culture of E12.5 periocular mesenchyme and (B) the immortalised E12.5POM cell line at passage 2. In both cases individual cells are elongated in areas of low confluency and appear rounder and more tightly packed when at high confluency.

To confirm the presence of the SV40 protein in the cell lines, immunocytochemistry was performed using a monoclonal anti-SV40 large T-antigen antibody derived from the Pab101 clone (ATCC TIB-117). In both the E12.5POM and E13.5POM cell lines SV40 expression was noted in the nucleus of every cell (Figure 3.4 D-I). Staining was consistent with that seen in the Ψ2 SV40 producer cell line (Figure 3.4 A,B,C).

Normal (non-immortalised) mouse embryonic fibroblasts (MEFs) were used as control cells. When grown in the presence of 400µg/ml Geneticin all MEFs died after 7-10 days. Normal MEFs did not display positive staining for SV40 (results not shown).

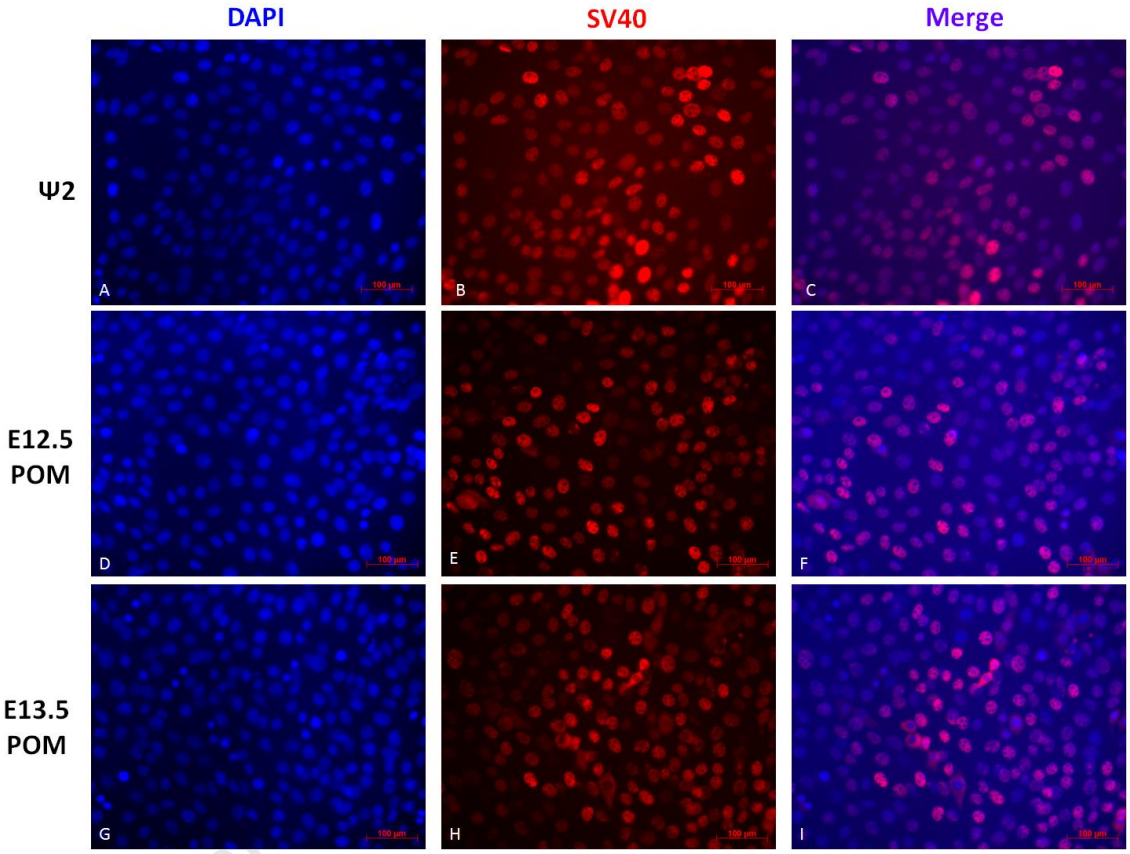

Figure 3.4: Immunodetection of SV40 large T-antigen in E12.5POM and E13.5POM compared to Ψ2 cells. (A-C) The Ψ2 producer cell line shows a clear nuclear localisation of SV40 large T-antigen in all cells. Both E12.5POM (D-F) and E13.5POM (G-I) show the same nuclear localisation of SV40 large T-antigen as the Ψ2 cell line.

3.2 Growth Characteristics of the E12.5POM and E13.5POM Cell Lines

The adult corneal endothelium has two characteristics that distinguish it from its precursor population of periocular mesenchyme. Firstly, it expresses both adherens and tight junctions. Secondly, the fully mature corneal endothelium is a single layer of cells that does not proliferate. Thus, in order to manipulate cells to form a corneal endothelium *in vitro*, one first needs to inhibit their proliferation to obtain a slowly dividing monolayer. Cell lines carrying a temperature sensitive mutant of the SV40 large T-antigen allow one to control the activity of the large T-antigen by changing the culture temperature. In this way the proliferation rate of the cells can be controlled. It was hypothesised that culture at 39°C, the non-permissive temperature of the SV40 large T-antigen, would slow the rate of proliferation and this would enable one to grow a monolayer of cells. The aim of the next series of experiments was therefore to compare the proliferation of the immortalised cell lines at the non-permissive (39°C) and permissive (33°C) temperatures over an 8 day culture period in DMEM with 10% foetal bovine serum (FBS).

Somewhat surprisingly, when grown at 33°C both cell lines showed a statistically similar rate of growth to that at 39°C with doublings times of approximately 24 hours (Figure 3.5 A and B). The control MEFs had a doubling time of approximately 24 hours at 39°C (Figure 3.5 C– Red line) but failed to proliferate at all at 33°C (Figure 3.5 C– Orange line). The similar proliferative rates at the permissive and non-permissive temperatures indicate that increasing the temperature is not sufficient to slow the proliferation of these immortal cell lines. Thus, other strategies had to be investigated in order to inhibit or slow down cell growth.

Proliferation in cell culture is driven by the addition of 10% FBS which contains high levels of embryonic growth promoting factors. It is known that the removal or reduction of the serum content in the culture medium is an effective method to slow cell growth. In order to quantify the effect that changing the serum content had on the growth rate of the cells, the proliferation of the E12.5POM cell line under a variety of conditions was measured.

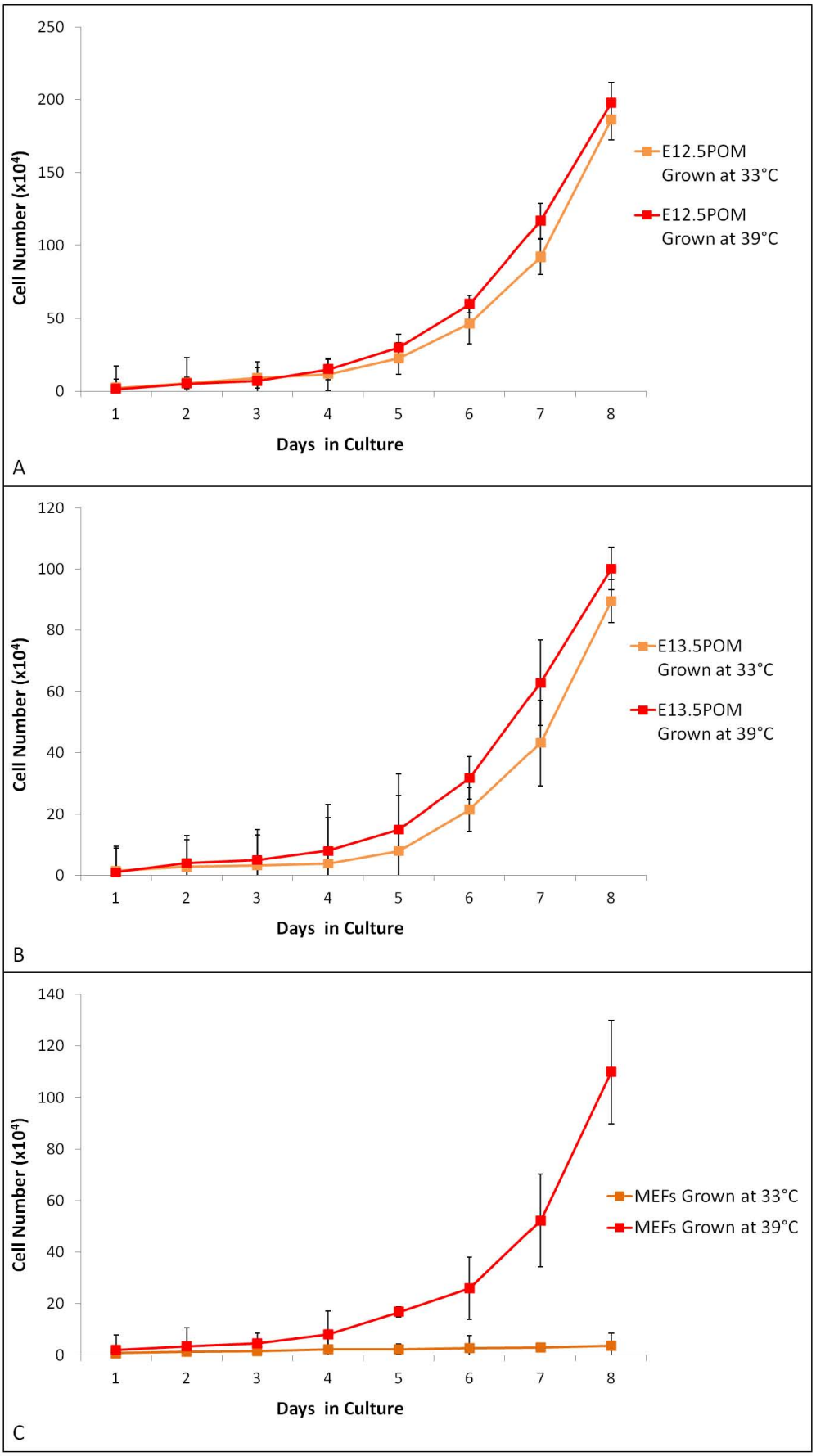

Figure 3.5: Growth curves of E12.5POM, E13.5POM, and MEFs at 33°C and 39°C. (A) E12.5POM cell line (B) E13.5POM cell line (C) Normal MEFs. MEFs did not proliferate at 33°C.

In the first set of experiments to inhibit proliferation, the FBS was removed from the culture medium and supplemented with 10% Knockout Serum Replacement (KOSR). KOSR is a defined formulation that contains no growth factors. E12.5POM cells were incubated for 8 days at 33°C in DMEM with 10% KOSR with or without the addition of 50ng/ml bFGF as a growth factor. When inspecting the cells grown in 10% KOSR with no serum it was noted that they were no longer adherent and grew as small spheres (Figure 3.6 A). This was true regardless of whether any bFGF was added. These spheres were evident even after 1 day of culture. In order to accurately quantify cell proliferation it is important that no cells are lost during the culturing period. To avoid losing any non-adherent cells, the medium in these cultures was never removed but topped up every second day. At the end of the 8 day incubation period there was a 4-fold decrease in the number of cells present when 10% KOSR was used instead of 10% FBS (Figure 3.6 B). The addition of bFGF rescued the growth rate of cells (Figure 3.6 B).

To establish whether the morphological changes observed (the formation of non-adherent spheres) were specific to the E12.5POM cell line, normal MEFs were grown in serum free medium with KOSR. In all cases the normal MEFs remained attached to the dish as a monolayer and did not form spheres (results not shown). To establish whether the morphological change was a consequence of infection with the SV40 large T-antigen the DMEL-2 cell line (dermal melanocytes cells that have been immortalised with the SV40 large T-antigen (Prince 1999)) was grown in serum free medium with KOSR. In all cases the DMEL-2 cell line remained attached to the dish as a monolayer and did not form spheres (results not shown). If the E12.5POM spheres were plated into fresh medium contain-ning 10% FBS they re-adhered and began to spread out over the dish (Figure 3.6 C). Furthermore, if the cells were initially seeded into medium containing 10% FBS and changed to medium containing 10% KOSR with no FBS after 24 hours, the cells would initially adhere to the dish but when changed into serum free conditions they clumped together, lifted off the dish and grew as floating spheres (Figure 3.6 D). These various lines of evidence indicate that it is specifically the E12.5POM cell line that grows as non-adherent spheres in serum free media and that neither MEFS nor another SV40 immortalized cell line (DMEL-2) grew as spheres.

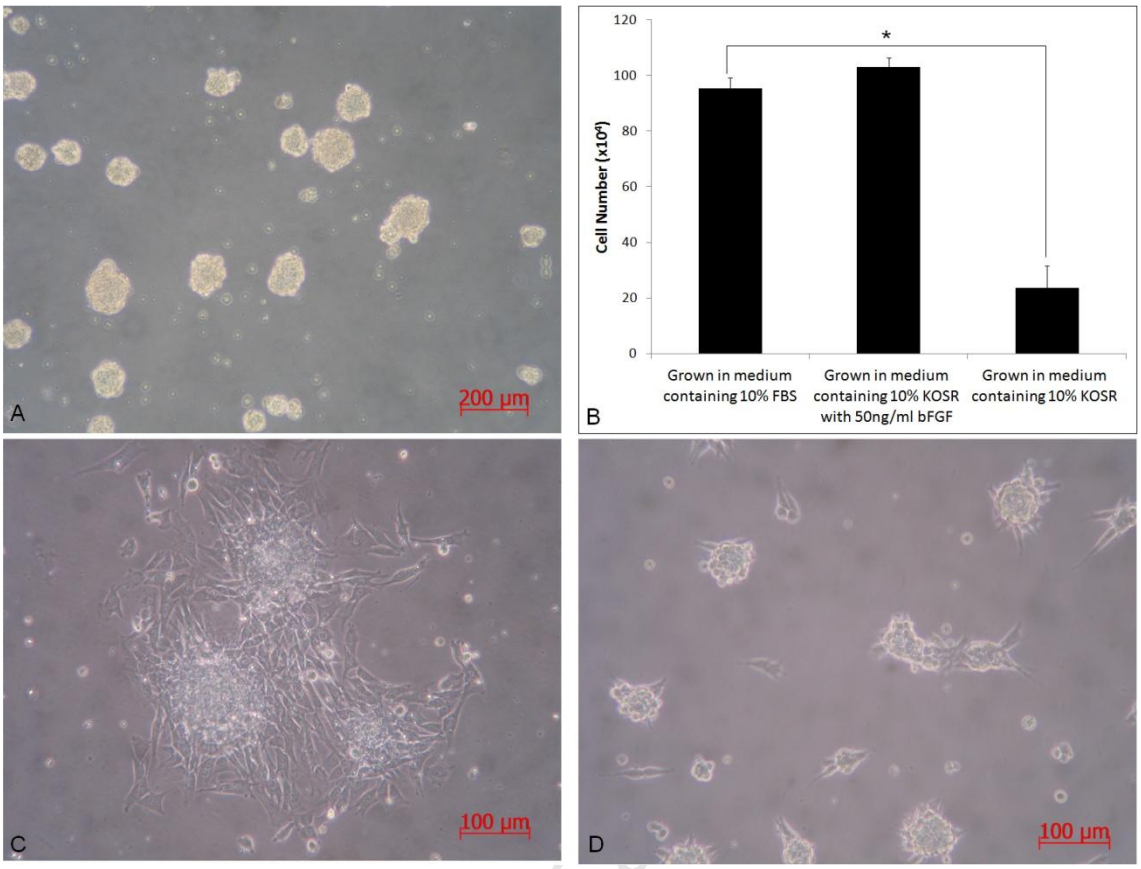

Figure 3.6: Proliferation and morphology of the E12.5POM cell line at 33°C under different conditions of growth. (A) Cells incubated at 33°C in 10% KOSR with bFGF formed small non-adherent spheres. (B) Graph showing number of cells present 8 days after seeding 5 x 10^4 cells in 35mm dishes under various conditions. (C) Spheres reattached when transferred into medium containing FBS. Cells were seen to spread out and proliferate. (D) Cells seeded in 10% FBS containing medium and then changed to medium containing 10% KOSR initially formed a monolayer and then clumped together and began to lift and form spheres once FBS was replaced with KOSR.

* indicates statistical significance ($p<0.05$) analysed by one way ANOVA.

Following these results, it was clear that further modifications would be were needed to inhibit cell growth while maintaining adhesion to the culture dish. It was reasoned that reducing but not eliminating the serum, and thus reducing the level of growth factors present, might be an effective method to slow proliferation while maintaining cell adhesion. Thus, the next experiment measured the proliferation of E12.5POM cells in reduced serum containing media at 33°C. When cells were grown in serum reduced medium containing either 2% or 1% FBS there was a significant 2-fold reduction in the number of cells present when compared to those grown in 10% FBS (Figure 3.7 A). Additionally, cells grown in reduced serum medium grew as a monolayer and maintained the cell morphology of those seen in 10% FBS (Figure 3.7 B). Thus, a

reduction in serum and incubation at 33°C resulted in an inhibition of the proliferation rate of the E12.5POM cell line while maintaining the adhesive properties of the cells.

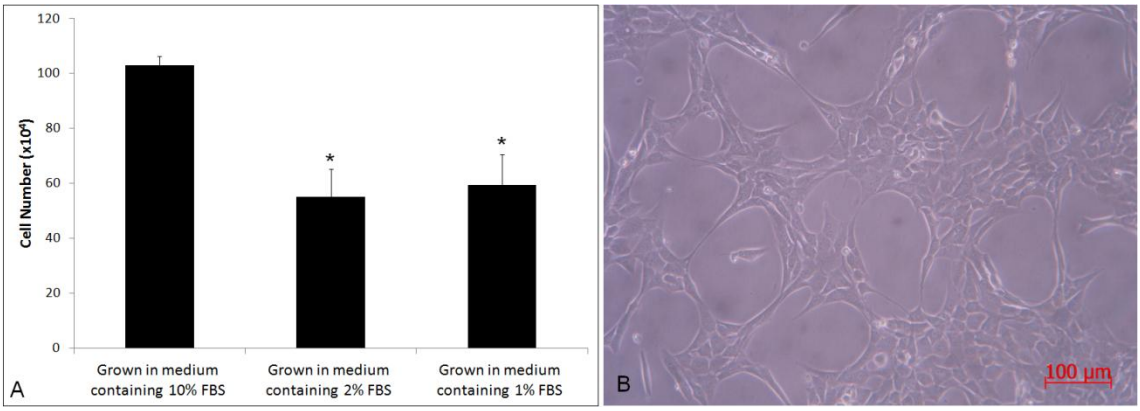

Figure 3.7: Proliferation and morphology of the E12.5POM cell line incubated at 33°C in different media. (A) Graph showing number of cells present 8 days after seeding 5 x 10^4 cells in 35mm dishes at 33°C in different media. (B) Morphology of cells grown in 2% FBS containing medium.
* indicates statistical significance ($p<0.05$) analysed by one way ANOVA.

The E12.5POM cells were next cultured in serum reduced conditions at the non-permissive temperature for the SV40 large T-antigen, 39°C, in order to determine if the increase in temperature could reduce the proliferation of the cells when in low serum even further. In 1% FBS at 39°C all cells died by the end of the growth period (Figure 3.8 A). In 2% FBS a significant 4-fold reduction in cellular proliferation was observed when compared to those grown in 10% FBS at the same temperature (Figure 3.8 A). When compared to cells grown at 33°C in 2% FBS a 1.9-fold decrease in cellular proliferation was noted (Figure 3.7 A and Figure 3.8 A). The increase in temperature thus reduced the proliferation of cells grown in 2% FBS even further.

Most interestingly, a very distinct change in cell shape was also observed when cells were incubated at 39°C in 2% FBS. The cells appeared to have a polygonal, epithelial-like morphology with bright, defined edges and grew in small, tightly packed groups. (Figure 3.8 B). They were noticeably different in appearance from the stellate cells that were present at 33°C in 2% FBS (Figure 3.7 B). Furthermore it took +/- 5 minutes to lift all the cells using trypsin/EDTA in this culture compared to the 10 seconds needed to lift the cells at 33°C in any percentage of FBS. This signifies an increase in the adhesive properties of the cells both to the culture dish and to each other when incubated at 39°C in 2% FBS.

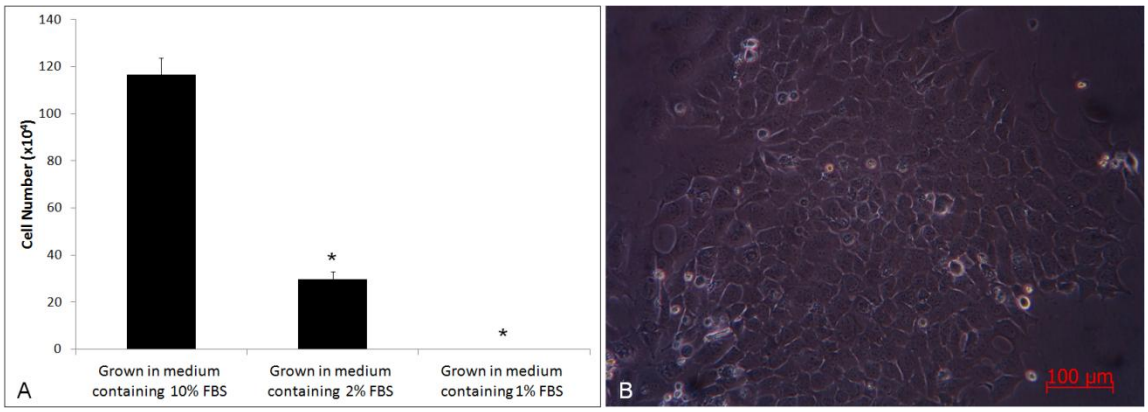

Figure 3.8: Proliferation and morphology of the E12.5POM cell line incubated at 39°C in different media. (A) Graph showing number of cells present 8 days after seeding 5 x 10^4 cells in 35mm dishes at 39°C in different media. In 1% FBS all cells died before they could be counted. (B) Morphology of cells grown in 2% FBS containing medium. Cells grew in small tightly packed groups with each cell having a defined, bright edge. Cells appeared to have a polygonal epithelial-like morphology.
* indicates statistical significance ($p<0.05$) analysed by one way ANOVA.

Thus, a suitable method was established to hinder the growth rate of the E12.5POM cell line by incubating the cells at 39°C in 2% FBS. Growing the cells under these conditions also induced an interesting change in cell morphology. With this in mind these conditions of growth were taken forward for further experimentation on both E12.5POM and E13.5POM. From this point onwards cells at **33°C in 10% FBS** are considered to be under the **proliferative conditions** while cells at **39°C in 2% FBS** are considered to be under the **non-proliferative conditions**.

3.3 Developmental Gene Expression Patterns of the E12.5POM and E13.5POM Cell Lines under Proliferative and Non-Proliferative Conditions

The next series of experiments had two aims. Firstly, to establish whether the gene expression pattern in the immortal cell lines under proliferative conditions was similar to the gene expression profile of the *in vivo* periocular mesenchyme. Secondly, to analyse the change in developmental gene expression induced by culturing the cell lines in the non-proliferative conditions (where the morphology of the cells was markedly different). To compare mRNA expression, qPCR reactions were run on cDNA reverse transcribed from mRNA extracted from both cell lines. Expression was analysed using the $2^{-\Delta\Delta Cq}$ method (Livak et al. 2001) and normalised to the reference gene Glucuronidase B (*Gus*).

In wildtype mice, *Foxc1* is highly expressed in the periocular mesenchyme from E11.5-E12.5 with reduced expression at E13.5 (Kidson et al. 1999; Ittner et al. 2005). In this study, under the proliferative conditions at passage 15, the E12.5POM cell line expressed over 2.6 times more *Foxc1* mRNA than its E13.5 counterpart (Figure 3.9). An identical expression pattern was obtained from cells at passage 30 (Figure 3.10). These results show that the down-regulation of *Foxc1* in E13.5POM when compared to E12.5POM is similar to the down-regulation that is seen *in vivo*. Additionally, the *Foxc1* expression pattern noted in the E12.5POM and E13.5POM cell lines is maintained over time in culture. When at the non-proliferative conditions E12.5POM showed a 4.3-fold decrease and E13.5POM a 2.6-fold decrease in *Foxc1* expression when compared to those grown under the proliferative conditions (Figure 3.9). The increase in serum and reduction in temperature thus induced a significant drop in *Foxc1* gene expression.

To establish whether the gene expression profiles observed in the cell lines were unique to the periocular mesenchyme, qPCR reactions were also under taken using MEF cDNA. It was previously noted that MEFs fail to multiply at 33°C in 10% FBS, the proliferative conditions for the immortal cell lines (Figure 3.5 C– Orange line). Thus, in order to obtain a sufficient number of MEFs to study, they were first incubated at 37°C until confluent. The MEFs were then transferred to 33°C and cultured at this

temperature for the same length of time as the experimental samples. This same method was used for all molecular studies that required MEFs to be incubated in the proliferative conditions. Following this method it was found that MEFs did not express *Foxc1* under either the proliferative or non-proliferative conditions (Figure 3.9).

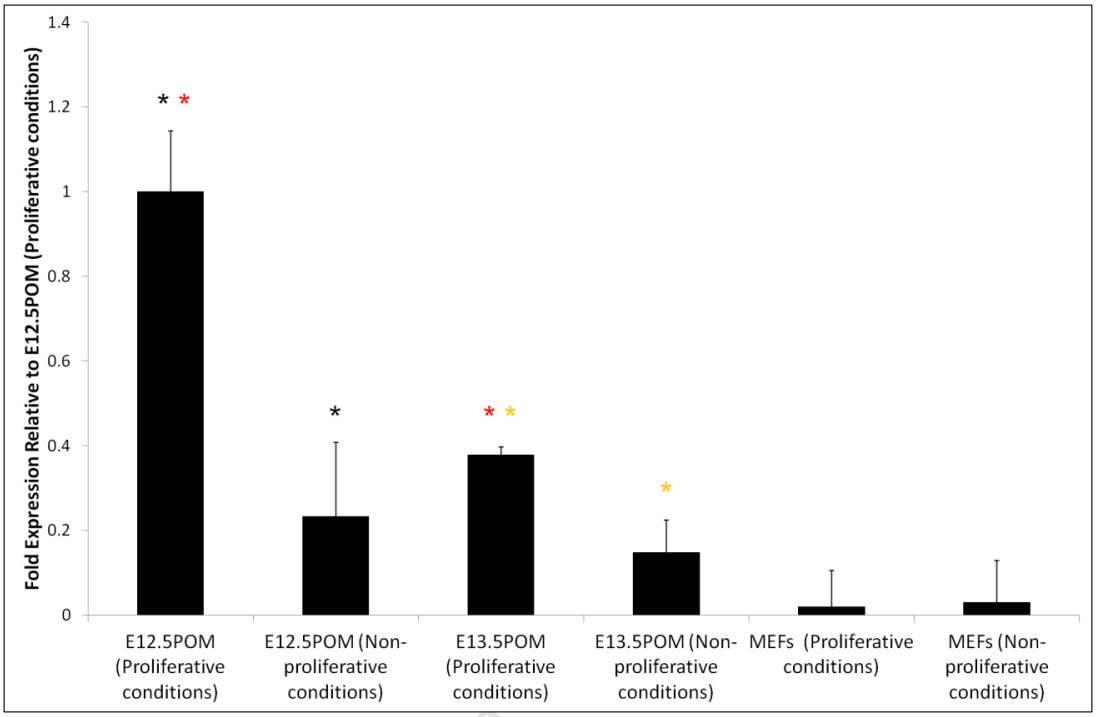

Figure 3.9: *Foxc1* mRNA expression in E12.5POM, E13.5POM and MEFs at passage 15 incubated in the proliferative and non-proliferative conditions. Relative fold expression was analysed by qPCR and normalised to the reference gene *Gus*. *,*,* indicates statistical significance ($p<0.05$) with different coloured pairs indicating significance relative to one another.

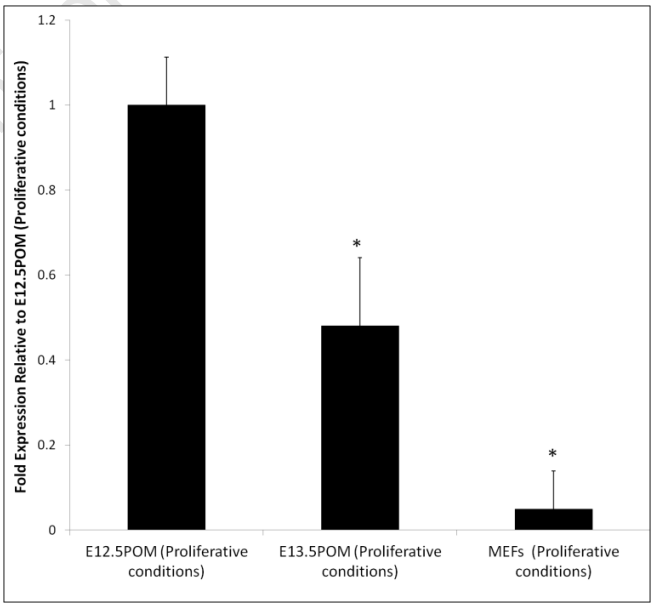

Figure 3.10: *Foxc1* mRNA expression in E12.5POM, E13.5POM and MEFs at passage 30 when incubated in the proliferative conditions. Relative fold expression was analysed by qPCR and normalised to the reference gene *Gus*. * indicates statistical significance. ($p<0.05$).

Tgfβ1i4 has been reported to be negatively regulated by *Foxc1,* and *Foxc1* null mutant mice show expanded and stronger expression of *Tgfβ1i4* than wildtype embryos (Sommer et al. 2006). Strong *Tgfβ1i4* expression has also been noted *in vivo* in E13.5 embryos in the periocular mesenchyme with lower expression at E12.5 (Napier 2005; Sommer et al. 2006). Furthermore, the postnatal corneal endothelium expresses high levels of *Tgfβ1i4* (Thut et al. 2001). In this study, the E13.5POM cell line showed an almost 2.5 fold increase in *Tgfβ1i4* expression when compared to the E12.5POM cell line under proliferative conditions (Figure 3.11). MEFs expressed moderate levels of *Tgfβ1i4* under these conditions (Figure 3.11). *Tgfβ1i4* had the inverse expression pattern of what was observed with *Foxc1* (Figure 3.9). These results show that the up-regulation of *Tgfβ1i4* in E13.5POM when compared to E12.5POM is similar to the up-regulation that is seen at these time points *in vivo*.

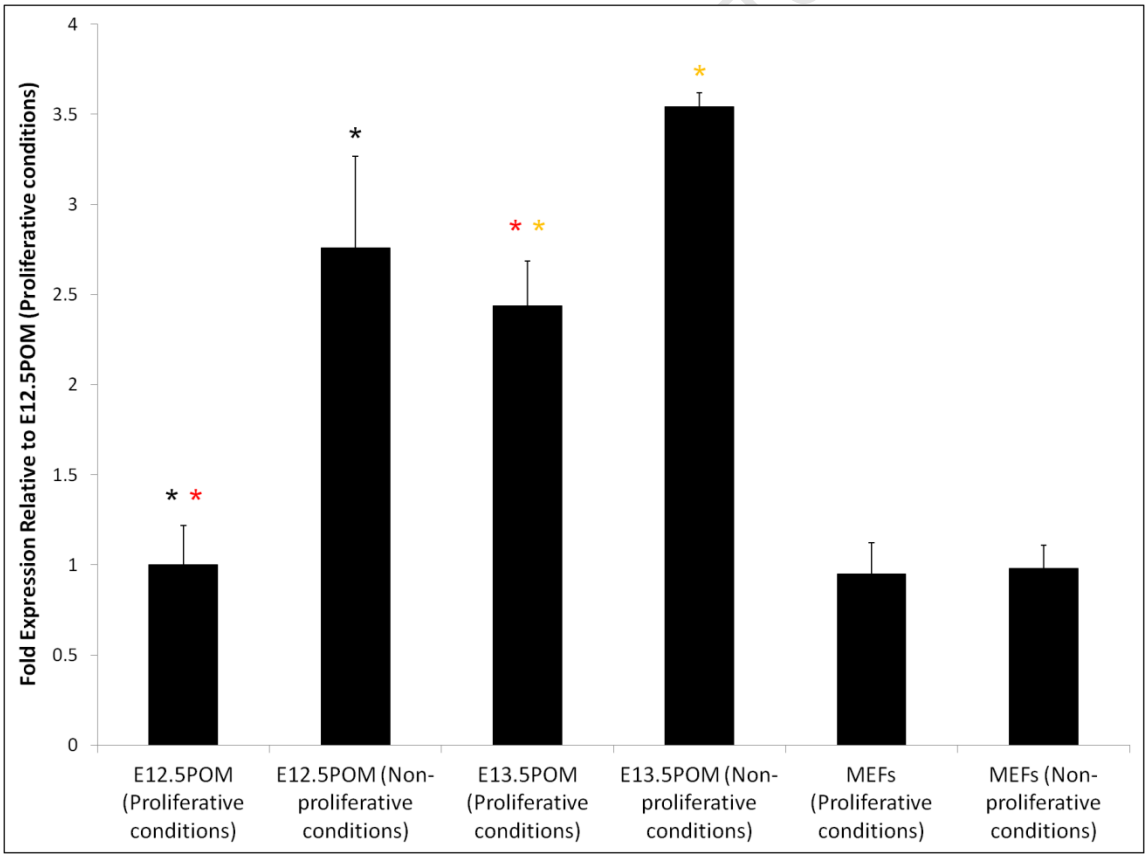

Figure 3.11: *Tgfβ1i4* mRNA expression in E12.5POM, E13.5POM and MEFs incubated in the proliferative and non-proliferative conditions. Relative fold expression was analysed by qPCR and normalised to the reference gene *Gus*. *,*,* indicate statistical significance ($p<0.05$) with different coloured pairs indicating significance relative to one another.

The E12.5POM cell line showed a 2.7-fold increase while E13.5POM showed a 1.4-fold increase in *Tgfβ1i4* expression when at the non-proliferative conditions compared to proliferative conditions (Figure 3.11). Normal MEFs did not have a significant difference in *Tgfβ1i4* expression when compared between the two conditions (Figure 3.11). The increase in *Tgfβ1i4* expression has a strong relationship with the decrease in *Foxc1* expression when grown under the non-proliferative conditions (Figure 3.9) and this would provide further evidence for the role of *Foxc1* in repressing *Tgfβ1i4* expression.

Pitx2 is strongly expressed in E12.5 mouse embryos in the periocular mesenchyme and expression is maintained in the developing corneal stroma and endothelium by E14.5 (Kitamura et al. 1999; Gage et al. 1999). In this study, high levels of *Pitx2* were found in the primary tissue of whole E12.5 mouse eyes (Figure 3.12). However, *Pitx2* was not detected in either cell line or in normal MEFs under proliferative or non-proliferative conditions (Figure 3.12). The lack of *Pitx2* expression in the cell lines therefore differs from what was found in the *in vivo* tissue. *Pitx2* is therefore not necessary for *Foxc1* expression in the immortal cell lines.

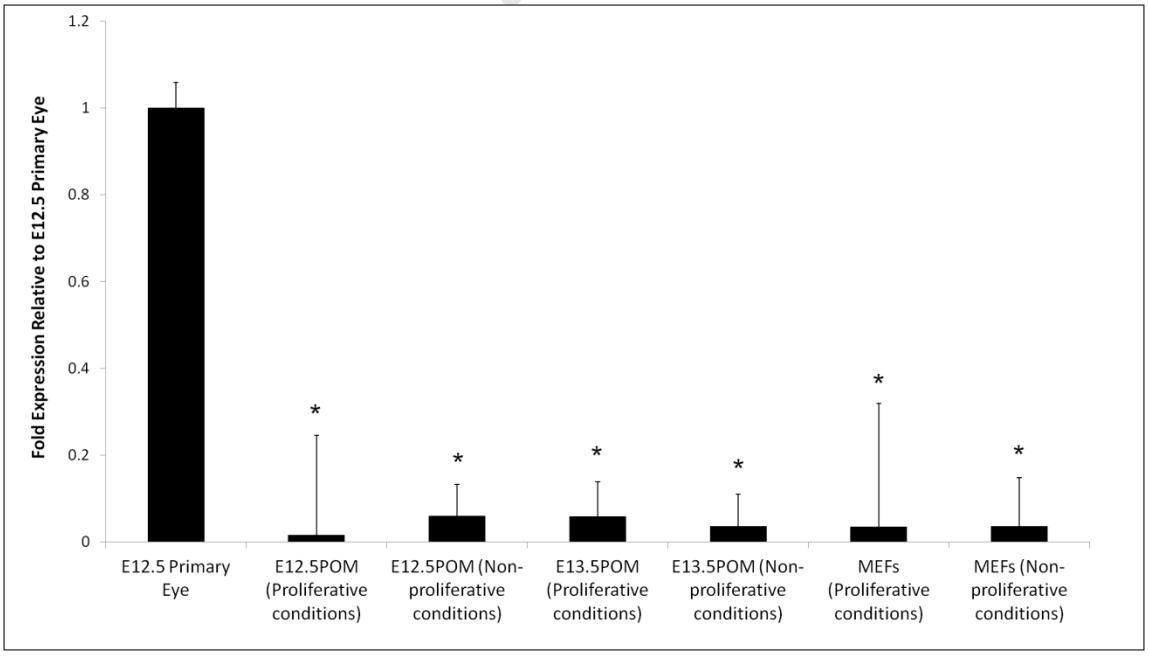

Figure 3.12: *Pitx2* mRNA expression in E12.5POM, E13.5POM and MEFs incubated in the proliferative and non-proliferative conditions. Relative fold expression was analysed by qPCR and normalised to the reference gene *Gus*. * indicates statistical significance ($p<0.05$).

Numerous attempts were also made to measure the expression of *Lmx1b,* a gene highly expressed in the periocular mesenchyme at E12.5 and E13.5 (Pressman et al. 2000), in the cell lines at both the proliferative and non-proliferative conditions. However, the conditions for the qPCR reaction using the *Lmx1b* primer set could not be optimised.

In conclusion, the *Foxc1* and *Tgfβ1i4* gene expression patterns of the E12.5POM and E13.5POM cell lines at the proliferative conditions are similar to gene expression of the endogenous periocular mesenchyme at both E12.5 and E13.5. When cultured at the non-proliferative conditions there was a decrease in *Foxc1* and a subsequent increase in *Tgfβ1i4* in both cell lines. The adult corneal endothelium does not express *Foxc1* (Kidson et al. 1999; Berry et al. 2006) but does express *Tgfβ1i4* (Thut et al. 2001; Napier 2005). The gene expression pattern of the cell lines at the non-proliferative conditions is thus more similar to what would be expected in the adult corneal endothelium than the periocular mesenchyme.

3.4 Junction Formation in the E12.5POM and E13.5POM Cell Lines under Proliferative and Non-Proliferative Conditions

In normal development *in vivo* the formation of the fully mature corneal endothelium is marked by the presence of adherens and tight junctions. It was reasoned that an investigation into the expression of cell junctions in the cell lines under the proliferative and non-proliferative conditions would enable one to differentiate between periocular mesenchymal and adult corneal endothelial cells. To identify the presence of cell junctions immunostaining was undertaken for N-cadherin and ZO-1 which are expressed in adherens and tight junctions respectively (Lodish et al. 2008).

3.4.1 Adherens junction formation

Adherens junctions start to form during periocular mesenchyme differentiation and are present in early corneal endothelial progenitors as well as the adult corneal endothelium (Beebe et al. 2000; Joyce 2003; Zhang et al. 2007). In order to establish a protocol to identify N-cadherin (a marker of adherens junctions), the immunostaining procedure was first optimised using HeLa cells, which are known to express N-cadherin.

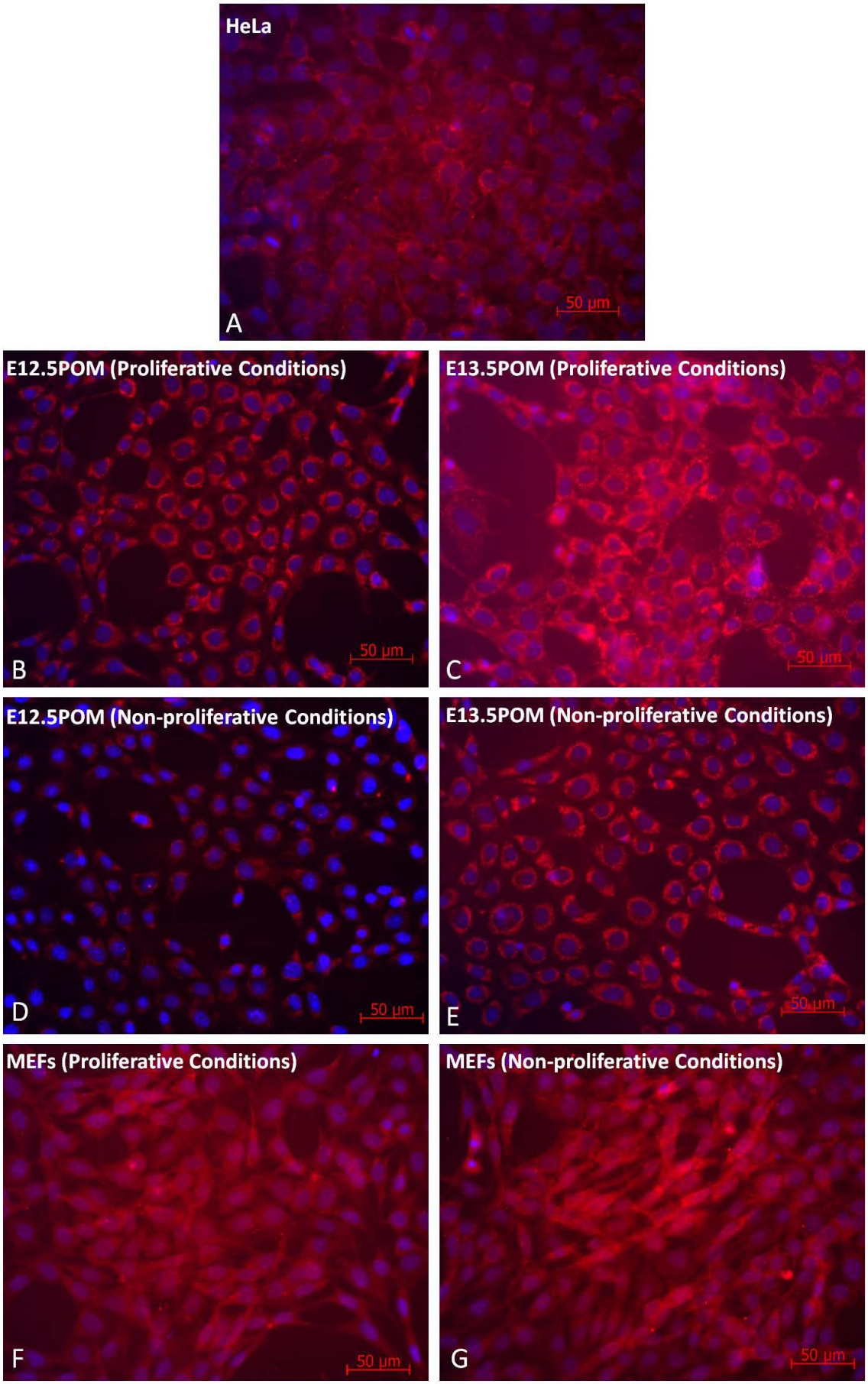
HeLa
50 µm
A
E12.5POM (Proliferative Conditions)
50 µm
B
E13.5POM (Proliferative Conditions)
50 µm
C
E12.5POM (Non-proliferative Conditions)
50 µm
D
E13.5POM (Non-proliferative Conditions)
50 µm
E
MEFs (Proliferative Conditions)
50 µm
F
MEFs (Non-proliferative Conditions)
50 µm
G

Figure 3.13: Immunodetection of N-cadherin in E12.5POM, E13.5POM and MEFs incubated in the proliferative and non-proliferative conditions compared to HeLa cells. (A) HeLa cells have peri-nuclear staining of N-cadherin. E12.5POM and E13.5POM also have peri-nuclear staining of N-cadherin at both the proliferative (B,C) and non-proliferative (D,E) conditions. (F,G) MEFs did not express any N-cadherin under either condition.

In HeLa cells a peri-nuclear pattern of N-cadherin expression was observed (Figure 3.13 A). All cells of both the E12.5POM and E13.5POM cell lines expressed N-cadherin in the same peri-nuclear pattern under both the proliferative and non-proliferative conditions in all six independent experiments (Figure 3.13 B-E). No staining was evident for normal MEFs under either condition (Figure 3.13 F.G).

In order to more closely examine the N-cadherin staining pattern, the E12.5POM cell line grown under the non-proliferative conditions was visualised using confocal microscopy. Clear expression of N-cadherin in discrete spots along the cell membrane of connecting cells was noted when viewed under higher power (Figure 3.14 A – white arrowheads). In both experiments that were visualised using confocal microscopy every connected cell had membrane bound expression of N-cadherin. The membrane staining was easily distinguishable from the cytoplasmic staining. Using differential interference contrast microscopy the junction between the two membranes could be visualised (Figure 3.14 B – black arrowheads) and a merged image confirmed the presence of N-cadherin at this junction (Figure 3.14 D – purple arrowheads). In the confocal images cytoplasmic N-cadherin expression appeared as small brightly stained vesicles (Figure 3.14 A – white arrows) that surrounded the nucleus (Figure 3.14 D-nucleus in blue).

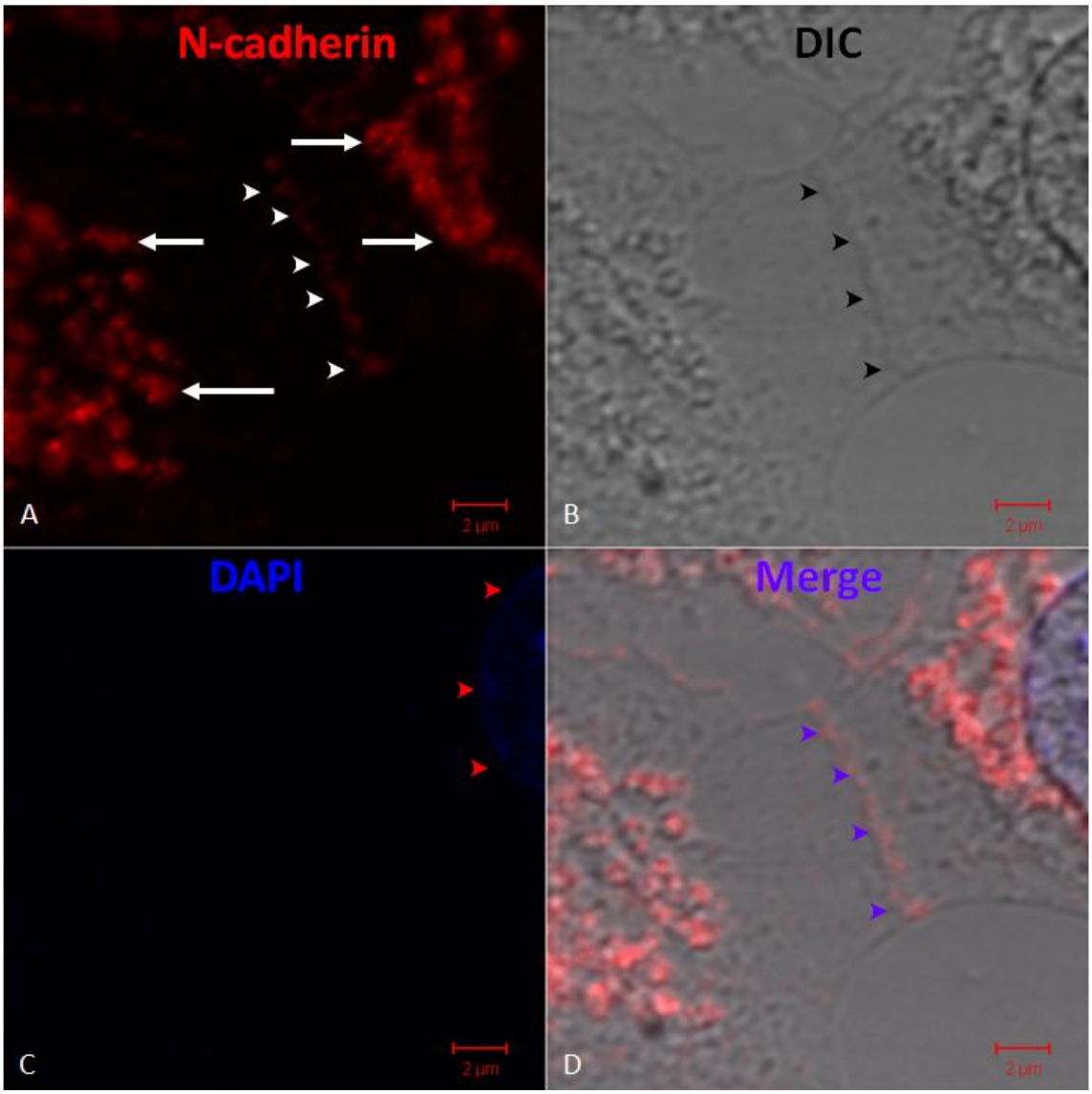

Figure 3.14: Confocal microscopy visualisation of N-cadherin in the E12.5POM cell line incubated in the non-proliferative conditions. (A) N-cadherin can be seen to be localised in two distinct regions in the cell. In vesicles within the cytoplasm surrounding the nucleus (white arrows) as well as in a line at the junction where the cellular membranes meet (white arrowheads). Pinhole size 110µm (B) Using differential interference contrast (DIC), the junction where the plasma membranes meet can be easily identified (black arrowheads). (C) Only one nucleus, stained with DAPI, is visible (red arrowheads). Pinhole size 1000µm (D) A merged image clearly shows that N-cadherin is present in the cell membranes of the contacted cells (purple arrowheads).

3.4.2 Tight junction formation

Tight junctions are present in the adult corneal endothelium but not the periocular mesenchyme (Petroll et al. 1999; Zhang et al. 2007). In order to establish a protocol to identify ZO-1 (a marker of tight junctions), the immunostaining procedure was first optimised using MDCK cells, which are known to have tight junctions. In MDCK cells membrane bound ZO-1 expression was observed in almost every cell (Figure 3.15 A).

ZO-1 staining was strongest at the vertices of the adjoining cells (Figure 3.15 A - white arrowheads). In all six experiments undertaken no expression of ZO-1 was noted in either E12.5POM or E13.5POM under the proliferative conditions (Figure 3.15 B,C). In contrast, strong membrane staining of ZO-1, indicative of tight junction formation, was observed in many adjoining cells in the non-proliferative conditions in all experiments undertaken (Figure 3.15 D,E – examples indicated by white arrowheads). MEFs by comparison did not express any ZO-1 under either condition (Figure 3.15 F,G).

Immunostaining of ZO-1 in the E12.5POM cell line under non-proliferative conditions was examined using confocal microscopy in order to confirm that the ZO-1 was expressed along the cell membrane. The strong band of staining between the adjacent cells could be more easily visualised using confocal microscopy (Figure 3.16 A - white arrowheads). When differential interference contrast microscopy was used the junction between the two membranes was very apparent (Figure 3.16 B – black arrowheads) and a merged image confirmed that ZO-1 was specifically expressed along the points where the two adjoining cell membranes met (Figure 3.16 D – purple arrowheads). The same results were noted in both experiments visualised in this manner.

It is common for tight junction expressing epithelial cells, such as the MDCK cells, to grow in very tightly packed groups with no spaces between the individual cells and tight junctions around the entire circumference of every cell. It was thus of interest to note that the tight junction expressing E12.5POM and E13.5POM cell lines were not as tightly packed as the MDCK cells and had numerous gaps between cells. These gaps were most notable at the apexes of adjoining cells (Figure 3.15 D,E – white arrows).

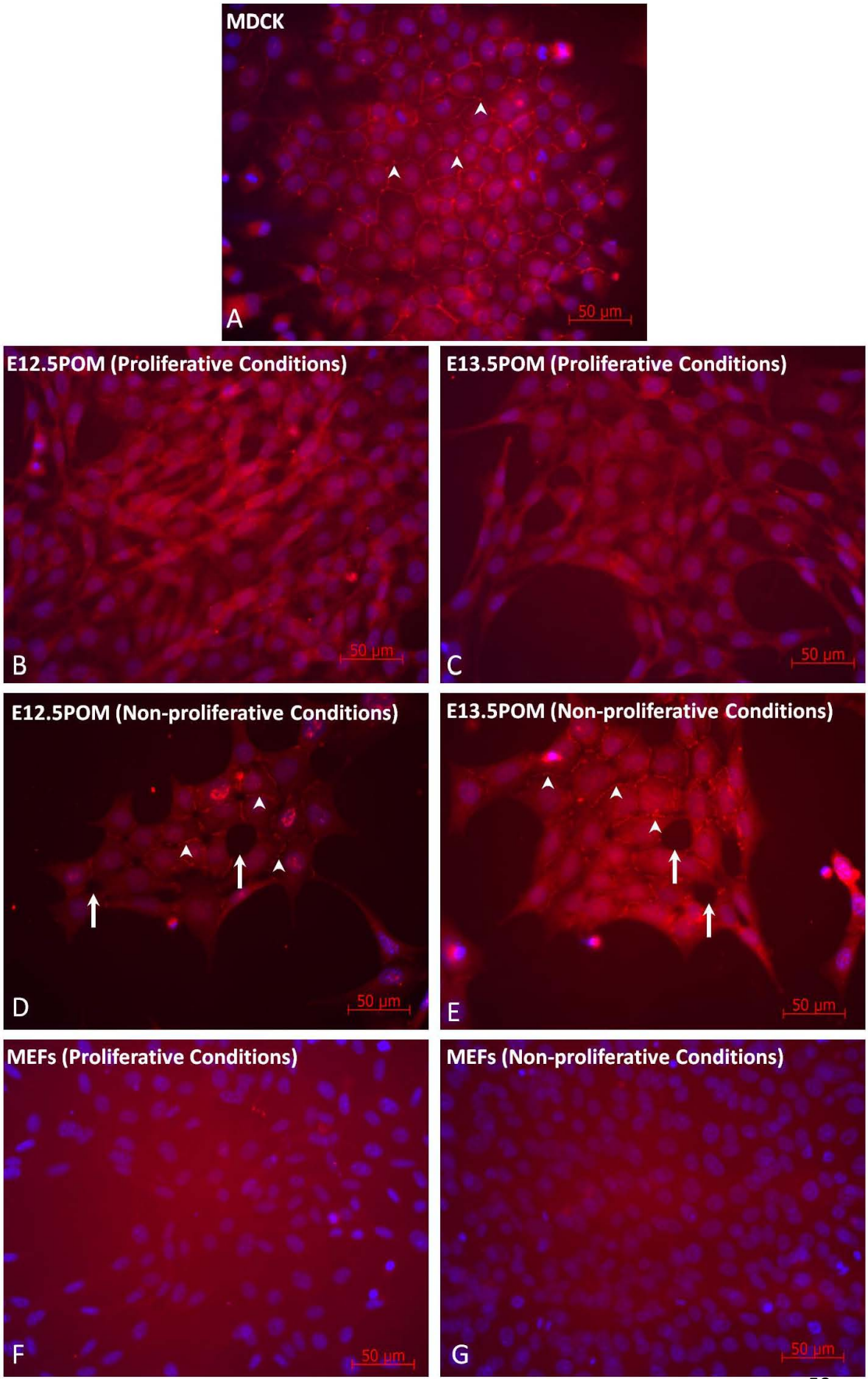
MDCK
A
50 µm
E12.5POM (Proliferative Conditions)
B
50 µm
E13.5POM (Proliferative Conditions)
C
50 µm
E12.5POM (Non-proliferative Conditions)
D
50 µm
E13.5POM (Non-proliferative Conditions)
E
50 µm
MEFs (Proliferative Conditions)
F
50 µm
MEFs (Non-proliferative Conditions)
G
50 µm

Figure 3.15: Immunodetection of ZO-1 in E12.5POM, E13.5POM and MEFS incubated in the proliferative and non-proliferative conditions compared to MDCK cells. (A) MDCK cells express ZO-1 protein the cell membranes of the closely associated cells. The vertices of the cell membranes showed the strongest ZO-1 staining (white arrowheads). Both E12.5POM (B) and E13.5POM (C) did not express the ZO-1 protein under proliferative conditions. When in the non-proliferative conditions both E12.5POM (D) and E13.5POM (E) expressed ZO-1 in the membranes of adjoining cells (white arrowheads). Numerous gaps were noted in between the clusters of cells (white arrows). (F,G) MEFs under either condition did not express any ZO-1.

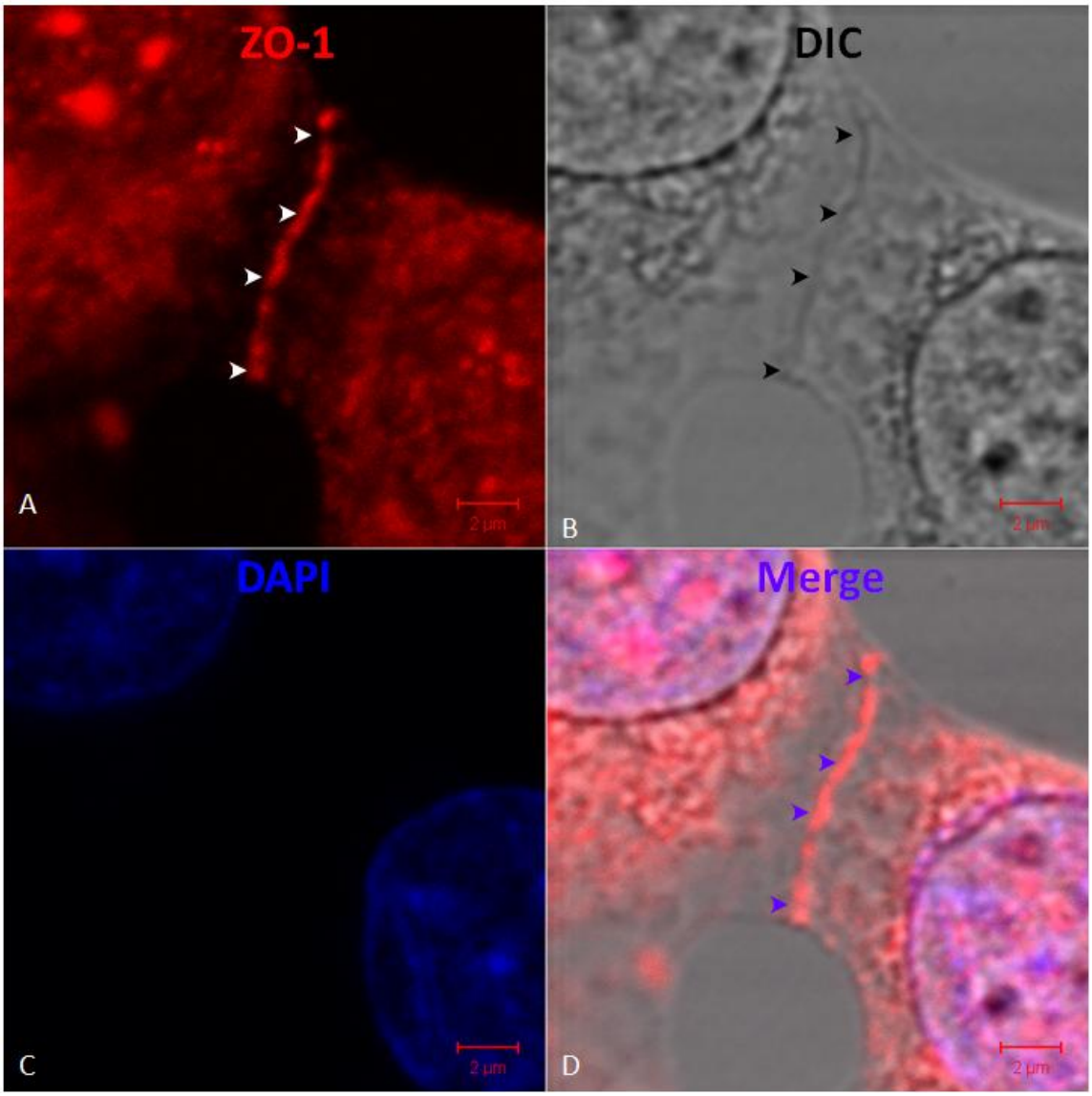

Figure 3.16: Confocal microscopy visualisation of ZO-1 in the E12.5POM cell line incubated in the non-proliferative conditions. (A) Strong ZO-1 staining is clearly visible at the junction where the cellular membranes of the two cells meet (white arrowheads). Pinhole size 110µm (B) Using differential interference contrast (DIC), the junction where the plasma membranes meet can be easily identified and appeared as a strong band (black arrowheads). (C) Nuclei, stained with DAPI, are clearly visible as dark blue circles on either side of the field of view. Pinhole size 1000µm (D) A merged image clearly shows that ZO-1 has localised to cell membrane at the points of contact between the two cells (purple arrowheads).

3.4.3 Formation of a functional barrier

The gold standard test to investigate the functionality of a barrier-forming endothelial or epithelial cell monolayer in culture is to measure the TEER. The higher the TEER levels, the tighter the barrier that has formed. The ability of the E12.5POM and E13.5POM cell lines to form a functional barrier was thus determined by making TEER measurements. The TEER levels of MDCK cells, which are known to form a functional barrier *in vitro*, were also measured in order to verify the accuracy of the experimental procedure. Cells at a concentration of 10^5cells/cm were seeded onto 12mm Transwell 0.4µm pore polycarbonate membranes. Resistance across the membrane was measured using silver electrodes with a multimeter over the course of 4 days. Triplicate readings were obtained from three sets of filters for each cell line under each condition. Resistance readings of blank filters were subtracted from experimental readings of filters with cells and resistance was then calculated per cm^2.

On days 1 and 2 no increase in TEER was noted for either the MDCK cells or periocular mesenchyme cells under either condition (Figure 3.17). By day 3 there was a large increase in the TEER levels of MDCK cells that was maintained over day 4 (Figure 3.17). No increase in TEER levels was observed over the course of 4 days for any experiment using either periocular mesenchyme cell line under either condition (Figure 3.17). This suggests that even though the cell lines express tight junctions when in the non-proliferative conditions, they do not form a functional barrier. The inability to form a barrier can most easily be explained by the presence of large gaps between the E12.5POM and E13.5POM cells that expressed tight junctions as visualised previously (Figure 3.15 D,E white arrows).

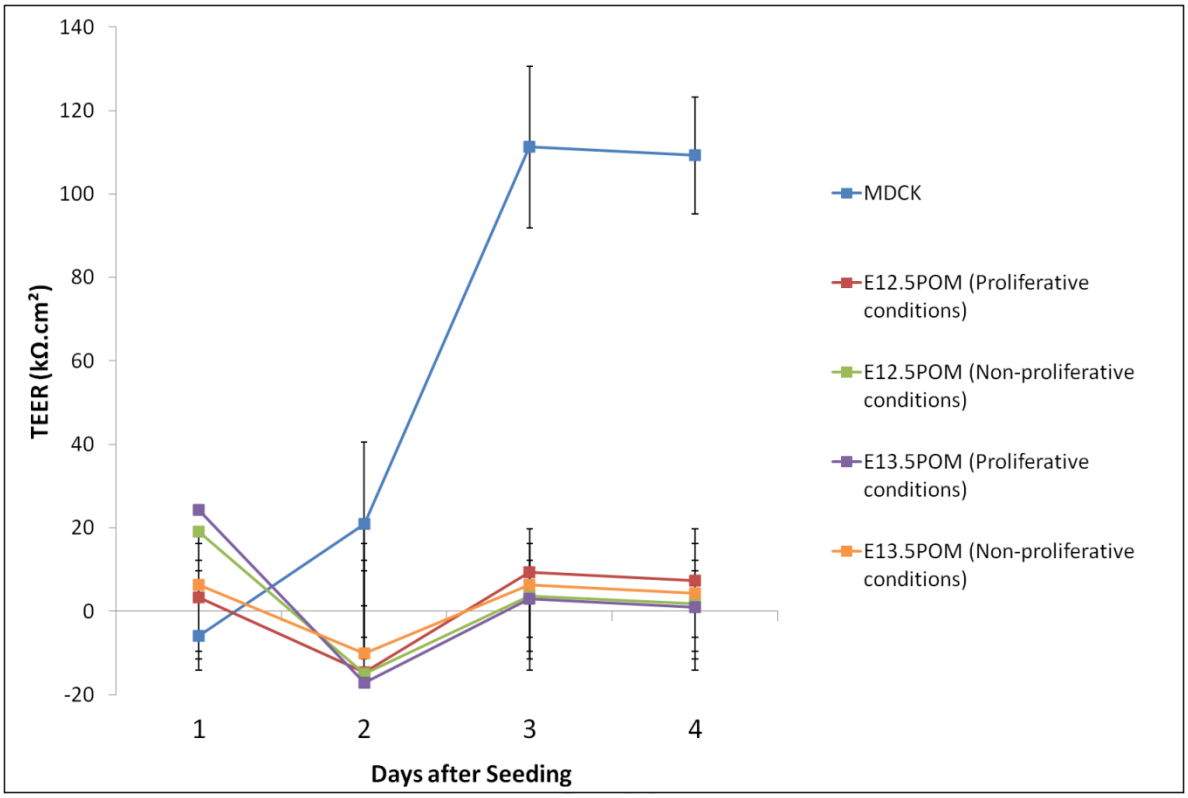

Figure 3.17: TEER measurements over 4 days for E12.5POM and E13.5POM incubated in the proliferative and non-proliferative conditions compared to MDCK cells. MDCK cells showed an increase in TEER levels after 3 days. This increase was maintained to day 4. None of the experiments using either the E12.5POM or E13.5POM cell lines resulted in any increase in TEER levels.

3.5 Culture of an Adult Corneal Endothelial Cell Line

One of the difficulties of attempting to study the development of the corneal endothelium *in vitro* is that there is no definitive molecular marker of the adult corneal endothelium. Relying on a single marker has previously led to some questionable results (Introduction and Aims - Section 1.3.1.2). In the present study it was thought that deriving an adult mouse corneal endothelial cell line would prove useful in the study of corneal endothelial development, proliferation and junction formation.

Corneas were dissected from the adult eyes and adherent tissue removed. However, it was apparent that it would be impossible to separate the endothelium from the rest of the cornea as has been reported for human corneas (Yue et al. 1989; Bednarz et al. 2001; Chen et al. 2001; Gao et al. 2010). Attempts were made to enzymatically

separate the corneas by treatment with 0.05% trypsin/EDTA or 5mg/ml Dispase (Sigma-Aldrich, USA) for 5-10 minutes at 37°C but these both proved to be unsuccessful.

An alternative approach was to culture the entire cornea, endothelial side down, on 35mm culture dishes with a coverslip flattening the cornea onto the surface of the dish to enable maximum contact between the endothelium and the dish (Figure 3.18 A). This technique resulted in the outgrowth of cells from the periphery of the cornea after just 1 day (Figure 3.18 B). These cells displayed either a fibroblastic or an epithelial morphology (Figure 3.18 C). After three days the cover slip as well as the cornea was removed, leaving only the cells that had become attached or had migrated away from the explants (Figure 3.18 D). These cells had, almost exclusively, a fibroblast morphology and, most likely, had migrated out from the corneal stroma. There were some hexagonal epithelial-type cells present that could either have been derived from the endothelium or the epithelium, but they could not be isolated or cultured alone as they were surrounded by fibroblasts. Therefore, despite many attempts, a homogenous culture of adult corneal endothelial cells could not be obtained and a cell line could not be derived from them.

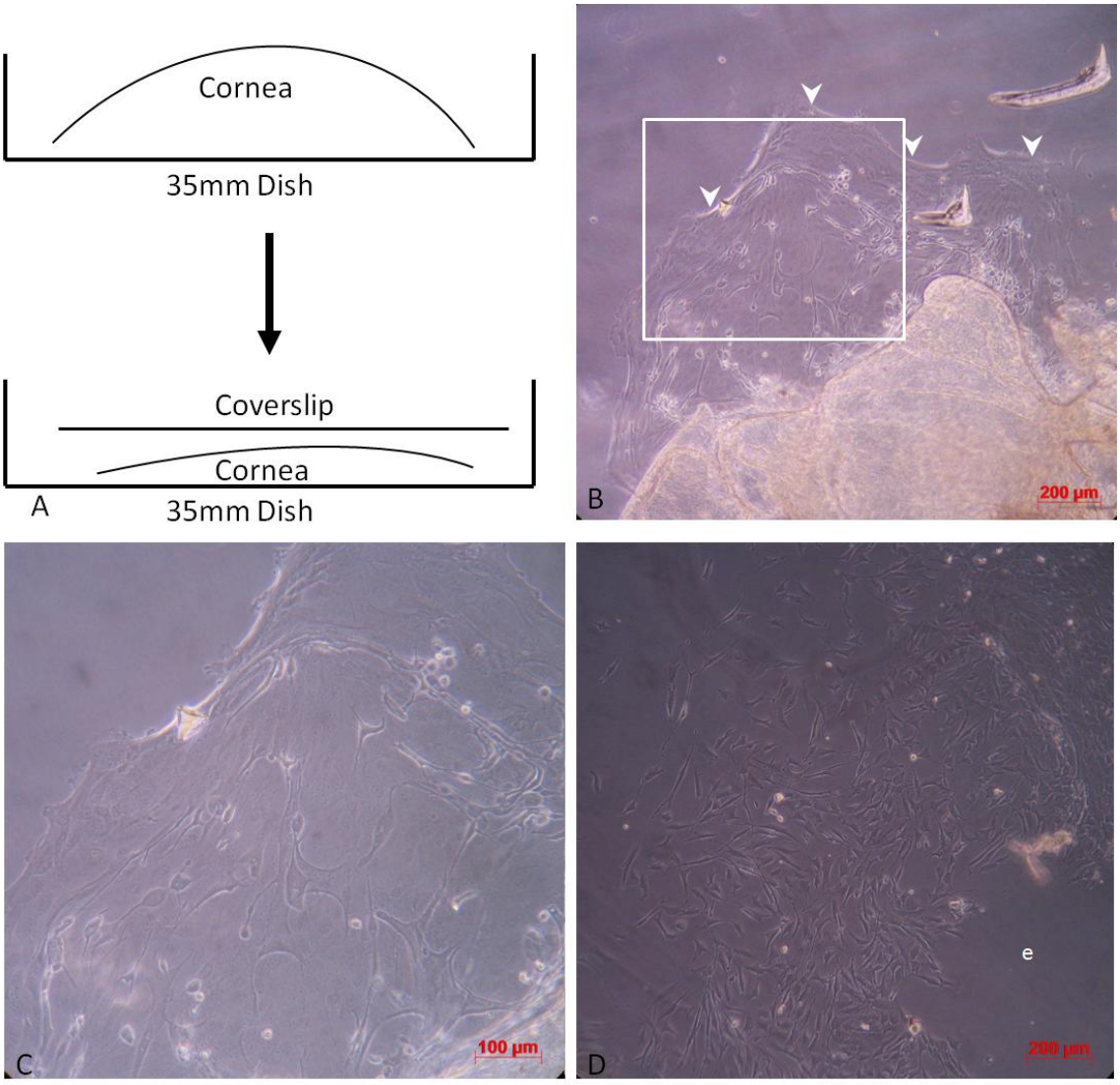

Figure 3.18: Primary cultures of adult mouse whole corneas. (A) Schematic representation (not to scale) of culturing technique for adult mouse corneas. Whole corneas were placed, endothelial side down, on 35mm tissue culture dishes. The cornea was then flattened onto the dish by placing a coverslip on it. (B) 1 day after plating. White arrowheads indicate border of migrating cells. The white box indicates the area represented by image C (C) Higher power magnification of the cells that have migrated away from the explant. (D)Cornea removed after 72 hours. 'e' indicates space where cornea used to be. Only migrated cells remain attached to the dish.

3.6 Culture of E12.5 and E13.5 Lenticular Epithelial Cell Lines

Signalling from the embryonic lens has already been determined to be critical to the development of the corneal endothelium (Genis-Galvez 1966). In particular, the lens epithelium has a crucial role to play in the proper formation of the anterior segment and in the differentiation (Beebe et al. 2000; Zhang et al. 2007) and migration (Lwigale et al. 2009) of the periocular mesenchyme. However, very little is known about the molecular basis of the role of the lens epithelium in development. In order to carry out analyses of lenticular epithelial cells, attempts were made to derive lenticular epithelial cell lines from E12.5 and E13.5 embryos. After isolating whole embryonic lenses by micro-dissection a variety of different techniques were attempted to grow and immortalise the embryonic lens epithelial cells. A summary of these methods is presented in Table 3.1.

Table 3.1: Culture Techniques Attempted to Derive a Lens Epithelial Cell Line

Medium*	**Coating on Dishes**	**Age of Lens**	**Form of Lenses**
DMEM	None	E12.5 and E13.5	Whole
DMEM	None	E12.5 and E13.5	Fragmented
DMEM	Laminin*[3]	E12.5 and E13.5	Whole
DMEM	Laminin	E12.5	Fragmented
DMEM	Polylysine*[4]	E12.5	Whole
DMEM	Polylysine	E12.5	Fragmented
DMEM	Polylysine	E12.5	Whole
DMEM	Polylysine	E12.5	Fragmented
DMEM/F12*[2]	Polylysine	E12.5	Whole
DMEM/F12	Polylysine	E12.5	Fragmented

* This indicates the basic medium used. All media contained antibiotics and 10% FBS

*[2] DMEM/F12 is a premade medium available from Gibco (Gibco, USA)

*[3] Refer to appendix B.6 for details of laminin coating of dishes

*[4] Refer to appendix B.7 for details of polylysine coating of dishes and wells

In the first series of experiments whole lenses from E12.5 and E13.5 embryos were cultured on 35mm plates (+/- 5 per dish), but they did not attach and remained as

floating spheres (Figure 3.19 A,B). These lenses were monitored over the course of a few days and were not seen to expand or grow in any way and eventually all lens tissues cultured in this manner died. The next technique attempted was to fragment the lens using tungsten needles and to seed the fragments into tissue culture dishes. It was hoped that the fragments containing the lens epithelial cells would be able to adhere and the cells would grow out while the developing fibre mass would remain non-adherent. However, none of the fragments adhered.

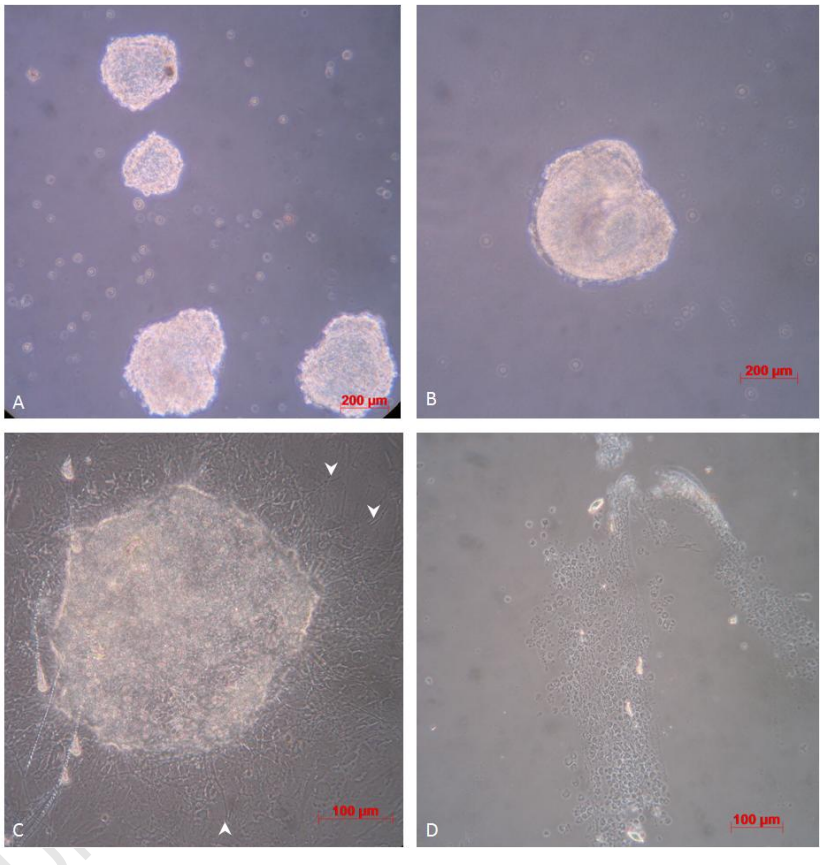

Figure 3.19: Primary cultures of E12.5 and E13.5 lenses derived from mouse embryos. (A-B) Whole lenses do not adhere to themselves or the uncoated tissue culture dishes. (C) Whole lenses attached to a poly-lysine coated dishes. Thin dendritic process extending away from the lens were visible (white arrowheads). (D) Small fragments of cuboidal shaped cells in culture containing fragmented lenses.

When dishes were coated with either laminin or polylysine an increase in the attachment of both whole lenses and lens fragments was seen on dishes coated with polylysine (Figure 3.19 C, D). No difference in attachment was noted on laminin coated dishes. In the case of the whole lenses, long thin processes were seen to grow out from the periphery of the lens (Figure 3.19 C – white arrowheads). It is possible that these

were fibres from adhering fibroblasts that had remained attached to the lens during the dissection. Patches of cuboidal cells were noted in two samples containing lens fragments (Figure 3.19 D). Due to their size and shape it was thought that these might be cells of the lens epithelium. The putative lens epithelial cells were dark and very small and did not proliferate for over 14 days in culture before finally senescing. Lastly, attempts to culture lenses in DMEM/F12 (Gibco, USA) instead of standard DMEM were not successful in promoting cell proliferation.

In summary, despite the multiple intensive efforts, all attempts to establish an embryonic lens epithelial cell line were unsuccessful.

3.7 Identification of a Presumptive Signalling Molecule Expressed in the Embryonic Lens

Numerous papers have identified the importance of the lens epithelium during the development of the corneal endothelium (Genis-Galvez 1966; Genis-Galvez et al. 1967; Beebe et al. 2000; Saika et al. 2001; Zhang et al. 2007). However, no candidate signalling molecules that could be responsible for the differentiation of periocular mesenchyme cells into corneal endothelial cells have been identified. Following the failure to establish lenticular epithelial cell lines in this study an alternative approach was required to identify signalling molecules expressed in the lens epithelium.

As part of the search for this elusive signal Prof. Beebe (Washington University in St. Louis) kindly shared some of his unpublished data. His laboratory carried out experiments using laser dissections which separated the E12.5 mouse lens epithelium from the E12.5 lens fibre mass. Microarrays were then used to compare the gene expression in the lens epithelium vs. the fibre mass. This series of experiments identified genes specifically expressed at E12.5 in the lens epithelium.

The aim was to identify a signalling molecule that is specifically expressed in the E12.5 lens epithelium that could potentially have a role to play in corneal endothelial development. To do this the microarray data from Prof. Beebe was mined for any genes

that could be of interest using KEGG. Numerous genes from the MAPK and Wnt signalling pathways were identified that were specifically expressed in the E12.5 lens epithelium (Beebe, unpublished data). Of particular interest, the analysis revealed that the signalling molecule follistatin (*Fst*) had a 94-fold up-regulation in the E12.5 lens epithelium when compared to the fibre mass.

One would expect a signalling molecule that is critical to the development of the corneal endothelium to be highly expressed during the period when differentiation of the periocular mesenchyme is occurring, with reduced expression during later developmental stages and in the adult lens. The expression of *Fst* in E12.5 (when the migrated periocular mesenchyme begins to differentiate into corneal endothelium), E15.5 (when the corneal endothelium is completely formed) and adult mouse lenses was therefore investigated using semi-quantitative RT-PCR.

RT-PCR reactions using primers specific to *Fst* were run on cDNA reverse transcribed from mRNA extracted from primary lenses. The PCR products were resolved on 2% agarose gels and bands were visualized by staining with ethidium bromide. The bands were then digitized in order to quantify the expression levels by examining the pixel density compared to the no template control. To establish whether the differences in expression were due to differences in total mRNA levels, RT-PCR reactions for the presence of the reference gene *Gus* were undertaken and quantified using the same protocol.

In all three experiments undertaken strong *Fst* expression was noted in the embryonic lenses with far less *Fst* in the adult lens (Figure 3.20 A). When quantified it was found that the E12.5 lens expressed 1.3 times more *Fst* than the E15.5 lens and 8.6 times more than the adult (Figure 3.20 B). There was no statistical difference in *Gus* expression in all three samples in any of the experiments (Figure 3.20 C,D). This result shows that *Fst* is highly expressed in the embryonic lens at E12.5 when the corneal endothelium is being formed (Kidson et al. 1999) and could possibly be a developmentally important signalling molecule involved in anterior segment formation.

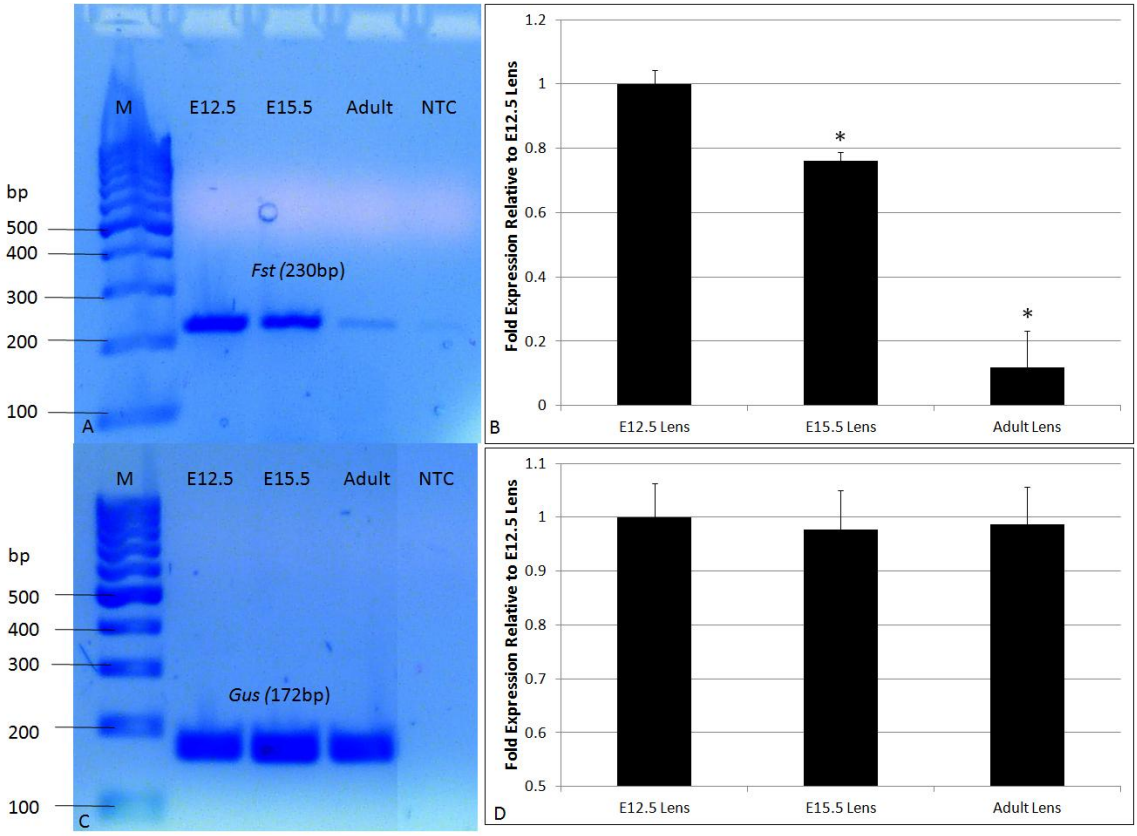

Figure 3.20: *Fst* mRNA expression in whole E12.5, E15.5 and adult mouse lenses. (A) RT-PCR analysis of *Fst* expression. (B) Digital quantification of *Fst* PCR gel by analysing pixel density (C) RT-PCR analysis of *Gus* expression. (D) Digital quantification of *Gus* PCR gel by analysing pixel density.
* indicates statistical significance ($p<0.05$). M = molecular weight marker, E12.5 = Lenses extracted from embryos at the E12.5 developmental stage, E15.5 = Lenses extracted from embryos at the E15.5 developmental stage, Adult = Lenses extracted from adult mice. NTC = No template control.

The potential effect that the presence of *Fst* would have was analysed by using KEGG. When processed using KEGG, *Fst* was identified as a signalling molecule involved in the Nodal signalling pathway (Figure 3.21). When up-regulated, *Fst* inhibits activin which, in turn, leads to an up-regulation of Nodal. Nodal is able to bind its receptors in the cell membrane and activate a cascade of Smad proteins which leads to the expression of a variety of genes involved in differentiation processes. One of the targets in this pathway is *Pitx2* which, as already mentioned, has an important role to play in the anterior segment. This, together with the lack of *Pitx2* expression in either of the immortalised cell lines (Figure 3.12) means that there is a distinct potential for Nodal derived *Pitx2* expression to play an important role in the formation of the cornea. *Fst*, produced by the lens epithelium, could potentially be the signal which leads to an up-

regulation, through the Nodal pathway, of *Pitx2* which in turn negatively regulates *Foxc1* and leads to the differentiation of periocular mesenchyme into corneal endothelial cells. Due to this reasoning *Fst* was identified as a presumptive lenticular-based signal to be studied further.

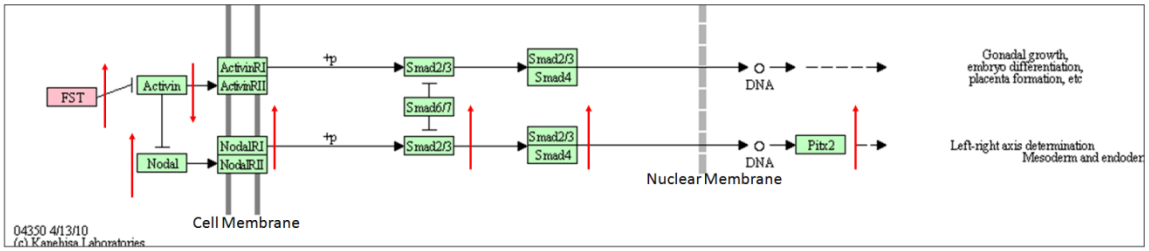

Figure 3.21: Selected overview of Nodal signalling pathway. Blocks in green represent selected proteins in Nodal signalling pathway. Red arrows represent the cascade of events that occur due to an increase in *Fst*, highlighted in red.
Image adapted from:
http://www.genome.jp/kegg-bin/show_pathway?1331653910753/mmu04350.args

3.8 The Effect of *Fst* on the E12.5POM and E13.5POM Cell Lines

As reasoned above, *Fst* could potentially be an embryonic lens derived signalling molecule with a role to play in the differentiation of periocular mesenchyme into corneal endothelium. To test this hypothesis human recombinant *Fst* produced in *E. coli* (Prospecbio, USA) was added to the culture medium of both the E12.5POM and E13.5POM cell lines.

To establish a suitable concentration of *Fst* with which to treat the cell lines, a range of concentrations from 10ng/ml - 100ng/ml of *Fst* were added to the 35mm dishes of confluent E12.5POM cells at the non-proliferative conditions. It was found that all cultures with an *Fst* concentration higher than 50ng/ml resulted in complete cell death after 3 days. This is consistent with *Fst* activating Nodal whose signalling pathway is known to be an inducer of apoptosis (reviewed by Wang et al. 2007). At 50ng/ml and below cell death still occurred but cultures were able to survive over a 10 day culture period. The effects of *Fst* have been tested on human endometrial stromal cells, embryonic stem cells and pituitary tumour cells (Tierney et al. 2004; Gerrard et al. 2005; Kanasaki et al. 2011). While all three of the above mentioned studies had different experimental designs and objectives, they all found that *Fst* at a concentration of 50ng/ml was suitable to induce a variety of effects on the cells in question.

Furthermore, *Fst* concentrations lower than 50ng/ml were not sufficient to induce any significant changes in human endometrial stromal cells and embryonic stem cells (Tierney et al. 2004; Gerrard et al. 2005). For this reason, in this preliminary study, 50ng/ml was used to treat the E12.5POM and E13.5POM cell lines at the non-proliferative conditions.

When *Fst* was added to the culture medium of cells incubated under the non-proliferative conditions the cells retained their polygonal morphology and grew in small tightly packed groups as before (Figure 3.22 A,B). Growth rate analyses could not be accurately completed due to the partial cell death that occurred.

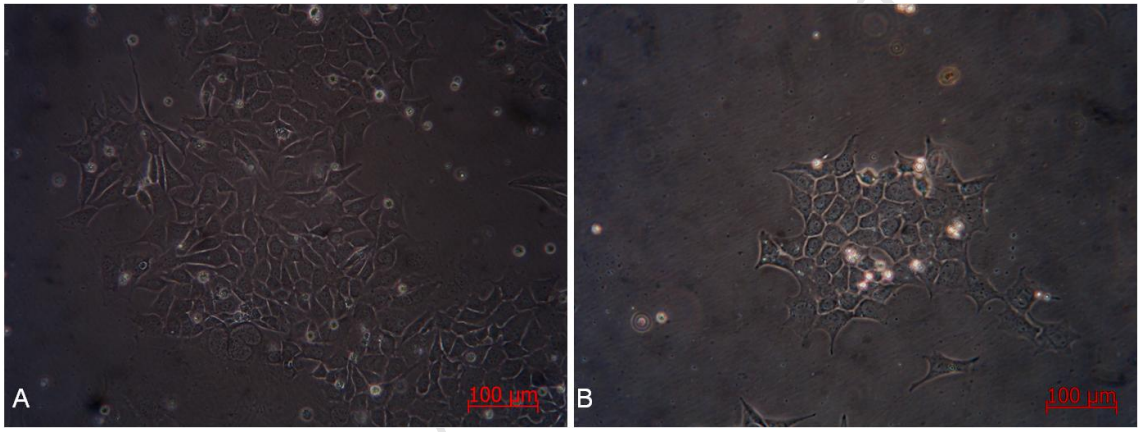

Figure 3.22: Morphology of *Fst* treated E12.5POM and E13.5POM cell lines. (A) E12.5POM and (B) E13.5POM cell lines incubated at non-proliferative conditions with 50ng/ml *Fst*. Both cell lines grew in small tightly packed groups with each cell having a defined, bright edge and polygonal epithelial-like morphology.

It was hypothesised that the addition of 50ng/ml *Fst* to the culture medium would result in a change in gene and protein expression in the cell lines. Gene expression analyses using qPCR and ICC for the presence of N-cadherin and ZO-1, as has been done above, were thus undertaken on *Fst* treated E12.5POM and E13.5POM. *Fst* treatment had no statistically significant effect on *Foxc1* expression, though a slight down-regulation of *Foxc1* expression in *Fst* treated cells was noted in both cell lines (Figure 3.23). A 1.6-fold down-regulation of *Tgfβ1i4* expression in E12.5POM and a 1.7-fold down-regulation of *Tgfβ1i4* expression in the E13.5POM was observed in cells treated with *Fst* (Figure 3.24). E12.5POM and E13.5POM cells cultured with *Fst* did not express any *Pitx2* (Figure 3.25).

Both cell lines had a peri-nuclear pattern of N-cadherin expression when treated with *Fst* (Figure 3.26). The same pattern of expression was observed when *Fst* was left out the culture medium (Figure 3.13 D,E). The cell lines had membrane bound ZO-1 expression when treated with *Fst* (Figure 3.27). The same ZO-1 expression pattern was noted when *Fst* was left out the culture medium (Figure 3.15 D,E) *Fst* did not increase TEER levels in either cell line with readings being statistically equivalent to zero (Figure 3.28). Thus, this preliminary study indicates that *Fst* does not have an effect on the gene or protein expression of the cell lines.

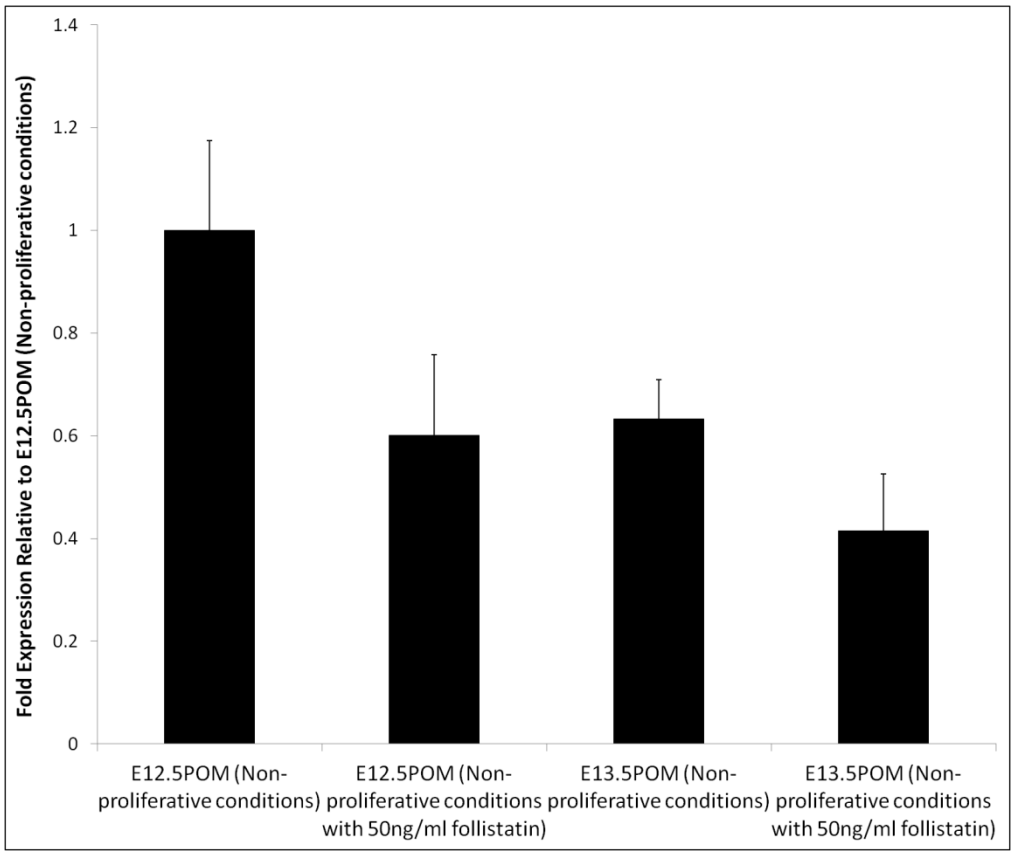

Figure 3.23: *Foxc1* mRNA expression in the E12.5POM and E13.5POM cell lines incubated at the non-proliferative conditions with and without 50ng/ml *Fst*. Relative fold expression was analysed by qPCR and normalised to the reference gene *Gus*.

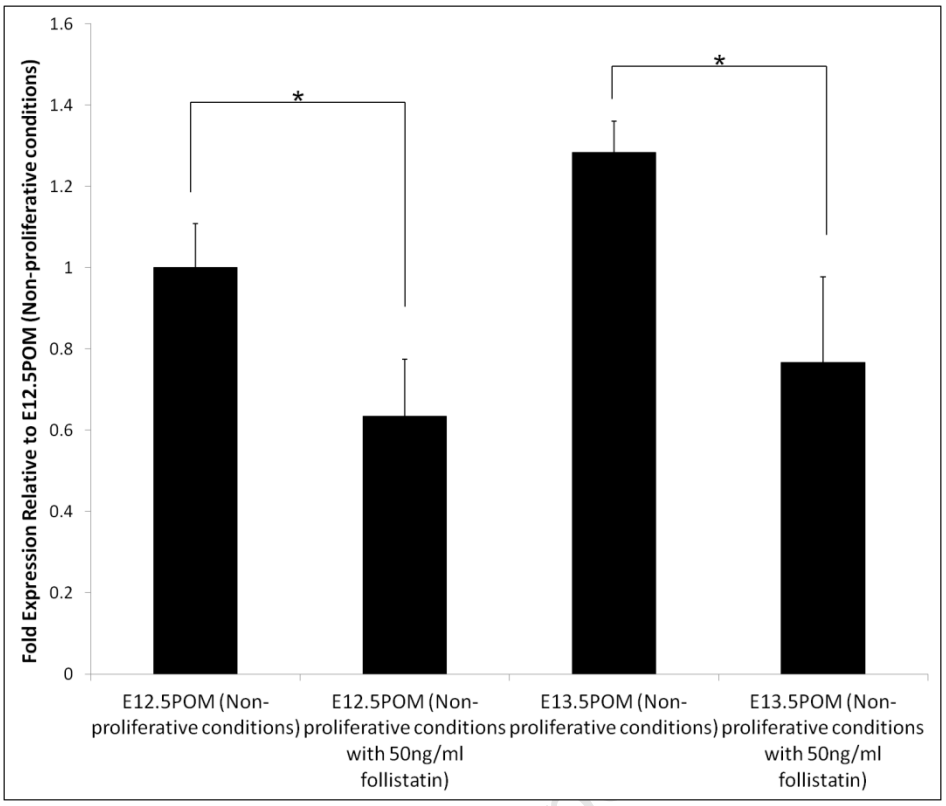

Figure 3.24: *Tgfβ1i4* mRNA expression in the E12.5POM and E13.5POM cell lines incubated at the non-proliferative conditions with and without 50ng/ml *Fst*. Relative fold expression was analysed by qPCR and normalised to the reference gene *Gus*. * indicates statistical significance ($p<0.05$).

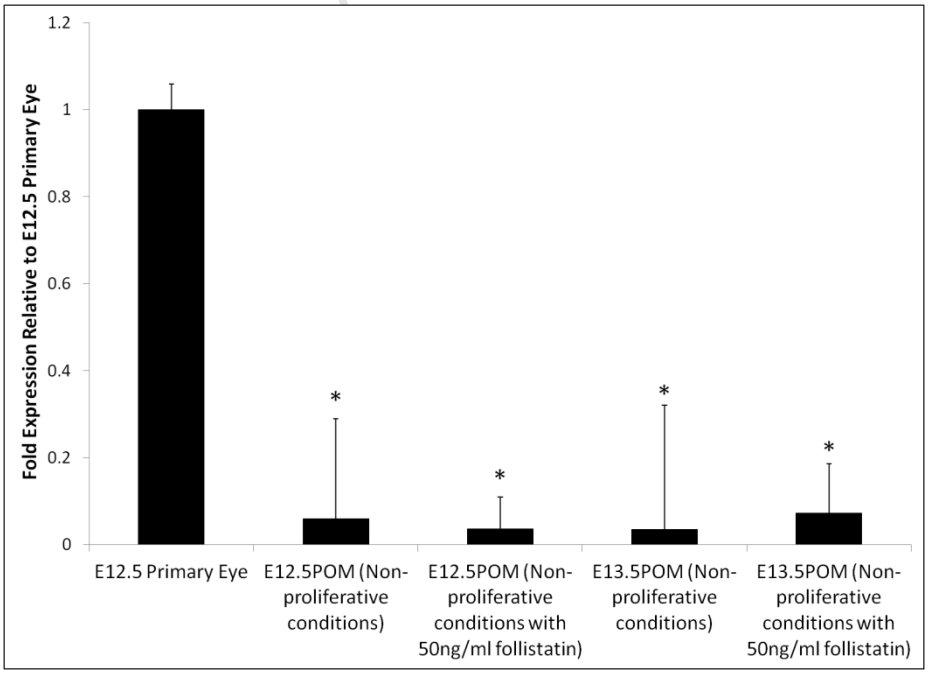

Figure 3.25: *Pitx2* mRNA expression in the E12.5POM and E13.5POM cell lines incubated at the non-proliferative conditions with and without 50ng/ml *Fst*. Relative fold expression was analysed by qPCR and normalised to the reference gene *Gus*. * indicates statistical significance ($p<0.05$).

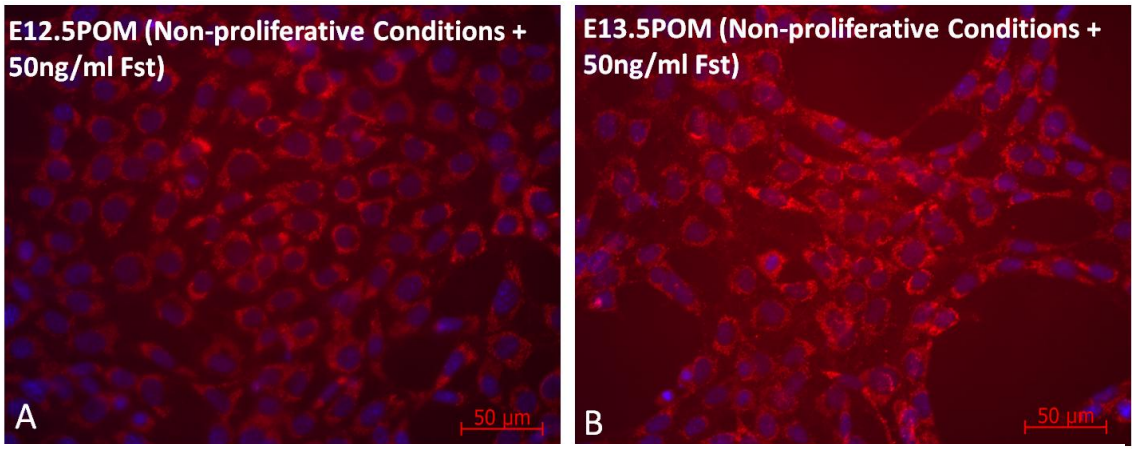

Figure 3.26: Immunodetection of N-cadherin in the E12.5POM and E13.5POM cell lines incubated at the non-proliferative conditions with 50ng/ml *Fst*. Both E12.5POM (A) and E13.5POM (B) had a very strong peri-nuclear localisation of N-cadherin in every cell.

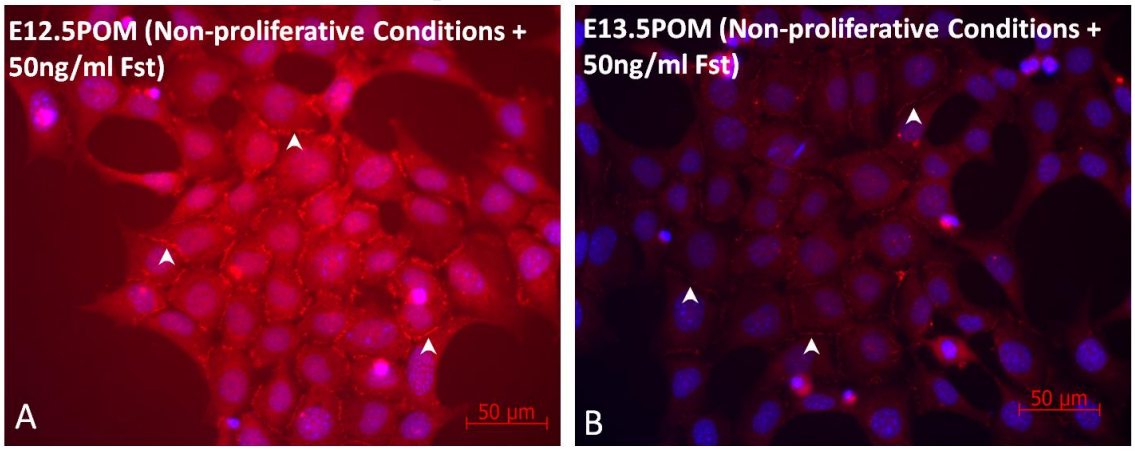

Figure 3.27: Immunodetection of ZO-1 in the E12.5POM and E13.5POM cell lines incubated at the non-proliferative conditions with 50ng/ml *Fst*. Both E12.5POM (A) and E13.5POM (B) showed the presence of ZO-1 in junctions between cellular membranes in the large majority of cells (examples indicated by white arrowheads).

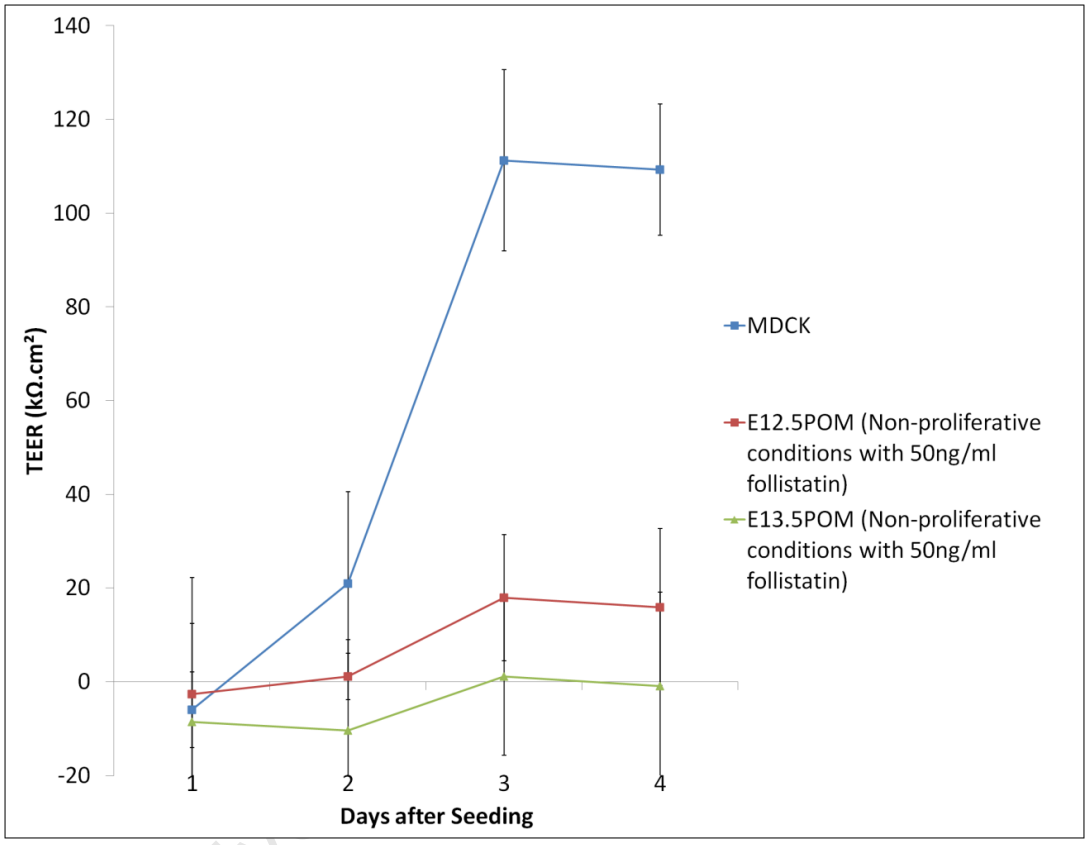

Figure 3.28: TEER measurements over 4 days for E12.5POM and E13.5POM incubated in non-proliferative conditions with 50ng/ml *Fst* compared to MDCK cells. MDCK cells showed an increase in TEER levels after 3 days. This increase was maintained to day 4. The E12.5POM and E13.5POM cell lines did not have any increase in TEER levels.

Chapter 4: Discussion

The vertebrate eye is one of the most intricate and important organs in the human body. It requires a host of different tissues to work in perfect synergy in order to function correctly. This complexity is reflected in the involved and multi-faceted developmental process that brings together cells from the neuroectoderm, ectoderm, and the surrounding mesenchyme. This developmental process is dependent on many temporal and spatial molecular cues which guide and direct the multipotent embryonic tissues into specialised adult ones.

In all these regards the cornea, a highly specialised and integral part of the eye, is certainly no exception. The complexity of the cornea stems from the fact that it not only acts as a physical barrier to the environment and protects the eye, but also has a critical role to play in the optical pathway. To fulfil these dual roles the cornea has certain specific characteristics that make it unique; transparency, strength and lack of a vascular system. These qualities also make it the perfect candidate for transplantation and regenerative medicine. So, for example, when there is a decrease in density in the corneal endothelium through aging, glaucoma or Fuchs' dystrophy and corneal opacity and loss of visual function occurs, penetrating or endothelial keratoplasty can be highly successful (Price et al. 2010). However, the severely short supply of donor corneas (Lai et al. 2006; Price et al. 2010; Peh et al. 2011), rapid loss of endothelial cells post-surgery (Laing et al. 1976; Price et al. 2010; Peh et al. 2011), and low proliferation rate of adult corneal endothelial cells (Joyce et al. 1996) all suggest that more novel therapeutic strategies are required to replenish damaged and diseased corneas.

An ideal avenue of treatment would be to use induced pluripotent stem (iPS) cells. Theoretically, patient derived iPS cells could be multiplied *in vitro* until a sufficient number were obtained and then directed to differentiate into corneal endothelial cells to be transplanted. Multiplying iPS cells in culture would overcome two of the major obstacles hindering the effectiveness of keratoplasty, namely, the short supply of donor corneas and the inability to proliferate adult corneal endothelial cells *in vitro*.

Furthermore, iPS cells offer a potentially unlimited source of personalised adult cells, allowing for multiple treatments to overcome any further damage or loss of corneal endothelial cells over time.

For stem cell derived therapies to come to fruition one would need to be able to successfully direct the differentiation of iPS cells into corneal endothelial cells. In order to do this the developmental processes that control the change from embryonic cell to adult cell need to be recapitulated *in vitro*. Thus, a deeper understanding of the precise molecular mechanisms and cellular events that control periocular mesenchyme migration and differentiation into corneal endothelium is vital.

Studies into the development of mammalian corneas *in vivo* are complicated due to lack of access to the developing embryonic eye. One approach would be to study the development of the corneal endothelium using an *in vitro* model. The overall objective of this project was to develop an *in vitro* system in which one could study the development of the corneal endothelium from its presumptive precursor population, the periocular mesenchyme.

4.1 Characterisation of the E12.5POM and E13.5POM cell lines

In order to obtain cell lines from the mouse periocular mesenchyme that could be used to model the formation of the corneal endothelium the correct developmental stages had to be identified. At E12.5, mesenchymal migration into the space between the surface ectoderm and the lens vesicle is at its peak and it is the periocular mesenchyme cells that migrate adjacent to the developing lens epithelium and go on to form the corneal endothelium (Kidson et al. 1999). At E13.5 the developing cornea begins to separate from the lens epithelium to form the anterior chamber (Kidson et al. 1999). These two time points mark the key developmental events that initiate the formation of the fully mature corneal endothelium. Thus, mouse periocular mesenchyme from the E12.5 and E13.5 developmental stages was cultured. These primary cultures were then immortalised using the SV40 large T-antigen and named E12.5POM and E13.5POM respectively. The cell lines derived by this method formed homogenous cultures of

stellate cells and expressed the SV40 oncoprotein in the nucleus of every cell. Both the E12.5POM and E13.5POM cell lines were passaged over 40 times with no significant changes in the cell growth or morphology. Taken together these results indicate that stable cell lines of the E12.5 and E13.5 periocular mesenchyme were established.

The first step in characterising the cell lines was to examine their proliferative ability in the presence or absence of the oncoprotein. At 33°C, the permissive temperature for the activation of the large T-antigen, both cell lines grew rapidly while MEFs failed to proliferate. Proliferation at this temperature was therefore reasoned to be due to the activation of the large T-antigen in the cell lines. The failure of the non-immortalised MEFs to proliferate at 33°C suggests that this is not a suitable temperature to grow normal cells. A previous study came to the same conclusion when they found that non-immortalised MEFs did not multiply at 33°C (Jat et al. 1991).

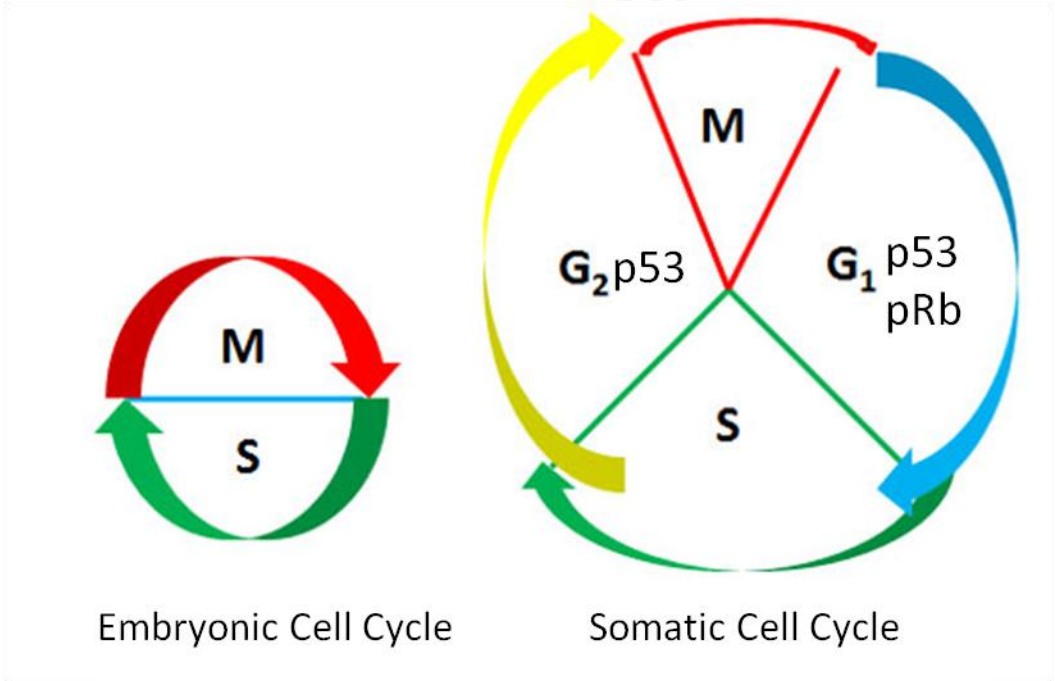

Figure 4.1: Comparison of the embryonic and somatic cell cycles. (adapted from Tang 2010)

At 39°C the large T-antigen is inactive and therefore growth at this temperature is not due to the oncogene. It was expected that the immortal cell lines at 39°C would grow at a slower rate than the cell lines at 33°C (when the large T-antigen is active). Surprisingly, the cell lines in this study grew at a similar rate at both the non-permissive

and permissive temperatures. A possible explanation as to why the cell lines grew at the non-permissive temperature is due to the embryonic origin of the cell lines and their unique cell cycle as compared to adult cells. Adult somatic cells are delayed at the G1/S regulation checkpoint by the tumour suppressors p53 and retinoblastoma (pRB) and at the G2/M checkpoint by p53 (Figure 4.1). Thus, at both these points, cell division in adult cells is delayed for an interval (the time varies depending on the cell type and the environment). When adult cells are infected with the SV40 large T-antigen both p53 and retinoblastoma are inactivated. This allows cells to pass through both the G1/S and G2/M checkpoints unchecked which results in their rapid proliferation in culture. When SV40 is inactivated, both p53 and retinoblastoma are once again functional and can delay cell division at the G1/S and G2/M checkpoints once more.

Embryonic cells have a markedly different cell cycle to somatic cells. Embryonic cells express an abundance of p53 but all p53-mediated responses are inactive as p53 is unable to translocate to the nucleus and activate its downstream targets (Hansen et al. 1997). Embryonic cells also express a large amount of pRB, but the vast majority of the pRB is in the inactive hyperphosphorylated form meaning that it too is also unable to activate its downstream targets (Savatier et al. 1994). The inactivity of both p53 and pRB means that embryonic cells lack G1/S and G2/M checkpoints and as such do not undergo cell cycle arrest (reviewed by Tang 2010 - Figure 4.1). This allows them to proliferate rapidly, a property that is necessary during development.

So, when embryonic cells, such as those from the periocular mesenchyme as used in this study, are immortalised with SV40, inactivating the large T-antigen will not delay cellular proliferation. Cell lines derived from embryonic tissues would thus proliferate at the same rate as any other embryonic cells, which explains why the growth rate of normal MEFs at 39°C was similar to the immortal cell lines.

In order for the cell lines to serve as a useful tool for understanding the development of the corneal endothelium it was essential to demonstrate that they maintained the endogenous expression levels of key genes. qPCR analyses showed that the *in vivo* *Foxc1* expression pattern was retained in the E12.5POM and E13.5POM cell lines.

Tgfβ1i4 has been described as been repressed by *Foxc1* and is highly expressed at E13.5 *in vivo* (Napier 2005; Sommer et al. 2006). In the present study qPCR analyses for *Tgfβ1i4* indicated that the cell lines retained their *in vivo* expression pattern and the relationship between *Tgfβ1i4* and *Foxc1* was similar to what has been noted in the periocular mesenchyme at E12.5 and E13.5. The gene expression analyses undertaken were not broad enough to prove that the immortal cell lines had maintained their endogenous gene expression profiles. To establish this, global gene expression studies using microarrays or deep RNA sequencing would have to be undertaken.

It was also found that the cell lines did not express *Pitx2*. *In vivo, Pitx2* is strongly expressed in E12.5 in the periocular mesenchyme of the mouse embryo (Semina et al. 1996) and expression is maintained in the developing corneal stroma and endothelium by E14.5 (Kitamura et al. 1999; Gage et al. 1999). The lack of *Pitx2* in either cell line is thus different from what would be expected in the native tissue. It is possible that the isolation and immortalisation procedure has altered the gene expression of the periocular mesenchyme cells. Caution must thus be taken when extrapolating the *in vitro* results to the *in vivo* development of the corneal endothelium because even though the E12.5POM and E13.POM cell lines are highly similar to the native tissues at E12.5 and E13.5, they are not identical.

4.2 Inducing a Mesenchymal-to-Epithelial Transition (MET) in the E12.5POM and E13.5POM Cell Lines

MET is the essential developmental process that involves the transition from an unspecialised, loosely packed, motile, group of mesenchymal cells to a differentiated, densely packed, polygonal, continuous sheet of epithelial cells. MET has been extensively studied in the transition of kidney mesenchymal cells to kidney epithelium (Ekblom 1989; Rothenpieler et al. 1993; Barasch et al. 1999; Cheng et al. 2003). While studying MET in the kidney has allowed the morphological changes that occur during this transition to be well characterised, the molecular mechanisms responsible for this phenotypic change remain to be elucidated. Furthermore, the MET that occurs in the anterior segment when periocular mesenchymal cells differentiate into corneal

endothelium has not been studied. Cells from the periocular mesenchyme region migrate into the space between the lens and the surface ectoderm. During this migratory period the cells are influenced by signals from the surrounding tissue and microenvironment that induce a reduction in growth rate, changes in morphology and gene expression and initiate the formation of cell junctions. These changes induce a shift in the cells from a mesenchymal to an epithelial phenotype. The cells that have migrated directly adjacent to the lens are influenced by additional paracrine signalling from the lens that transforms them into fully mature corneal endothelial cells (Beebe et al. 2000; Zhang et al. 2007).

The main aim of this study was to encourage the differentiation of the E12.5POM and E13.5POM cell lines into corneal endothelial cells by inducing a MET in culture. Following the ineffectiveness of culture at the non-permissive temperature to hinder cell growth an alternative approach was needed to obtain a slowly dividing monolayer of cells. Cell proliferation was thus inhibited by reducing the level of growth factors present in the culture medium by decreasing the serum concentration. Reducing the serum concentration to 2% FBS was most effective in reducing proliferation when the cells were cultured at 39°C and so these conditions were considered the non-proliferative conditions.

Culture at the non- proliferative conditions resulted in both cell lines changing to a polygonal, epithelial like shape and growing in a tessellated, cobblestone pattern. These morphological characteristics are similar to what has been noted in human and murine corneal endothelial cells when they have been cultured *in vitro* (Fabricant et al. 1981; Hyldahl 1984; Engelmann et al. 1989; Joo et al. 1994; Joyce et al. 1996). The morphology of the cell lines was thus more similar to corneal endothelial cells than to mesenchymal cells at the non-proliferative conditions. This morphology change is a good initial indicator that MET had taken place.

The change in morphology instigated an investigation into the gene expression of the two key developmental genes, *Foxc1* and *Tgfβ1i4*. It was found that there was a shift in gene expression with a significant decrease in *Foxc1* and an increase in *Tgfβ1i4.*

A reduction in *Foxc1* has been shown to reduce the proliferative ability of embryonic periocular mesenchyme cells *in vivo* (Iwao et al. 2009) as well as cardiac neural crest cells *in vitro* (Seo et al. 2006). The down-regulation of *Foxc1* has also found to be necessary for the development of the cornea, lacrimal gland and skeletal muscles into fully mature adult cells (Kidson et al. 1999; Mattiske et al. 2006; Saleem et al. 2001; Savage et al. 2010). Similarly, increased levels of *Tgfβ1i4* have been shown to inhibit the proliferation of a variety of cancer cell lines (Kawamata et al. 2004; Gupta et al. 2003; Kester et al. 1997) and are associated with the promotion of differentiation in the transition from mouse periocular mesenchyme into corneal endothelium (Thut et al. 2001; Sommer et al. 2006) and rat cardiac myofibroblasts into cardiac muscle (Yan et al. 2011).

The change in morphology together with the shift in gene expression indicates that the E12.5POM and E13.5POM cell lines represent a population of cells that have initiated a progression to a less proliferative and more differentiated state and are now are more similar to adult corneal endothelial cells than periocular mesenchyme cells.

The most critical step in the transition from loosely associated periocular mesenchyme cells to a continuous sheet of corneal endothelial cells is the formation of cell junctions. Adherens junctions start to form during periocular mesenchyme migration and provide a scaffold that triggers the formation of tight junctions in a discontinuous band around the apical surface of mature corneal endothelial cells. However, the mechanisms controlling the formation of cell junctions are poorly understood. With the view of improving the current understanding of the requirements for cell junction formation a preliminary study investigating the presence of adherens and tight junctions in the E12.5POM and E13.5POM cell lines was undertaken.

Under any conditions both cell lines had vast intracellular stores of N-cadherin and were able to form adherens junctions. It was deduced that the cytoplasmic stores of N-cadherin in the cell lines were situated in vesicles in the Golgi apparatus based on their location and the fact that N-cadherin has previously been shown to be present in the Golgi apparatus of both rat fibroblasts and mouse myoblasts (Mary et al. 2002). Mary

et al. (2002) also showed that that cell-to-cell contact promoted N-cadherin redistribution to the cell membrane. These findings support the theory that cell-to-cell contact could mediate the rapid formation of adherens junctions in the migrating periocular mesenchyme.

It has previously been shown that *Foxc1*$^{-/-}$ periocular mesenchyme cells *in vitro* express intracellular N-cadherin but do not form adherens junctions (Mgwebi 2004; Napier 2005). It is thus suggested that *Foxc1* expression plays a crucial role in regulating the distribution of N-cadherin to the cell membrane and is necessary for the initial establishment of adherens junctions in the periocular mesenchyme. It is possible that the failure to traffic N-cadherin in *Foxc1*$^{-/-}$ cells is a result of their inability to perceive cell-cell contact. However, the mechanism of how *Foxc1* might control the shuttling of N-cadherin has not been studied.

There is a large body of evidence to suggest that in the transition towards an epithelial phenotype adherens junctions act as a trigger for the formation of tight junctions (reviewed by Steed et al. 2010). In the present study tight junctions only formed in the cell lines when *Foxc1* was down-regulated. Cells that maintained *Foxc1* expression did not form tight junctions. In fact, no ZO-1 expression of any form was ever noted in these cells. This was an interesting result as the cell lines that maintained *Foxc1* expression were able to form adherens junctions which creates an appropriate scaffold for the formation of tight junctions. Additionally, cell lines that did not express any initial *Foxc1* did not form tight junctions in the same culture system. It is thus suggested that the presence of adherens junctions together with the **transient** expression of *Foxc1* is necessary for the formation of tight junctions.

The transient expression of *Foxc1* may act as the trigger for the initiation of tight junction formation but is not sufficient by itself to form a tight junction. ZO-1 connects tight junctions to the actin cytoskeleton of the cell and thus its expression must also be up-regulated in order for tight junctions to form. In the present study ZO-1 was only expressed in the cell lines when in reduced serum indicating that there is an activity in serum that inhibits ZO-1 expression and thus inhibits the formation of tight junctions.

Furthermore, ZO-1 expression in MDCK cells was not affected by the presence of serum which suggests that the activity of serum on ZO-1 is specific to the periocular mesenchyme cell lines. It is likely that a similar inhibitory signal prevents ZO-1 expression in the periocular mesenchyme *in vivo*. It is suggested that an unknown signal inhibits the expression of ZO-1 in the periocular mesenchyme cells when the cells surround the optic cup and before they begin to migrate. As the periocular mesenchyme cells then ingress into the region between the lens and surface ectoderm they are no longer acted upon by this inhibitory signal. When the periocular mesenchyme cells reach the front of the eye, signalling from the developing lens is able to induce complete differentiation of periocular mesenchyme into corneal endothelial cells by activating the transcription of ZO-1 and the subsequent formation of tight junctions.

If serum had an inhibitory activity on the cell lines then one would expect additional changes in the cell lines in the complete absence of serum. When the E12.5POM cell line was grown in serum free conditions the cells no longer adhered to the culture dish and grew as spheres. It is hypothesised that in the complete absence of serum there is nothing inhibiting the formation of tight junctions in these cells. This results in the formation of tightly packed balls of cells that adhere more strongly to one another than to the culture dish. Investigations into the presence of cell junctions in these spheres would support this theory.

It is interesting to note that the spheres in the present study were similar to those induced using sphere forming assays (Yokoo et al. 2005; Mimura, et al. 2005a; Yamagami, Yokoo, et al. 2006; Amano et al. 2006; Huang et al. 2010; Yu et al. 2011). In all of these studies the researchers attempted to isolate bovine (Huang et al. 2010; Yu et al. 2011 - Figure 4.2), rabbit (Mimura, et al. 2005a), or human (Yokoo et al. 2005; Yamagami, Yokoo, et al. 2006; Amano et al. 2006) corneal endothelial precursors *in vitro*. To do this the corneas were divided into peripheral and central regions and cultured in DMEM/F12 medium with bFGF (from 20-40ng/ml) and EGF (from 20-40ng/ml) added as growth factors. In all cases serum free media was used to culture the endothelial precursor cells and under these conditions they formed spheres in

culture (Figure 4.2). It was also found that the rate of sphere formation from the peripheral cells was significantly higher than from the central region of the cornea in rabbit, cows and humans. These various studies came to the same two conclusions. Firstly, that culturing the peripheral region of the cornea in serum free medium allows one to isolate corneal endothelial precursor cells and secondly, that these precursor cells are located in the limbus. The theory that corneal endothelial precursors are located in the limbus is supported by the fact that corneal progenitor spheres have also been isolated from primary cultures of adult trabecular meshwork, contained within the limbus, by using serum free media (Gonzalez et al. 2006). Furthermore, rabbit precursor spheres were able to form adult corneal endothelial like cells when transplanted into corneal endothelial-deficient rabbits (Mimura et al. 2005b). It was proposed that the spheres were able to differentiate into adult like cells due to inductive signals from the surrounding environment after transplantation.

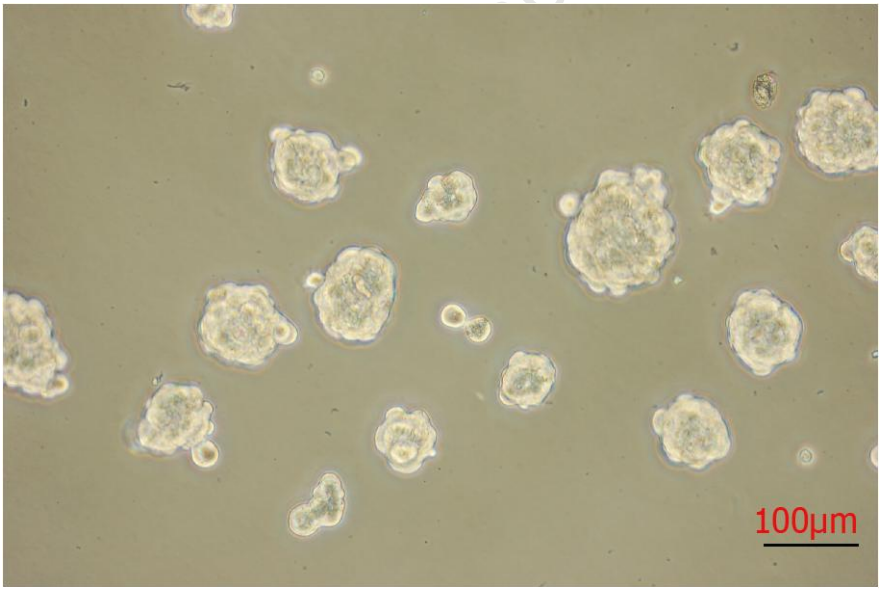

Figure 4.2: Bovine corneal endothelial progenitor cells in serum free medium. (taken from Yu et al. 2011)

The highly similar morphology of the spheres formed by the E12.5POM cell line in the present study compared to corneal endothelial progenitors (Figure 4.2) under similar culture conditions suggests two things. Firstly, that in absence of all inhibitory factors that are present in serum the E12.5POM cell line initiates MET and forms adult corneal endothelial precursor cells. This is similar to what is hypothesised to occur *in vivo* as

the periocular mesenchyme cells that have ingressed into the region over the lens epithelium have migrated away from the inhibitory activity that holds the cells in a mesenchymal phenotype and can thus undergo MET.

Secondly, these results suggest that the E12.5POM cell line has retained its ability to differentiate into a fully mature adult corneal endothelium but that this differentiation requires additional inductive signals to complete the transformation. This is similar to the *in vivo* development of the corneal endothelium as the completion of MET requires inductive signals that originate from the lens epithelium.

One of the broad aims of the present study was to investigate the effect of a candidate signalling molecule, expressed by the embryonic lens, on the E12.5POM and E13.5POM cell lines. Analyses of microarray data (generously shared by Prof. Beebe) indicated that *Fst* had a 94-fold up-regulation of expression in the E12.5 lens epithelium vs. the E12.5 lens fibre mass. The results from the present study showed that high levels of *Fst* were expressed in the mouse E12.5 lens with lower expression in the E15.5 lenses and very little *Fst* in the adult lens. A drawback of the *Fst* gene expression results in the present study was that mRNA was extracted from the entire lens and not just the lens epithelium. The lens epithelium forms only a small fraction of the cells in the embryonic lens and thus the expression of *Fst* could not be proven to originate from the lens epithelium. What the results do suggest is that *Fst* is highly expressed in the E12.5 embryonic lens and thus, could be the inductive signal that transforms the periocular mesenchyme cells that have migrated over the lens at this developmental stage into a fully mature corneal endothelium.

When *Fst* was included in the culture media in this preliminary study it had little effect on the E12.5POM and E13.5POM cell lines. The only significant differences were an increase in cell death and a drop in *Tgfβ1i4* expression after *Fst* treatment. The increase in cell death can easily be explained by the fact that *Fst* activates the Nodal pathway which has been shown to induce apoptosis in a variety of cell lines (Munir et al. 2004; Xu et al. 2004; Wang et al. 2007). The decrease in *Tgfβ1i4* expression due to treatment with *Fst* can be explained by examining the relationship between *Fst* and the known

transcriptional regulators of *Tgfβ1i4*. *Tgfβ1i4* is up-regulated by *TGFβ1* as well as follicle-stimulating hormone (*FSH*) (Dohrmann et al. 1999) both of which *Fst* binds and inactivates (Patel 1998; Nakamura et al. 1990). This provides a mechanism by which the expression of *Tgfβ1i4* is inhibited by *Fst*. Interestingly, it was noted that *Fst* had no effect on inducing *Pitx2* expression in the cell lines. It was initially hypothesised that the presence of *Fst* would up-regulate Nodal expression and one of the downstream consequences of this would be an increase in *Pitx2*. However, the results in the present study suggest that *Fst* is not sufficient to induce *Pitx2* expression.

There are a number of possible explanations for the ineffectiveness of *Fst* to induce a change towards a mature corneal endothelial phenotype in the cell lines. It is possible that high levels of *Fst* in the embryonic lens are involved in the patterning and differentiation of the lens itself and not the corneal endothelium and thus the presence of *Fst* would have no effect on periocular mesenchyme cells. This could be confirmed by creating a lens specific *Fst* knockout mouse which would enable one to visualise the developmental dysgenesis that occurs as a result. It is also possible that the high levels of cell death caused by the inclusion of *Fst* in the culture medium masked any other effects that *Fst* was having. The most likely explanation is that the addition of just *Fst* to the culture medium is not sufficient to drive differentiation. It is hypothesised that, *in vivo, Fst* acts in conjunction with a host of other cytokines and signalling molecules expressed by the embryonic lens epithelium to induce the final stages of MET in the periocular mesenchyme cells lines and so form the fully mature corneal endothelium. Thus, without the presence of the full host of factors secreted by the lens epithelium in culture, the differentiation of periocular mesenchymal cells into mature adult corneal endothelial cells is not possible.

4.3 Technical Considerations

In the present study it was reasoned that deriving an embryonic lenticular cell line would provide one with a way to identify signalling molecules expressed by the developing lens epithelium that could be involved in the formation of the corneal

endothelium. However, despite the numerous attempts made and different techniques used, a lenticular epithelial cell line was never successfully established.

Another technique that was attempted in order to investigate the effect of the lens on the immortal cell lines was the use of hanging drop cultures co-cultures consisting of E12.5POM and primary E12.5 mouse lenses. However, histological analyses of these hanging drops revealed numerous artefacts, in the form of spaces between many of the cells. These artefacts limited the conclusions that could be drawn from these experiments as it could not be determined if the results were a true interaction between the E12.5POM cell line and the E12.5 lens or simply an artefact of the processing procedure. Details of the experimental procedure and subsequent results can be found in appendix D.

Attempts were made to establish an adult corneal endothelial cell line in order to investigate the normal function and formation of cell junctions in the corneal endothelium. However, none of techniques used were successful. Besides the fact that a homogenous population of corneal endothelial cells could never be isolated, the immortalisation protocol is only effective on mitotically active cells. Since adult corneal endothelial cells have a very limited proliferative ability (Joyce et al. 1996) it would be almost impossible to immortalise them using the SV40 large T-antigen and other immortalising approaches would be needed.

The measurements of TEER levels were unsuccessful in this study. A more sensitive system of measurement would be required to pick up the small increase in TEER induced by incomplete tight junction formation. An example of such a system is to directly coat cells onto gold electrodes and take electrical impedance readings using specialised commercial equipment (Srinivas et al. 2004; Ma et al. 2007). This system can pick up very small increases in TEER levels and has been used to measure the TEER levels of bovine and rabbit adult corneal endothelium which range between 15-25 $\Omega.cm^2$ (Srinivas et al. 2004; Ma et al. 2007). Such a system would prove useful in order measure the tightness of the barrier formed by the E12.5POM and E13.5POM cell lines under different conditions.

4.4 Concluding Remarks

The results achieved in this study can be viewed in conjunction with the current body of knowledge in order to form an updated model of the development of the corneal endothelium.

During neurulation, neural crest cells delaminate from the junction of the closing neural tube and ectoderm and migrate to become committed to numerous lineages during embryogenesis. A small sub-population of cranial neural crest cells migrate along the optic vesicle into the presumptive eye, undergo an epithelial to mesenchymal transition (EMT). EMT is the reverse process of MET and results in a loss of adhesion and polarity and an increase in motility (reviewed by Chen et al. 2012). Both EMT and MET are fundamental developmental processes that control the switching between different cell types in the embryo (reviewed by Chen et al. 2012). The cranial neural crest cells that had undergone EMT and together with the ocular mesoderm, form the *Foxc1* expressing periocular mesenchyme population that surrounds the developing optic cup (Figure 4.3 – E11.5). While in this region the cells are maintained in an undifferentiated state due to undetermined signal secreted by the surrounding microenvironment which inhibits their differentiation.

At E12.5 the periocular mesenchyme cells begin to migrate towards the lens and away from the source of the morphogen that inhibits their differentiation (Figure 4.3 – E12.5). Thus the migrating mesenchyme cells can begin to undergo MET to form corneal endothelial cells. One of the changes as part of this MET is the formation of adherens junctions as the migrating cells make cell-to-cell contact.

By E13.5 the periocular mesenchyme cells have migrated over the lens and are sufficiently far away from the inhibitory morphogen that they can undergo complete MET (Figure 4.3 – E13.5). The principle change that occurs is a down-regulation in *Foxc1* which initiates a cascade of gene and protein expression changes in the migrated cells including the formation of tight junctions. Further signalling, by unknown

molecules/mechanisms, originates from the lens epithelium and aids the completion of MET.

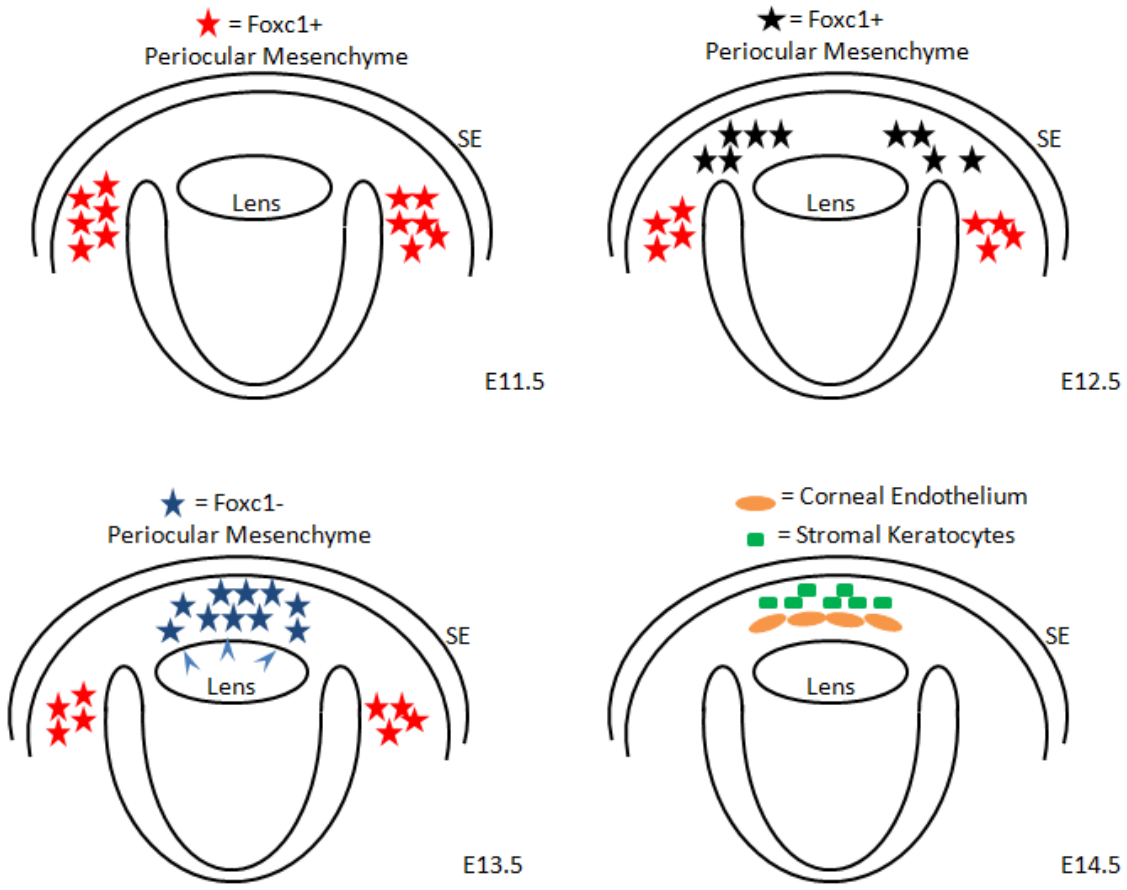

Figure 4.3: A model of corneal endothelial development. E11.5 - *Foxc1* expressing periocular mesenchyme cells surround the developing optic cup. E12.5 - the periocular mesenchyme cells begin to migrate towards the lens and start to undergo MET. E13.5 – *Foxc1* is down-regulated in the migrated mesenchymal cells. This induces a change towards an epithelial phenotype. Signals from the lens aid in the completion of this MET. E14.5 - the cells closest to the lens differentiate into mature, fully functional corneal endothelial cells. Those more distal to the lens are not influenced by paracrine signalling from the lens epithelium and form stromal keratocytes.

By E14.5 lens derived signals have assisted in the formation of a fully mature, functional adult corneal endothelium in the mesenchymal cells closest to the lens (Figure 4.3 – E14.5). Cells that are not in direct contact with the lens go on to form the stromal keratocytes (Figure 4.3 – E14.5). The differentiated corneal endothelial cells then separate from the lens which is the crucial event in the formation of the anterior chamber.

In conclusion, a protocol was derived that could differentiate immortal embryonic periocular mesenchyme cells into corneal endothelial like cells. In this way an *in vitro* model within which one can study the development of the corneal endothelium from the periocular mesenchyme precursor cells was established. It is hoped that future research using this model will ultimately lead to a more complete understanding of corneal endothelial development.

Chapter 5: Appendices

Appendix A – Recipes, Reagents and Molecular Weight Marker

A.1 1x PBS

Dissolve 8g NaCl, 1.26g Na_2HPO_4, 0.2g KCl, and 0.2g KH_2PO_4 in 800ml of distilled water. pH to 7.4 and make up to 1 litre. Autoclave to sterilise and store at 4°C.

A.2 0.05% trypsin/EDTA

Dissolve 0.05g trypsin (Sigma-Aldrich, USA) in 100ml 1xPBS. Add 0.02g EDTA (Sigma-Aldrich, USA) and stir to dissolve. Filter sterilize through 0.22µm filter and aliquot into 50ml tubes. Store at -20°C.

A.3 4% Paraformaldehyde in PBS

Add 4g PFA (Merck, Germany) to 80ml of 1xPBS in fume hood. While in fume hood dissolve by heating and pH to 7.4. Make up to 100 ml and store at 4°C.

A.4 1x TBE

Dissolve 10.8g tris (Merck, Germany), 5.5g boric acid (Sigma-Aldrich, USA), and 0.75g EDTA (Sigma-Aldrich, USA) in 900ml distilled H_20. Adjust pH to 8.0. Adjust volume to 1 litre and store at room temperature.

A.5 Chromic Acid Solution

Dissolve 30g potassium dichromate (Merck, Germany) in 100ml distilled water. Slowly add 450ml concentrated sulphuric acid while constantly stirring and cooling. Make up to 1 litre using distilled water.

A.6 Molecular Weight Marker - O'Generuler 100bp DNA ladder

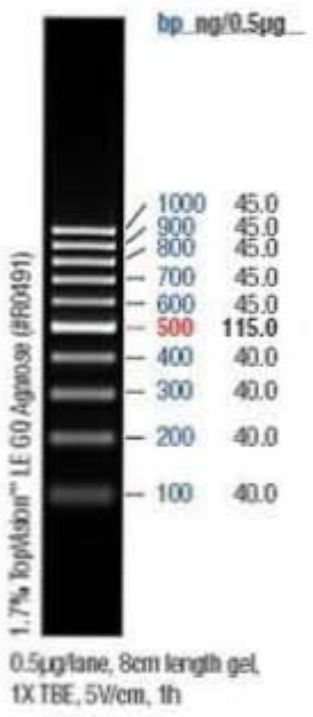

Appendix B – Additional Methods

B.1 Freezing down cells

Cells were lifted with 0.05% trypsin/EDTA, re-suspended in freezing medium (DMEM with 20% FBS and 10% dimethyl sulfoxide (Merck, Germany)), placed in cryogenic tubes and transferred to -80°C overnight. The following day they were placed in liquid nitrogen storage.

B.2 Testing for *Mycoplasma* infection

The presence of a *Mycoplasma* infection in cell lines was tested for by using a Hoechst nuclear stain and standard operating procedure (Chen 1977). Stained cells were visualised using a Zeiss Axiovert 200M fluorescent microscope (Carl Zeiss, Germany). Since none of the cell lines were found to be infected with *Mycoplasma* during this study treatment options were never considered.

B.3 RNA extraction using TriPure Isolation Reagent (Roche, Germany)

For adherent cell lines, cells were first lifted using trypsin/EDTA and centrifuged. After aspirating the medium, 1ml of cold TriPure was added to the pellet. Primary tissues on the other hand were homogenised using corex tubes in 1ml of cold TriPure. Both cells and tissues were lysed by repeated trituration. Lysate was transferred to a 1.5ml Eppendorf tube at room temperature for 5 minutes ensuring dissociation of the nucleoprotein complexes. 100µl of pure chloroform was added and vortexed vigorously for 20 seconds after which it was left at room temperature for 10 minutes. Samples were centrifuged for 15 minutes at 4°C at 12000g. 200µl of the uppermost layer, containing the RNA was transferred to a new 1.5ml Eppendorf tube and 250µl of cold isopropanol was added. Tubes were gently inverted several times by hand and RNA was precipitated at -20°C overnight.

The next morning samples were centrifuged at 12000g for 10minutes at 4°C. Supernatant was discarded and the pellet washed with 75% ethanol and vortexed briefly, followed by re-centrifuging for a further 10 minutes. Ethanol was then removed

by drying under a vacuum for 10 minutes with further air-drying as necessary. RNA pellets were then re-suspended in an appropriate volume of SABAX water (Adcock Ingram, South Africa).

B.4 Siliconising corex tubes

Corex tubes were soaked in chromic acid (Appendix A.5) overnight. They were then rinsed 10 times in tap water followed by 3 rinses in distilled water and dried in an 80°C oven for 30 minutes. The tubes were then filled with siliconising fluid (4% solution of dichlorodimethylsilane in carbon tetrachloride filtered through Whatman paper) in a fume hood and allowed to soak for 10 minutes. After this the tubes were drained and baked for 2 hours in a 180°C oven before being cooled and rinsed 3 times with distilled water. The tubes were then treated with a 0.01% diethylpyrocarbonate (DEPC) solution made in 1xPBS at 37°C for 2 hours and then autoclaved in order to inactivate the DEPC.

B.5 Details of primer design

Sequences from Entrez Gene

Sequences of the genes of interest were obtained from Entrez Gene (maintained by the National Center of Biotechnology Information, USA).

Table B.1: Sequence Accession Numbers for Genes Used in Primer Design

Gene	Sequence accession Number
Glucuronidase B (Gus)	NM_023048.5
Forkhead Box C1 (*Foxc1*)	NM_008592.2
Transforming growth factor beta 1 induced transcript 4 (*Tgfβ1i4*)	NM_010286.3
Paired-like homeodomain transcription factor 2 (*Pitx2*)	NM_011098.3
Follistatin (*Fst*)	NM_008046.2

Parameters for primer design in Primer-BLAST

PCR product size; 100-200bp (in the case of FOXC1 this was changed to 100-600 as no appropriate primer sets could be found the initial conditions)

Primer Melting Temperature; Minimum - 55°C, Optimum - 57°C, Maximum - 60°C

Organism; Mus Musculus

All other parameters in the programme were left as the default values.

Properties of primers in IDT OligoAnalyzer

Hairpins, self-dimers and hetero-dimers had to have individual Delta G values of more than -9 kcal/mole. Any value for any dimer or hairpin formed by a primer set that was less than this threshold was not suitable for use and another primer set was designed.

Reconstituting primers

Primers received from Whitehead Scientific (Whitehead Scientific, South Africa) were made up, according to their instructions, to a 100µM concentration in 1xTris/EDTA (pH 7.4). This stock solution was then diluted in distilled water to a concentration of 10 µM for use in PCR reactions.

B.6 Laminin coating of dishes

Laminin (Sigma-Aldrich, USA) was used to coat tissue culture dishes. A 100µg/ml stock solution of laminin was made in distilled water and filter sterilised using a 0.22µm filter. Stock was diluted to 10µg/ml in distilled water to make a working solution. 1ml of working solution was added to 35mm dishes and left on for 4 hours at 37° in a sterile incubator. After this time the laminin solution was removed and the dish was washed 3 times with 1xPBS. Dishes were stored at 37°C until needed

B.7 Polylysine coating of dishes and wells

Polylysine (Sigma-Aldrich, USA) was used to coat dishes and wells of plates as follows. A 1mg/ml stock solution of polylysine was made in distilled water and filter sterilised using a 0.22µm filter. Stock was diluted to 0.1mg/ml in distilled water to make a working solution. Sufficient working solution was added to the wells or dishes so that the entire surface was covered. The working solution was left in the well/dish for 1 hour at room temperature in the lamina flow. After this time the polylysine was removed and the well/dish was washed 3 times with 1xPBS. Plates and dishes were stored at 37°C until needed.

Appendix C – qPCR Validation

C.1 mRNA integrity

All RNA samples used for cDNA synthesis were analysed for their integrity in accordance with the MIQE guidelines (Bustin et al. 2009). When quantified, only RNA samples with high yields (above 1000ng of RNA) and $OD_{260/280}$ readings of between 1.8 and 2.2 were determined to be suitable for qRT-PCR reactions (as reviewed by Fleige et al. 2006). RNA samples were also run on a 1% (w/v) agarose gel as per methods section 2.4.2. Three bands, the 28s, 18s and 5s should be present with the 28s band approximately 1.8-2 times more intense than the 18s band. There should be no additional high molecular weight fragments or any smearing between the two bands (Fleige et al. 2006). An example of mRNA considered to be of high enough quality to use in this study is presented in figure 5.1.

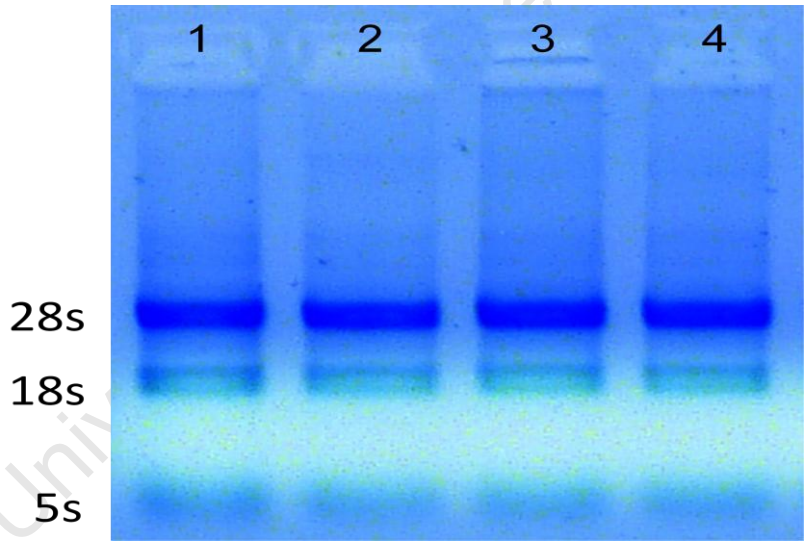

Figure 5.1: Example of agarose gel analysis (1% (w/v) agarose, 100V) indicating mRNA integrity of various experimental samples. The 28s, 18s and 5s ribosomal RNA bands are indicated.
Lane 1 – E12.5POM (Proliferative conditions)
Lane 2 – E12.5POM (Non-proliferative conditions)
Lane 3 – E13.5POM (Proliferative conditions)
Lane 4 – E13.5POM (Non-proliferative conditions)

C.2 Primer efficiencies

In order to obtain accurate quantification of target genes using the $2^{-\Delta\Delta Cq}$ method the amplification efficiencies between the reference gene and the target genes must be highly similar (Livak et al. 2001). In order to evaluate the efficiencies of the primers, a serial dilution of template cDNA samples that were positive for each target gene was made. Each diluted sample of cDNA was then analysed by qPCR as per the standard conditions for each primer set. The log of the cDNA concentration was then plotted against the average C_q value for each target gene and the reference gene. The efficiency of the primer sets was calculated by using the formula $10^{-1/a}$ with 'a' representing the slope of the plotted graph. All the primer sets had efficiencies between 0.8 and 1.2 and were thus considered suitable for analysis using the $2^{-\Delta\Delta Cq}$ method (Livak et al. 2001). An example of an evaluation of primer efficiency is presented in figure 5.2 and the calculation below.

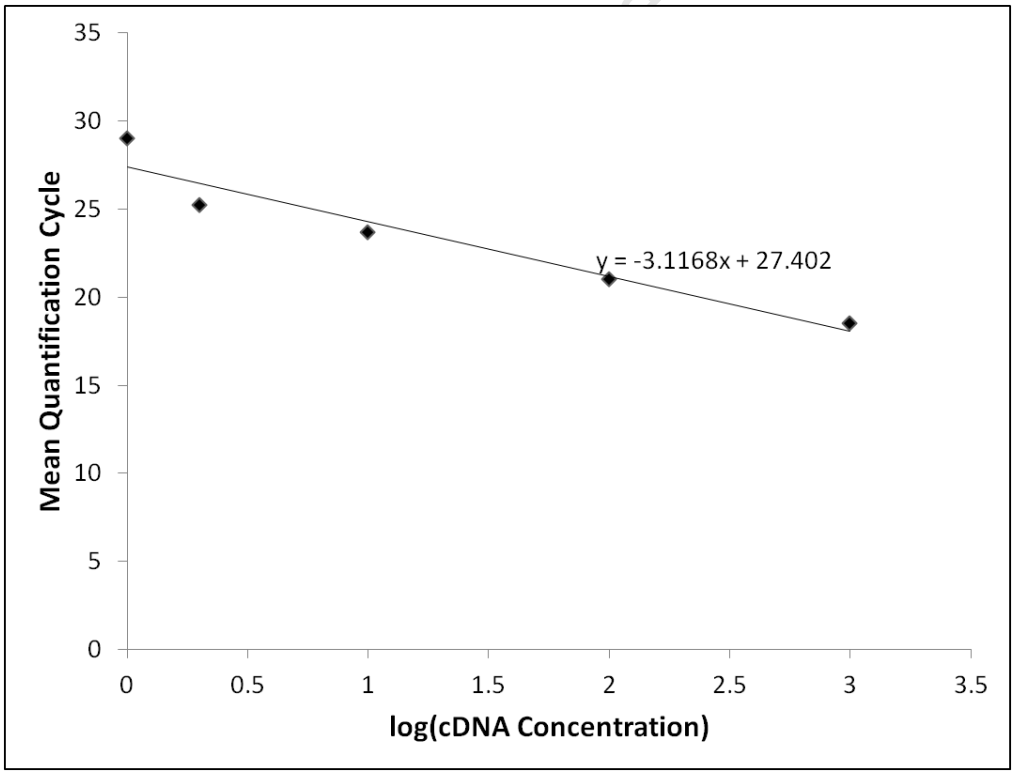

Figure 5.2: Quantification cycle vs. cDNA concentration for *Tgf*β*1i4* primer set.

The slope of the line of best fit of the graph in figure 5.2 is -3.1168.
Therefore;
*Tgf*β*1i4* primer efficiency = $10^{-1/-3.1168}$
*Tgf*β*1i4* primer efficiency = 1.093251

C.3 qPCR specificity

In order to confirm the specificity of each primer set the melting curves from each qPCR protocol as well as agarose gels were used. A single peak in the positive sample along with no significant peak of the same size in the no template control in the melting curve analysis indicates a single product. The correct size of the product was checked by running it on a 1% (w/v) agarose gel. Primer sets were only used if one single product of the correct size in the positive samples as well as no product of this size in the no template control was noted. An example of a qPCR specificity check is presented in figure 5.3 below.

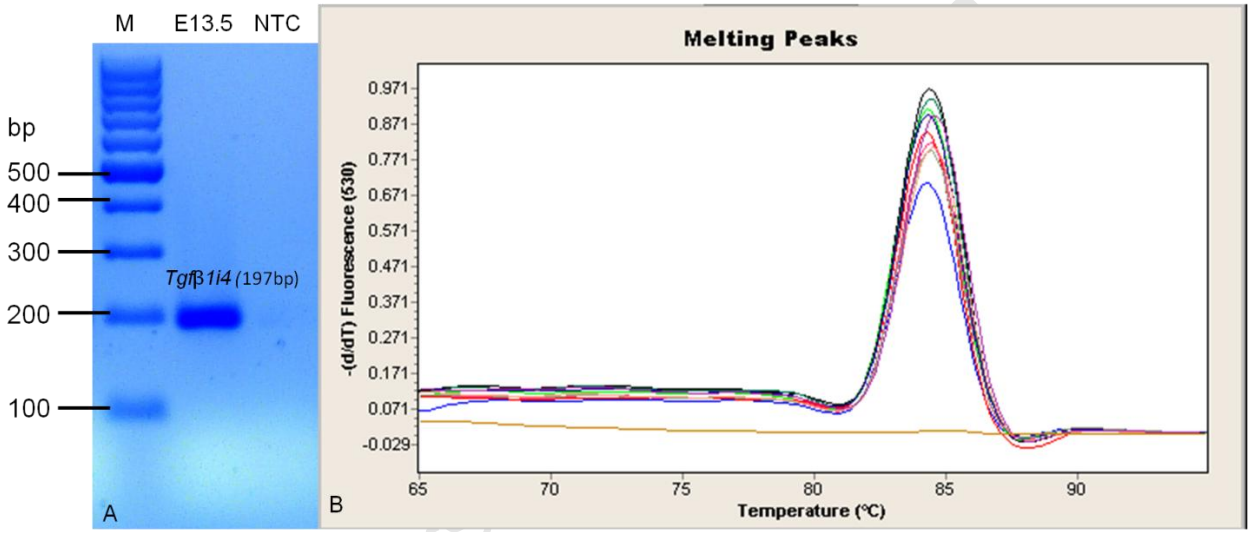

Figure 5.3: Melting curve and agarose gel analysis of *Tgfβ1i4* qPCR reaction. (A) Agarose gel analysis of *Tgfβ1i4* qPCR reaction shows a single amplification product at the correct calculated molecular weight in the positive sample (E13.5) with no product in the no template control (NTC). (B) Melting curve generated during the *Tgfβ1i4* qPCR reaction. Single peak noted in all the samples with no products in the no template control.
M – Molecular weight marker, O'Generuler 100bp DNA ladder
E13.5 - E13.5POM (Non-proliferative conditions)
NTC – No template control

Appendix D – Preliminary Study into the Physical Interaction Between the E12.5POM Cell Line and the E12.5 Embryonic Lens

Numerous reports have suggested that the physical presence of the lens itself has a role to play in the formation of the anterior segment (Genis-Galvez 1966; Beebe et al. 2000; Zhang et al. 2007). It was hypothesised in the present study that co-culture of primary embryonic lenses with the immortalised periocular mesenchyme cell lines would result in a physical interaction between the cells and the lens which would mimic *in vivo* the formation of the anterior chamber. In order to analyse the effect that embryonic mouse lenses had on the immortalised cell lines, hanging drop cultures were undertaken.

D.1 Methodology

A confluent plate of E12.5POM cells was trypsinised and re-suspended in approximately 1ml of medium (volume was adjusted to obtain 10^5cells/ml). To plate a hanging drop, a 30µl drop of re-suspended cells was positioned onto the lid of a 35mm culture dish. Primary lenses dissected from mice at the E12.5 developmental stage were then added to the hanging drops. Hanging drops without lenses were also plated as controls. The lid was then placed back onto the dish itself (which contained 2ml of medium) and left for 5 days at 37°C.

After this culture period the hanging drops were fixed and processed for histological staining. Medium was aspirated from the hanging drops and melted HistoGel (Richard-Allen Scientific, USA) was added and allowed to set for 5 minutes. Once set, cells suspended in the gel were fixed using 4% paraformaldehyde in PBS for 30 minutes at room temperature. The gel suspended drops were then processed by dehydration in an ethanol series (2 x 1 hour 70% ethanol (EtOh), 2 x 2 hours 96% EtOh, 3 x 2 hours 100% EtOh) and then cleared in xylol for 2 x 2 hours. During processing, samples were agitated in a Shandon Elliot Automatic Tissue Processor (Shandon Elliot, USA). Tissues were embedded in wax the next morning and sectioned using a Reichert-Jung 2040 Microtome (Reichert-Jung, Germany) at 4 µm intervals.

The wax sections were placed in a 60°C oven for 1 hour to melt the wax. Wax was then removed by 2 x 5 minute washes in xylol. Sections were then hydrated though an ethanol series (3 x 1 min absolute EtOh, 2 x 1 min 96% EtOh, 1 min in 70% EtOh) followed by washing in running tap water for 1 minute. Half the slides were then stained with haematoxylin and eosin and the other half with a periodic acid Schiff stain, used to indicate the presence of carbohydrates in the basement membrane.

Slides to be stained with haematoxylin and eosin were placed in haematoxylin for 5 minutes and then washed in running tap water for 1 minute. They were then stained in Scott's solution for 1 minute, rewashed, stained in eosin for 4 minutes and then washed once again.

Slides to be stained with the periodic acid Schiff stain were placed in 1% periodic acid (Sigma-Aldrich, USA) for 5 minutes and then washed in distilled water for 5 minutes. Following this, the slides were stained in Schiff's reagent (see below) for 15 minutes, rewashed, counter-stained with eosin for 4 minutes and then washed once again.

(To make Schiff's reagent 5g of basic fuchsin (Sigma-Aldrich, USA) was dissolved in 900ml of boiling distilled water. After cooling 50^{o}C 100ml of 1M hydrochloric acid (Merck, Germany) was added slowly. The solution was cooled once more to 25^{o}C and 10g of potassium metabisulfite ($K_2S_2O_5$ - Merck, Germany) was added and stirred for 5 minutes. The reagent was then incubated in the dark at room temperature for 24 hours. The next day 5 grams of fine activated charcoal was added and the solution was filtered through Whatman filter paper)

All the slides were then dehydrated using an ethanol series. (A few quick dips in 96% EtOh followed by a few in absolute EtOh). Finally, sections were cleared in xylol for 2 minutes and mounted with entellan (Merck, Germany) for visualisation. Four independent experiments, each consisting of 12 hanging drops were completed in this manner.

D.2 Results and Discussion

Haematoxylin and eosin stains of hanging drops containing only periocular mesenchyme cells consisted of a confluent sphere of cells (Figure 5.4 A). When a mouse lens was inserted into the middle of this culture it was easily distinguishable from the surrounding mesenchyme (Figure 5.4 B –black arrowheads). The lenses in these cultures appeared as densely packed balls of small cells and were always placed centrally within the hanging drop. When examining the interface between the lens and the mesenchyme (Figure 5.4 C) there appeared to be a gap between the two over one half of the lens (indicated by the black arrows in Figure 5.4 C). Similar gaps were noted in all four experiments undertaken.

No periodic acid Schiff staining was present in cultures containing only periocular mesenchyme (Figure 5.4 D). Mouse lenses were easily noted to be distinct from the surrounding mesenchyme (Figure 5.4 E – red arrowheads). Under high magnification some faint positive staining was noted (Figure 5.4 F). The majority of this staining was within the lens itself, but in numerous instances a border of staining surrounding the mesenchymal cells closest to the lens was evident in two of the four experiments (Figure 5.4 F – red arrows).

One potential explanation for these findings is that the interaction between the lens and the periocular mesenchyme cell line has resulted in the formation of an anterior chamber *in vitro*, potentially where the mesenchyme cells were in contact with the lens epithelium. This would explain why a gap had formed between the two over only one half of the lens. The faint basement membrane positive staining would suggest the initiation of the formation of a Descemet's membrane in a similar manner to what occurs during the development of the anterior chamber *in vivo*. However, the results from the hanging drops were not conclusive and artefacts, in the form of spaces between many of the cells, were prevalent. No matter what was changed in the culturing or processing of the hanging drops similar artefacts were always noted. Thus, it could not be determined if the results achieved in these experiments were due to the interaction between the E12.5POM cell line and the E12.5 lens or an artefact of the processing procedure.

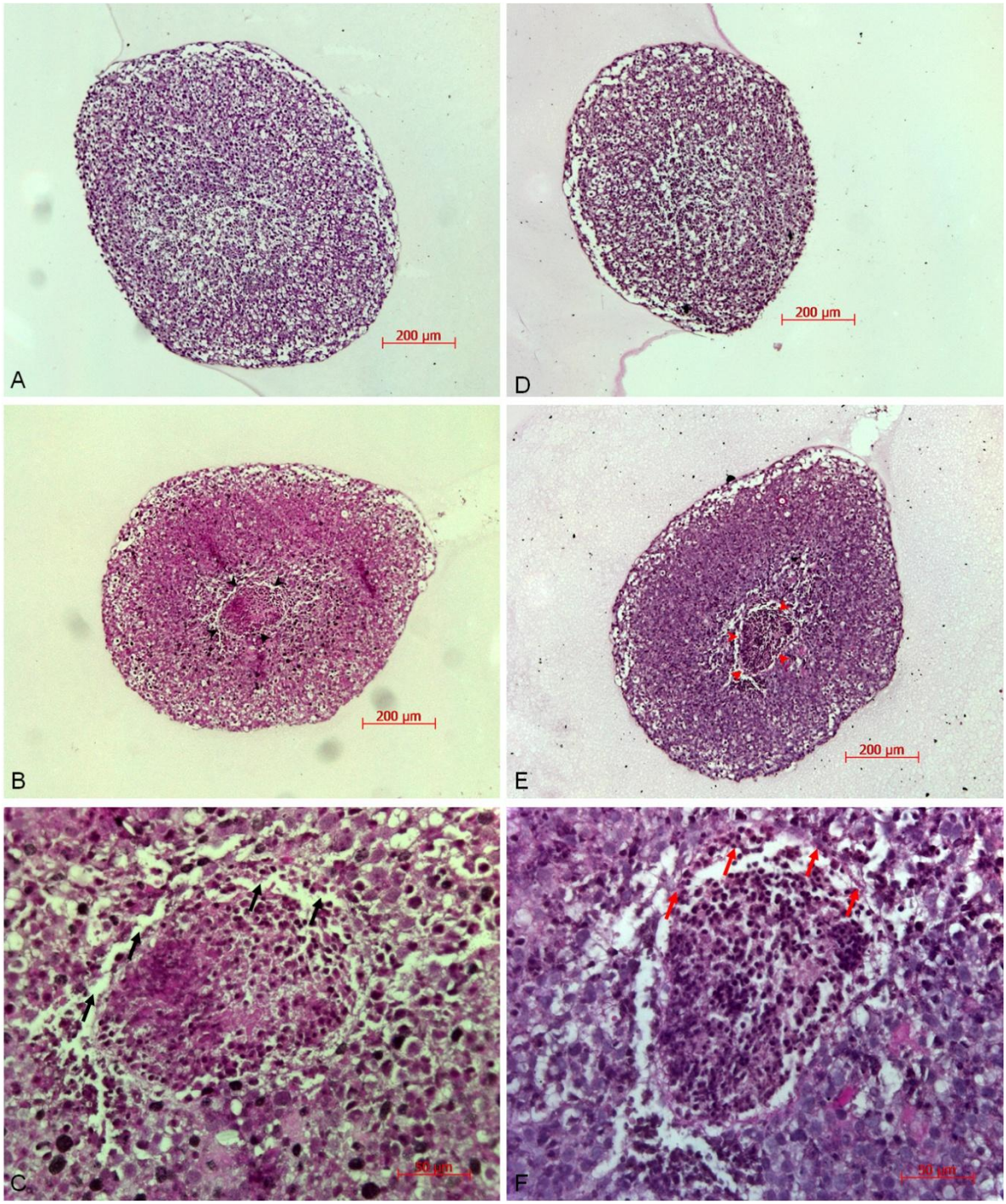

Figure 5.4: Histological analysis of hanging drop cultures containing the E12.5POM cell line and primary E12.5 lenses. A-C; Haematoxylin and eosin staining. D-F Periodic acid Schiff staining. (A) Hanging drop containing E12.5POM without the addition of a lens. (B) Hanging drop containing E12.5POM and E12.5 mouse lens. Boundary of lens indicated by the black arrowheads. (C) Higher magnification image of B. Black arrows indicate gap formed between the lens and the surrounding mesenchymal cells (D) Hanging drop containing E12.5POM without the addition of a lens. (E) Hanging drop containing E12.5POM and E12.5 mouse lens. Boundary of lens indicated by the red arrowheads. (F) Higher magnification image of E. Red arrows indicated areas of light pink staining in the periocular mesenchymal cells surrounding parts of the lens.

References

Aboalchamat, B., Engelmann, K., Böhnke, M., Eggli, P., and Bednarz, J. (1999). Morphological and functional analysis of immortalized human corneal endothelial cells after transplantation. Experimental Eye Research 69, 547-553.

Akitaya, T., and Bronner-Fraser, M. (1992). Expression of cell adhesion molecules during initiation and cessation of neural crest cell migration. Developmental Biology 194, 12-20.

Ali, S. H., and DeCaprio, J. A. (2001). Cellular transformation by SV40 large T antigen: interaction with host proteins. Seminars in Cancer Biology 11, 15-23.

Amano, S., Yamagami, S., Mimura, T., Uchida, S., and Yokoo, S. (2006). Corneal stromal and endothelial cell precursors. Cornea 25 Supp.1, S73-S77.

Balda, M. S., Gonzalez-Mariscal, L., Matter, K., Cereijido, M., and Anderson, J. M. (1994). Assembly of the tight junction: the role of diacylglycerol. The Journal of Cell Biology 123, 293-302.

Balda, M. S., and Matter, K. (2008). Tight junctions at a glance. Journal of Cell Science 121, 3677-3682.

Barasch, J., Yang, J., Ware, C. B., Taga, T., Yoshida, K., Erdjument-Bromage, H., Tempst, P., Parravicini, E., Malach, S., Aranoff, T., Oliver, J. A. (1999). Mesenchymal to epithelial conversion in rat metanephros is induced by LIF. Cell 99, 377-386.

Bednarz, J., Doubilei, V., Wollnik, P. C., and Engelmann, K. (2001). Effect of three different media on serum free culture of donor corneas and isolated human corneal endothelial cells. The British Journal of Ophthalmology 85, 1416-1420.

Bednarz, J., Teifel, M., Friedl, P., and Engelmann, K. (2000). Immortalization of human corneal endothelial cells using electroporation protocol optimized for human corneal endothelial and human retinal pigment epithelial cells. Acta Ophthalmologica 70, 130-136.

Beebe, D. C., and Coats, J. M. (2000). The lens organizes the anterior segment: specification of neural crest cell differentiation in the avian eye. Developmental Biology 220, 424-431.

Behrens, J., Birchmeier, W., Goodman, S. L., and Imhof, B. A. (1985). Dissociation of Madin–Darby canine kidney epithelial cells by the monoclonal antibody anti-arc-1: Cell, aspects and identification of the antigen as a component related to uvomorulin. Journal of Biology 101, 1307–1315.

Berry, F. B., Lines, M. A., Oas, J. M., Footz, T., Underhill, D. A., Gage, P. J., and Walter, M. A. (2006). Functional interactions between FOXC1 and PITX2 underlie the

sensitivity to FOXC1 gene dose in Axenfeld-Rieger syndrome and anterior segment dysgenesis. Human Molecular Genetics 15, 905-919.

Bourne, W. M. (2003). Biology of the corneal endothelium in health and disease. Eye 17, 912-918.

Bourne, W. M. (2010). Corneal endothelium-past, present, and future. Eye and Contact Lens 36, 310-314.

Braga, V. (2000). Epithelial cell shape: cadherins and small GTPases. Experimental Cell Research 261, 83-90.

Braga, V. (2002). Cell-cell adhesion and signalling. Current Opinion in Cell Biology 14, 546-556.

Bruewer, M., Hopkins, A. M., Hobert, M. E., Nusrat, A., and Madara, J. L. (2004). RhoA, Rac1, and Cdc42 exert distinct effects on epithelial barrier via selective structural and biochemical modulation of junctional proteins and F-actin. American Journal of Physiology - Cell Physiology 287, C327-C335.

Bustin, S. A., Benes, V., Garson, J. A., Hellemans, J., Huggett, J., Kubista, M., Mueller, R., Nolan, T., Pfaffl, M.W., and Shipley, G.L. (2009). The MIQE Guidelines - Minimum Information for Publication of Quantitative Real-Time PCR Experiments. Clinical Chemistry 55, 611-622.

Capella, J. A. (1972). Regeneration of endothelium in diseased and injured cornea. American Journal of Ophthalmology 74, 810-817.

Chen, J., Han, Q., and Pei, D. (2012). EMT and MET as paradigms for cell fate switching. Journal of Molecular Cell Biology4, 66-69.

Chen, K. H., Azar, D., and Joyce, N. C. (2001). Transplantation of adult human corneal endothelium ex vivo: a morphologic study. Cornea 20, 731-737.

Chen, T. (1977). In situ detection of mycoplasma contamination in cell cultures by fluorescent Hoechst 33258 stain. Experimental Cell Research 104, 255-262.

Cheng, H.-T., Miner, J. H., Lin, M., Tansey, M. G., Roth, K., and Kopan, R. (2003). Gamma-secretase activity is dispensable for mesenchyme-to-epithelium transition but required for podocyte and proximal tubule formation in developing mouse kidney. Development 130, 5031-5042.

Chomczynski, P., and Sacchi, N. (1987). Single-step method of RNA isolation by acid guanidinium thiocyanate-phenol-chloroform extraction. Analytical Biochemistry 162, 156-159.

Chow, R., and Lang, R. A. (2001). Early eye development in vertebrates. Annual Review of Cell and Developmental Biology 17, 255-296.

Clark, K. L., Halay, E. D., Lai, E., and Burley, S. K. (1993). Co-crystal structure of the HNF-3/fork head DNA-recognition motif resembles histone H5. Nature 364, 412-420.

Creuzet, S., Vincent, C., and Couly, G. (2005). Neural crest derivatives in ocular and periocular structures. The International Journal of Developmental Biology 49, 161-171.

Danielian, P. S., Muccino, D., Rowitch, D. H., Michael, S. K., and Mcmahon, A. P. (1998). Modification of gene activity in mouse embryos in utero by a tamoxifen-inducible form of Cre recombinase. Current Biology 8, 1323-1326.

Davanger, M., and Evensen, A. (1971). Role of the pericorneal papillary structure in renewal of corneal epithelium. Nature 229, 560-561.

Dohrmann, C. E., Belaoussoff, M., and Raftery, L. A. (1999). Dynamic expression of TSC-22 at sites of epithelial-mesenchymal interactions during mouse development. Mechanisms of Development 84, 147-151.

Dünker, N., and Krieglstein, K. (2001). Targeted mutations of transforming growth factor-β genes reveal important roles in mouse development and adult homeostasis. European Journal of Biochemistry 267, 6982-6988.

Ekblom, P. (1989). Developmentally regulated conversion of mesenchyme to epithelium. The FASEB Journal 3, 2141-2150.

Engelmann, K., and Friedl, P. (1989). Optimization of culture conditions for human corneal endothelial cells. In Vitro Cellular and Developmental Biology 25, 1065–1072.

Erlich, H. A. (1989). Polymerase chain reaction. Journal of Clinical Immunology 9, 437-447.

Fabricant, R., Alpar, A., Centifanto, Y., and Kaufman, H. (1981). Epidermal growth factor receptors on corneal endothelium. Archives of Ophthalmology 99, 305-308.

Fitch, K. L., and Nadakavukaren, M. J. (1986). Age-related changes in the corneal endothelium of the mouse. Experimental Gerontology 21, 31-35.

Fleige, S., and Pfaffl, M. W. (2006). RNA integrity and the effect on the real-time qRT-PCR performance. Molecular Aspects of Medicine 27, 126-139.

Gage, P. J., Rhoades, W., Prucka, S. K., and Hjalt, T. A. (2005). Fate maps of neural crest and mesoderm in the mammalian eye. Investigative Ophthalmology and Visual Science 46, 4200-4208.

Gage, P. J., Suh, H., and Camper, S. (1999). Dosage requirement of Pitx2 for development of multiple organs. Development 126, 4643-4651.

Gagnon, M., Boisjoly, H., Brunette, I., Charest, M., and Amyot, M. (1997). Corneal endothelial cell density in glaucoma. Cornea 16, 314-318.

Gao, Y., Zhou, Q., Qu, M., Yang, L., Wang, Y., and Shi, W. (2010). In vitro culture of human fetal corneal endothelial cells. Graefe's Archive for Clinical and Experimental Ophthalmology 249, 663-669.

Genis-Galvez, J. M. (1966). Role of the lens in the morphogenesis of the iris and cornea. Nature 210, 209-210.

Genis-Galvez, J. M., Santos-Gutierrez, L., and Rios-Gonzalez, A. (1967). Causal factors in corneal development: an experimental analysis in the chick embryo. Experimental Eye Research 6, 48-56.

Gerrard, L., Rodgers, L., and Cui, W. (2005). Differentiation of human embryonic stem cells to neural lineages in adherent culture by blocking bone morphogenetic protein signalling. Stem Cells 23, 1234-1241.

Gilbert, S. (2000). Developmental Biology 6th ed. (Sunderland, Massachusetts: Sinauer Associates).

Gonzalez, P., Epstein, D. L., Luna, C., and Liton, P. B. (2006). Characterization of free-floating spheres from human trabecular meshwork (HTM) cell culture in vitro. Experimental Eye Research 82, 959-967.

Goshima, Y., Sasaki, Y., Nakayama, T., Ito, T., and Kimura, T. (2000). Functions of semaphorins in axon guidance and neuronal regeneration. Japanese Journal of Pharmacology 82, 273-279.

Gupta, R. A., Sarraf, P., Brockman, J. A., Shappell, S. B., Raftery, L. A., Willson, T. M., and Dubois, R. N. (2003). Peroxisome proliferator-activated receptor y and transforming growth factor- B pathways inhibit intestinal epithelial cell growth by regulating levels of TSC-22*. The Journal of Biological Chemistry 278, 7431-7438.

Hansen, R., and Oren, M. (1997). p53; from inductive signal to cellular effect. Current Opinion in Genetics and Development 7, 46-51.

Hay, E. (1986). Development of the vertebrate cornea. International Review of Cytology 63, 263-322.

Hay, E., Linsenmayer, T. F., Trelstad, R. L., and Mark, K. V. D. (1979). Origin and distribution of collagens in the developing avian cornea. Current Topics in Eye Research 1, 1-35.

Hirsch, M., Renard, G., Faure, J., and Pouliquen, Y. (1977). Study of the ultrastructure of the rabbit corneal endothelium by the freeze- fracture technique: apical and lateral junctions. Experimental Eye Research 25, 277–288.

Hjalt, T. A., Semina, E. V., Amendt, B. A., and Murray, J. C. (2000). The Pitx2 protein in mouse development. Developmental Dynamics 218, 195-200.

Horn, D. L. Van, Sendele, D. D., Seideman, S., and Buco, P. J. (1977). Regenerative capacity of the corneal endothelium in rabbit and cat. Investigative Ophthalmology and Visual Science 16, 597-613.

Huang, L., Harkenrider, M., Thompson, M., Zeng, P., Tanaka, H., Gilley, D., Ingram, D., Bonanno, J., and Yoder, M. (2010). A hierarchy of endothelial colony forming cell activity is displayed by bovine corneal endothelial cells. Investigative Ophthalmology and Visual Science 51, 3943-3949.

Hyldahl, L. (1984). Primary cell cultures from human embryonic corneas. Journal of Cell Science 66, 343-351.

Ittner, L. M., Wurdak, H., Schwerdtfeger, K., Kunz, T., Ille, F., Leveen, P., Hjalt, T.A., Suter, U., Karlsson, S., Hafezi, F., and Born, W, (2005). Compound developmental eye disorders following inactivation of TGFB signaling in neural-crest stem cells. Journal of Biology 44, 11.1-11.16.

Iwamoto, T., and Smelser, G. (1965). Electron microscopy of the human corneal endothelium with reference to transport mechanisms. Investigative Ophthalmology and Visual Science 4, 270–279.

Iwao, K., Inatani, M., Matsumoto, Y., Ogata-Iwao, M., Takihara, Y., Irie, F., Yamaguchi, Y., Okinami, S., and Tanihara, H. (2009). Heparan sulfate deficiency leads to Peters anomaly in mice by disturbing neural crest TGF-β 2 signaling. The Journal of Clinical Investigation 119, 1997-2008.

Jat, P. S., Noble, M. D., Ataliotis, P., Tanakat, Y., Yannoutsost, N., Larsent, L., and Kioussist, D. (1991). Direct derivation of conditionally immortal cell lines from an H-2Kb-tsA58 transgenic mouse. Proceedings of the National Academy of Sciences 88, 5096-5100.

Jat, P. S., and Sharp, P. A. (1989). Cell lines established by a temperature-sensitive simian virus 40 large-T-antigen gene are growth restricted at the non-permissive temperature. Molecular and Cellular Biology 9, 1672-1681.

Johnston, M. C., Noden, D. M., Hazelton, R. D., Coulombre, J. L., and Coulombre, A. J. (1979). Origins of avian ocular and periocular tissues. Experimental Eye Research 29, 27-43.

Joo, C. K., Pepose, J. S., and Fleming, T. P. (1994). In vitro propagation of primary and extended life span murine corneal endothelial cells. Investigative Ophthalmology and Visual Science 35, 3952-3957.

Jou, T. S., Schneeberger, E. E., and Nelson, W. J. (1998). Structural and functional regulation of tight junctions by RhoA and Rac1 small GTPases. The Journal of Cell Biology 142, 101-115.

Joyce, N. C. (2003). Proliferative capacity of the corneal endothelium. Progress in Retinal and Eye Research 22, 359-389.

Joyce, N. C., Navon, S. E., Roy, S., and Zieske, J D (1996). Expression of cell cycle-associated proteins in human and rabbit corneal endothelium in situ. Investigative Ophthalmology and Visual Science 37, 1566-1575.

Joyce, N. C., and Zieske, J.D. (1997). Transforming growth factor-beta receptor expression in human cornea. Investigative Ophthalmology and Visual Science 38, 1922-1928.

Jun, A. S., Chakravarti, S., Edelhauser, H. F., and Kimos, M. (2006). Aging changes of mouse corneal endothelium and Descemet's membrane. Experimental Eye Research 83, 890-896.

Kanasaki, H., Oride, A., and Miyazaki, K. (2011). Paracrine control of gonadotrophs by somatolactotrophs through TRH- induced follistatin production. The Open Neuroendocrinology Journal 4, 102-110.

Kaufman, P., and Alm, A. (2003). Adler's physiology of the eye: clinical application Tenth Edit. (Maryland Heights, Missouri: Mosby).

Kawamata, H., Fujimori, T., and Imai, Y. (2004). TSC-22 (TGF-beta stimulated clone-22): a novel molecular target for differentiation-inducing therapy in salivary gland cancer. Current Cancer Drug Targets. 4, 521-529.

Kester, H. A., Leede, B. J. M. V. D., Saag, P. T. V. D., and Burg, B. V. D. (1997). Novel progesterone target genes identified by an improved differential display technique suggest that progestin-induced growth inhibition of breast cancer cells coincides with enhancement of differentiation *. The Journal of Cell Biology 272, 16637-16643.

Kidson, S. H., Kume, T., Deng, K., Winfrey, V., and Hogan, B. L. (1999). The forkhead/winged-helix gene, Mf1, is necessary for the normal development of the cornea and formation of the anterior chamber in the mouse eye. Developmental Biology 211, 306-322.

Kitamura, K., Miura, H., Miyagawa-Tomita, S., Yanazawa, M., Katoh-Fukui, Y., Suzuki, R., Ohuchi, H., Suehiro, A., Motegi, Y., Nakahara, Y., Kondo, S., and Yokoyama, M. (1999). Mouse Pitx2 deficiency leads to anomalies of the ventral body wall, heart, extra- and periocular mesoderm and right pulmonary isomerism. Development 126, 5749-5758.

Kulesa, P., Ellies, D. L., and Trainor, P. A. (2004). Comparative analysis of neural crest cell death, migration, and function during vertebrate embryogenesis. Developmental Dynamics 229, 14-29.

Kume, T., Deng, K. Y., Winfrey, V., Gould, D. B., Walter, M. A., and Hogan, B. L. (1998). The forkhead/winged helix gene Mf1 is disrupted in the pleiotropic mouse mutation congenital hydrocephalus. Cell 93, 985-996.

Lai, J., Chen, K., Hsu, W.-M., Hsiue, G.-H., and Lee, Y.-H. (2006). Bioengineered human corneal endothelium for transplantation. Archives of Ophthalmology 124, 1441-1448.

Laing, R., Sandstrom, M., Berrospi, A., and Leibowitz, H. (1976). Changes in the corneal endothelium as a function of age. Experimental Eye Research 22, 587-594.

Larsson, L.-I. (1988). Immunocytochemistry: Theory and practice (Boca Raton: CRC Press).

Larue, L., Ohsugi, M., Hirchenhain, J., and Kemler, R. (1994). E-cadherin null mutant embryos fail to form a trophectoderm epithelium. Proceedings of the National Academy of Sciences 91, 8263-8267.

Lehmann, O. J., Ebenezer, N. D., Jordan, T., Fox, M., Ocaka, L., Payne, A., Leroy, B. P., Clark, B. J., Hitchings, R. A., Povey, S., Khaw, P. T., and Bhattacharya, S. S. (2000). Chromosomal duplication involving the forkhead transcription factor gene FOXC1 causes iris hypoplasia and glaucoma. American Journal of Human Genetics 67, 1129-1135.

Lin, C. R., Kioussi, C., O'Connell, S., Briata, P., Szeto, D., Liu, F., Izpisua-Belmonte, C., and Rosenfeld, M. (1999). Pitx2 regulates lung asymmetry, cardiac positioning and pituitary and tooth morphogenesis. Nature 401, 279-282.

Livak, K. J., and Schmittgen, T. D. (2001). Analysis of relative gene expression data using real-time quantitative PCR and the 2(-Delta Delta C(T)) method. Methods 25, 402-408.

Lièvre, C. S. Le, and Douarin, N. M. Le (1975). Mesenchymal derivatives of the neural crest : analysis of chimaeric quail and chick embryos. Journal of Embryology and Experimental Morphology 34, 125-154.

Lodish, H., Berk, A., Zipursky, S. L., Matsudaira, P., Baltimore, D., and Darnell, J. (2008). Molecular cell biology 6th ed. (New York: W.H. Freeman).

Lovicu, F. J., and Robinson, M. L. (2004). Development of the ocular lens (Cambridge: Cambridge University Press).

Lu, M. F., Pressman, C., Dyer, R., Johnson, R. L., and Martin, J. F. (1999). Function of Rieger syndrome gene in left-right asymmetry and craniofacial development. Nature 401, 276-278.

Luetteke, N. C., and Lee, D. C. (1990). Transforming growth factor alpha: expression, regulation and biological action of its integral membrane precursor. Seminars in Cancer Biology 1, 265-275.

Luetteke, N. C., Qiu, T. H., Peiffer, R. L., Oliver, P., Smithies, O., and Lee, D. C. (1993). TGF alpha deficiency results in hair follicle and eye abnormalities in targeted and waved-1 mice. Cell 73, 263-278.

Lwigale, P. Y., and Bronner-Fraser, M. (2009). Semaphorin3A/neuropilin-1 signaling acts as a molecular switch regulating neural crest migration during cornea development. Developmental Biology 336, 257-265.

Ma, L., Kuang, K., Smith, R., Rittenband, D., Iserovich, P., Diecke, F., and Fischbarg, J. (2007). Modulation of tight junction properties relevant to fluid transport across rabbit corneal endothelium. Experimental Eye Research 84, 790-798.

Martinez-Morales, J. R., and Wittbrodt, J. (2009). Shaping the vertebrate eye. Current Opinion in Genetics and Development 19, 511-517.

Mary, S., Charrasse, S., Meriane, M., Comunale, F., Travo, P., and Blangy, A. (2002). Biogenesis of N-cadherin-dependent cell-cell contacts in living fibroblasts is a microtubule- dependent kinesin-driven mechanism. Molecular Biology of the Cell 13, 285-301.

Mattiske, D., Sommer, P., Kidson, S. H., and Hogan, B. L. (2006). The role of the forkhead transcription factor, Foxc1, in the development of the mouse lacrimal gland. Developmental dynamics 235, 1074-1080.

McLaughlin, B., Caldwell, R., Sasaki, Y., and Wood, T. (1985). Freeze-fracture quantitative comparison of rabbit corneal epithelial and endothelial membranes. Current Eye Research 4, 951-961.

McLennan, R., and Kulesa, P. (2007). In vivo analysis reveals a critical role for neuropilin-1 in cranial neural crest cell migration in chick. Developmental Biology 301, 227–239.

Mgwebi, T. (2004). Morphological investigations into the development of the mammalian corneal endothelium using the mouse model. PhD Thesis. University of Cape Town.

Mimura, T., Yamagami, S., Yokoo, S., Araie, M., and Amano, S. (2005a). Comparison of rabbit corneal endothelial cell precursors in the central and peripheral cornea. Investigative Ophthalmology and Visual Science, 3645-3648.

Mimura, T., Yamagami, S., Yokoo, S., Yanagi, Y., and Usui, T. (2005b). Sphere Therapy for Corneal Endothelium Deficiency in a Rabbit Model. Investigative Ophthalmology and Visual Science, 3128-3135.

Monier-Gavelle, F., and Duband, J. (1995). Control of N-cadherin-mediated intercellular adhesion in migrating neural crest cells in vitro. Journal of Cell Science 108, 3839-3853.

Munir, S., Xu, G., Wu, Y., Yang, B., Lala, P. K., and Peng, C. (2004). Nodal and ALK7 inhibit proliferation and induce apoptosis in human trophoblast cells. The Journal of Biological Chemistry 279, 31277-31286.

Murphy, C., Alvarado, J., Jusrer, R., and Maglio, M. (1984). Prenatal and postnatal cellularity of the human corneal endothelium: A quantitative histologic study. Investigative Ophthalmology and Visual Science 25, 312-322.

Nakamura, T., Takio, K., Eto, Y., Shibai, H., Titani, K., and Sugino, H. (1990). Activin-binding protein from rat ovary is follistatin. Science 247, 836-838.

Napier, H. R. L. (2005). Ontogenesis of the cornea and ciliary body: A morphological and molecular study. PhD Thesis. University of Cape Town.

Niessen, C. M. (2007). Tight junctions/adherens junctions: basic structure and function. The Journal of Investigative Dermatology 127, 2525-2532.

Nishimura, D. Y., Searby, C. C., Alward, W. L., Walton, D., Craig, J. E., Mackey, D. A., Kawase, K., Kanis, A. B., Patil, S. R., Stone, E. M., and Sheffield, V. C. (2001). A spectrum of FOXC1 mutations suggests gene dosage as a mechanism for developmental defects of the anterior chamber of the eye. American Journal of Human Genetics 68, 364-372.

Noden, D. M. (1983). The role of the neural crest in patterning of avian cranial skeletal, connective, and muscle tissues. . Developmental Biology 96, 144-165.

Noden, D. M. (1988). Interactions and fates of avian craniofacial mesenchyme. Development 103 Supplement, 121-140

Nusrat, A., Giry, M., Turner, J. R., Colgan, S. P., Parkos, C. A., Carnes, D., Lemichez, E., Boquet, P., and Madara, J. L. (1995). Rho protein regulates tight junctions and perijunctional actin organization in polarized epithelia. Proceedings of the National Academy of Sciences 92, 10629–10633.

Ohsugi, M., Larue, L., Schwarz, H., and Kemler, R. (1997). Cell-junctional and cytoskeletal organization in mouse blastocysts lacking E-cadherin. Developmental Biology 185, 261–271.

Osborne, N., Begbie, J., Chilton, J., Schmidt, H., and Eickholt, B. (2005). Semaphorin/neuropilin signaling influences the positioning of migratory neural

crest cells within the hindbrain region of the chick. Developmental Dynamics 232, 939–949.

Panicker, S. G., Sampath, S., Mandal, A. K., Reddy, A. B. M., Ahmed, N., and Hasnain, S. E. (2002). Novel mutation in FOXC1 wing region causing Axenfeld-Rieger anomaly. Investigative Ophthalmology and Visual Science 43, 3613-3616.

Patel, K. (1998). Follistatin. International Journal of Biochemistry and Cell Biology 30, 1087-1093.

Peh, G. S. L., Beuerman, R. W., Colman, A., Tan, D. T., and Mehta, J. S. (2011). Human Corneal Endothelial Cell Expansion for Corneal Endothelium Transplantation : An Overview. Transplantation 91, 811-819.

Pei, Y. F., and Rhodin, J. A. (1970). The prenatal development of the mouse eye. Anatomical Records 168, 105-125.

Pelton, R. W., Saxena, B., Jones, M., Moses, H. L., and Gold, L. I. (1991). Immunohistochemical localization of TGF beta 1, TGF beta 2, and TGF beta 3 in the mouse embryo: expression patterns suggest multiple roles during embryonic development. The Journal of Cell Biology 115, 1091-1105.

Petroll, W. M., Hsu, J. K. W., Bean, J., Cavanagh, H. D., and Jester, J. V. (1999). The spatial organization of apical junctional complex-associated proteins in feline and human corneal endothelium. Current Eye Research 18, 10-19.

Piatigorsky, J. (1981). Lens differentiation in vertebrates. A review of cellular and molecular features. Differentiation. 19, 134-153.

Pressman, C., Chen, H., and Johnson, R. L. (2000). LMX1B, a LIM homeodomain class transcription factor, is necessary for normal development of multiple tissues in the anterior segment of the murine eye. Genesis 26, 15-25.

Price, M. O., and Price, F. W. (2010). Endothelial keratoplasty - a review. Clinical and Experimental Ophthalmology 38, 128-140.

Prince, S. (1999). Regulation of melanogenesis in conditionally immortalised mouse melanocytes expressing a temperature-sensitve SV40 large T-antigen. PhD Thesis. University of Cape Town.

Radice, G., Ferreira-Cornwell, M., Robinson, S., Rayburn, H., Chodosh, L., Takeichi, M., and Hynes, R. (1997). Precocious mammary gland development in P-cadherin-deficient mice. The Journal of Cell Biology 139, 1025-1032.

Radice, G., Rayburn, H., Matsunami, H., Knudsen, K., Takeichi, M., and Hynes, R. (1997). Developmental defects in mouse embryos lacking N-cadherin. Developmental Biology 181, 64-78.

Ramalho, J. S., Gregory-Evans, K., Huxley, C., and Seabra, M. C. (2004). Mouse genetic corneal disease resulting from transgenic insertional mutagenesis. British Journal of Ophthalmology 88, 428-433.

Raymond, G. M., Jumblarr, M. M., Barrels, S. P., and Neufeld, A. H. (1986). Rabbit Corneal Endofhelial Cells in Vitro: Effects of EGF. Investigative Ophthalmology and Visual Science 27, 474-479.

Reneker, L. W., Silversides, D. W., Patel, K., and Overbeek, P. A. (1995). TGF alpha can act as a chemoattractant to perioptic mesenchymal cells in developing mouse eyes. Development 121, 1669-1680.

Reneker, L. W., Silversides, D. W., Xu, L., and Overbeek, P. A. (2000). Formation of corneal endothelium is essential for anterior segment development - a transgenic mouse model of anterior segment dysgenesis. Development 127, 533-542.

Rothenpieler, U. W., and Dressler, G. R. (1993). Pax-2 is required for mesenchyme-to-epithelium conversion during kidney development. Development 119, 711-720.

Saika, S., Liu, C. Y., Azhar, M., Sanford, L. P., Doetschman, T., Gendron, R. L., Kao, C. W., and Kao, W. W. (2001). TGFbeta2 in corneal morphogenesis during mouse embryonic development. Developmental Biology 240, 419-432.

Saleem, R. A., Banerjee-Basu, S., Berry, F. B., Baxevanis, A. D., and Walter, M. A. (2001). Analyses of the effects that disease-causing missense mutations have on the structure and function of the winged-helix protein FOXC1. American Journal of Human Genetics 68, 627-641.

Sanford, L. P., Ormsby, I., Groot, A., Sariola, H., Friedman, R., Boivin, G. P., Cardell, E. L., and Doetschman, T. (1997). TGFβ2 knockout mice have multiple developmental defects that are non- overlapping with other TGFβ knockout phenotypes. Development 124, 2659-2670.

Savage, J., Voronova, A., Mehta, V., Sendi-Mkasa, F., and Ilona, S. S. (2010). Canonical Wnt signaling regulates Foxc1 / 2 expression in P19 cells. Differentiation 79, 31-40.

Savatier, P., Huang, S., Szekely, L., Wiman, K. G., and Samarut, J. (1994). Contrasting patterns of retinoblastoma protein expression in mouse embryonic stem cells and embryonic fibroblasts. Oncogene 9, 809-818.

Schermer, A., Galvin, S., and Sun, T. T. (1986). Differentiation-related expression of a major 64K corneal keratin in vivo and in culture suggests limbal location of corneal epithelial stem cells. The Journal of Cell Biology 103, 49-62.

Schwartzkopff, J., Bredow, L., Mahlenbrey, S., Boehringer, D., and Reinhard, T. (2010). Regeneration of corneal endothelium following complete endothelial cell loss in rat keratoplasty. Molecular Vision 16, 2368-2375.

Semina, E. V., Reiter, R., Leysens, N. J., Alward, W. L., Small, K. W., Datson, N. A., Siegel-Bartelt, J., Bierke-Nelson, D., Bitoun, P., Zabel, B. U., Carey, J. C., and Murray, J. C. (1996). Cloning and characterization of a novel bicoid-related homeobox transcription factor gene, RIEG, involved in Rieger syndrome. Nature Genetics 14, 392-399.

Seo, S., and Kume, T. (2006). Forkhead transcription factors, Foxc1 and Foxc2, are required for the morphogenesis of the cardiac outflow tract. Developmental Biology 296, 421-436.

Sevel, D., and Isaacs, R. (1988). A re-evaluation of corneal development. Transactions of the American Ophthalmological Society 86, 178-207.

Snell, R. S., and Lemp, M. A. (1998). Clinical Anatomy of the Eye Second Edi. (Hoboken, New Jersey: Wiley-Blackwell).

Sommer, P., Napier, H. R. L., Hogan, B. L., and Kidson, S. H. (2006). Identification of Tgfβ1i4 as a downstream target of Foxc1. Development, Growth and Differentiation 48, 297- 308.

Srinivas, S. P. (2011). Cell signaling in regulation of the barrier integrity of the corneal endothelium. Experimental Eye Research, 1-8.

Srinivas, S. P., Satpathy, M., Gallagher, P., Larivière, E., and Driessche, W. V. (2004). Adenosine induces dephosphorylation of myosin II regulatory light chain in cultured bovine corneal endothelial cells. Experimental Eye Research 79, 543-551.

Steed, E., Balda, M. S., and Matter, K. (2010). Dynamics and functions of tight junctions. Trends in Cell Biology 20, 142-149.

Stiemke, M. M., McCartney, M. D., Cantu-Crouch, D., and Edelhauser, H. F. (1991). Maturation of the Corneal Endothelial Tight Junction. Investigative Ophthalmology and Visual Science 32, 2757-2765.

Stuart, R., Sun, A., Bush, K., and Nigam, S. (1996). Dependence of epithelial intercellular junction biogenesis on thapsigargin-sensitive intracellular calcium stores. Journal of Biological Chemistry 271, 13636-13641.

Svedbergh, B., and Bill, A. (1972). Scanning electron microscopic studies of the corneal endothelium in man and monkeys. Acta Ophthalmologica 50, 321-326.

Taddei, A., Giampietro, C., Conti, A., Orsenigo, F., Breviario, F., Pirazzoli, V., Potente, M., Daly, C., Dimmeler, S., and Dejana, E. (2008). Endothelial adherens junctions control tight junctions by VE-cadherin-mediated upregulation of claudin-5. Nature Cell Biology 10, 923-934.

Takaishi, K., Sasaki, T., Kotani, H., Nishioka, H., and Takai, Y. (1997). Regulation of cell-cell adhesion by rac and rho small G proteins in MDCK cells. The Journal of Cell Biology 139, 1047-1059.

Tang, Z. I. (2010). The Domino and Clock Models of Cell Cycle Regulation. Nature Education 3, 56.

Thut, C. J., Rountree, R. B., Hwa, M., and Kingsley, D. M. (2001). A large-scale in situ screen provides molecular evidence for the induction of eye anterior segment structures by the developing lens. Developmental Biology 231, 63-76.

Tierney, E. P., and Giudice, L. C. (2004). Role of activin A as a mediator of in vitro endometrial stromal cell decidualization via the cyclic adenosine monophosphate pathway. Fertility and Sterility 81 Suppl 1, 899-903.

Tümer, Z., and Bach-Holm, D. (2009). Axenfeld-Rieger syndrome and spectrum of PITX2 and FOXC1 mutations. European Journal of Human Genetics 17, 1527-1539.

Umeda, K., Ikenouchi, J., Katahira-Tayama, S., Furuse, K., Sasaki, H., Nakayama, M., Matsui, T., Tsukita, S., and Furuse, M. (2006). ZO-1 and ZO-2 independently determine where claudins are polymerized in tight-junction strand formation. Cell 126, 741-754.

Wang, H., and Tsang, B. K. (2007). Nodal signalling and apoptosis. Reproduction 133, 847-853.

Wilson, S. E., Lloyd, S. A., He, Y. G., and McCash, C. S. (1993). Extended life of human corneal endothelial cells transfected with the SV40 large T antigen. Investigative Ophthalmology and Visual Science 34, 2112-2123.

Wójciak-Stothard, B., Potempa, S., Eichholtz, T., and Ridley, A. J. (2001). Rho and Rac but not Cdc42 regulate endothelial cell permeability. Journal of Cell Science 114, 1343-1355.

Xu, G., Zhong, Y., Munir, S., Yang, B. B., Tsang, B. K., and Peng, C. (2004). Nodal induces apoptosis and inhibits proliferation in human epithelial ovarian cancer cells via activin receptor-like kinase 7. The Journal of Clinical Endocrinology and Metabolism 89, 5523-5534.

Yamagami, S., Yokoo, S., Mimura, T., Takato, T., Araie, M., and Amano, S. (2006). Distribution of precursors in human corneal stromal cells and endothelial cells. Ophthalmology 114, 433-439.

Yan, X., Zhang, J., Pan, L., Wang, P., Xue, H., Zhang, L., Gao, X., Zhao, X., Ning, Y., Chen, Y. (2011). TSC-22 promotes transforming growth factor β-mediated cardiac myofibroblast differentiation by antagonizing Smad7 activity. Molecular and Cellular Biology 31, 3700-3709.

Yokoo, S., Yamagami, S., Yanagi, Y., Uchida, S., and Mimura, T. (2005). Human corneal endothelial cell precursors isolated by sphere-forming assay. Investigative Ophthalmology and Visual Science 46, 1626-1631.

Yu, W. Y., Sheridan, C., Grierson, I., Mason, S., Kearns, V., Lo, A. C. Y., and Wong, D. (2011). Progenitors for the corneal endothelium and trabecular meshwork: a potential source for personalized stem cell therapy in corneal endothelial diseases and glaucoma. Journal of Biomedicine and Biotechnology 2011:41274, 1-13.

Yue, B. Y., Sugar, J., Gilboy, J. E., and Elvart, J. L. (1989). Growth of human corneal endothelial cells in culture. Investigative Ophthalmology and Visual Science 30, 248-253.

Zhang, Y., Overbeek, P. A., and Govindarajan, V. (2007). Perinatal ablation of the mouse lens causes multiple anterior chamber defects. Molecular Vision 13, 2289-2300.